STUDIES ON PDE4 CYCLIC AMP-SPECIFIC PHOSPHODIESTERASES

A thesis presented to the University of Glasgow

for the degree of Doctor of Philosophy

Jonathan Curtis O'Connell

Department of Biochemistry and Molecular Biology,

University of Glasgow, October 1996

Abstract

The type 4 family of phosphodiesterases (PDEs) are part of family of enzymes that provide the sole means of hydrolysing the ubiquitous second messenger, adenosine-3',5'-cyclic monophosphate. The PDE4 family is complex, consisting of four genes, each of which is alternatively spliced. Understanding the functional significance of the multiple species is crucial so as to enable the development of novel drugs to modulate their activities for the treatment of many disorders, including depression, asthma and arthritis.

In this study, the regulation of PDE4B splice variants by insulin in intact rat epididymal adipocytes was investigated and the expression of PDE4B species in a number of cell lines was detected using antisera designed to recognise the C-terminal region of PDE4B species. Described herein is the first demonstration of the interaction of PDE4 isoforms with Src homology-3 (SH3) domains. The PDE4A species, rpde6 (RNPDE4A5) and the PDE4D species PDE4D4, when expressed either transiently in COS cells or endogenously in brain, were shown to possess the ability to bind to SH3 domains of certain Src family tyrosyl kinases, that were expressed as glutathione-S-transferase (GST) fusion proteins. Neither PDE isoforms interacted with GST itself. PDE4D4 and rpde6 displayed little or no binding to the SH3 domains of the adapter proteins Grb2 and Crk, thus displaying specificity for the SH3 domains with which they interacted. Interaction was determined by the N-terminal splice region of rpde6 since the PDE4A splice variant rpde39, which differs from rpde6 at the N-terminus failed to interact with SH3 domains at all. This occurred both when rpde39 was either transiently expressed in COS cells or endogenously expressed in testes. The interaction of PDE4D4 with SH3 domains appeared to be determined by its N-terminal splice region since the other PDE4D splice variants, PDE4D3 and PDE4D5, which differ from PDE4D4 only in their extreme N-terminally spliced regions, did not interact with SH3 domains. rpde6 but not PDE4D4 was shown to interact with the SH3 domains of Crk, Lck and Csk, as well as the cytoskeletal protein fodrin, leading to a perturbation of the catalytic activity of rpde6. In contrast, association with the SH3 domains of Src family tyrosyl kinases, Src, Fyn and Lyn did not effect the catalytic activity, K_m or sensitivity to the PDE4 specific inhibitor rolipram of rpde6. The basis and possible functional significance of such interactions is described.

Acknowledgements

First and foremost, thanks to the Department of Biochemistry and Molecular Biology at Glasgow University for the use of their facilities and to the MRC for the studentship which funded this research. Sincere thanks to Professor Miles Houslay for all his help and guidance over the last three years. I would also like to thank every one in the Gardiner Lab for attempting to keep me sane during the more stressful periods of my Ph.D. Special thanks to Clodagh and Adrienne, I would not have survived the write up without them. Most of all, thanks to my parents for their help and support during my seven years at university.

CONTENTS

CHAPTER 2 MATERIALS AND METHODS

List of Figures

List of Tables

Abbreviations

AC	adenylyl cyclase
AKAP	PKA anchor proteins
AMP	adenosine monophosphate
ANP	A-type natriureic peptide
ATP	adenosine triphosphate
BNP	B-type natriureic peptide
BSA	bovine serum albumin
CaM	calmodulin
cAMP	adenosine-3',5'-cyclic monophosphate
CAT	chloramphenicol acetyl transferase
cGMP	guanosine-3',5'-cyclic monophosphate
CNP	C-type natriureic peptide
CRE	cAMP response element
CREB	cAMP response element binding protein
DMEM	Dulbecco's Modified Eagle's Medium
DMSO	Dimethyl sulphoxide
DTT	dithiothreitol
EDTA	Ethylenediaminetetra-acetic acid
EGTA	ethylene glycolbis(β-aminoethylether)-N,N,N',N'-tetra-acetic acid
EGF	epidermal growth factor
GC	guanylyl cyclase
GDP	guanine diphosphate

G-Protein	guanine triphosphate binding protein
Grb2	growth factor receptor binding protein 2
GTP	guanine triphosphate
HARBS	high affinity rolipram binding site
Hepes	N-2-Hydroxyethylpiperazine-N'-2-ethanesulfonic acid
HRP	horse radish peroxidase
IBMX	isobutylmethylxanthine
IgG	immunoglobulin G
IRS 1	insulin receptor substrate 1
IRS 2	insulin receptor substrate 2
KHD	kinase homology domain
LDL	low density lipoprotein
MAP	mitogen activated protein
MOPS	3-[N-Morpholino]propane sulphonic acid
PAGE	polyacrylamide gel electrophoresis
PBS	phosphate buffered saline
PCR	polymerase chain reaction
PDE	phosphodiesterase
PDGF	platelet derived growth factor
PGE_2	prostaglandin E_2
PH	pleckstrin homology domain
PI3K	phosphotidylinositol 3'-kinase
PKA	protein kinase A

PKG	cGMP dependent protein kinase
PLC	phospholipase C
PTB	phosphotyrosine binding
P-Tyr	phosphorylated tyrosine residue
RTK	receptor tyrosine protein kinase
SDS	Sodium dodecyl sulphate
SH2	Src homology domain 2
SH3	Src homology domain 3
TBS	Tris buffered saline
TEA	triethanolamine
TEMED	N,N,N',N'-tetramethylethylenediamine
TNFα	Tumour necrosis factor-alpha
TSH	thyroid stimulating hormone
UCR	upstream conserved region
cGI-PDE	cGMP-inhibited PDE, PDE3
TYK2	Non-receptor tyrosine kinase 2

Chapter 1

Introduction

1.1. INTRODUCTION

This thesis describes work which investigates the regulation and interactions of type 4 phosphodiesterases which specifically breakdown the second messenger adenosine-3',5'-cyclic monophosphate. It pays particular attention to the function of the multiple splice variants of these genes in order to decipher the functional role of their N-terminal splice regions in determining protein-protein interactions.

1.2. CYCLIC NUCLEOTIDE SIGNALLING

1.2.1. Background

Two cyclic nucleotides are known to be involved in intracellular signalling processes. These are adenosine-3',5'-cyclic monophosphate (cAMP) and guanosine -3',5'-cyclic monophosphate (cGMP). Such second messengers are generated as a result of the action of adenylyl cyclase which produces cAMP and guanylyl cyclase which produces cGMP. These enzymes can be activated in response to external stimuli such as hormones or neurotransmitters. Cellular responses to these second messengers are mediated through their activation of protein kinases which phosphorylate target proteins, leading, in turn to a cellular response.

1.2.2. cAMP generation

Binding of an effector to a cell surface receptor transmits its signal to adenylyl cyclase via heterotrimeric GTP-binding proteins (G-proteins). These G-

proteins can either stimulate, in the case of G_s, or inhibit, via G_i, adenylyl cyclase. cAMP if produced can bind to the regulatory subunits of protein kinase A (PKA), causing the dissociation and subsequent activation of the catalytic subunits which then phosphorylate target proteins. The regulatory subunits are then involved in transport of cAMP either to the nucleus where it is believed to bind to DNA and effect transcriptional events or to the cytoplasm where the complex may have post-translational effects.

cAMP levels must be regulated. While desensitisation plays a role in decreasing cAMP synthesis after stimulation, a mechanism is also required for degrading the second messenger. Such a mechanism is provided by a family of enzymes known as cyclic nucleotide phosphodiesterases (PDEs) which hydrolyse both cAMP and cGMP into their corresponding 5'-monophosphate.

1.2.2. G-proteins

G-proteins are a heterologous, but related, group of membrane-associated proteins that functionally link surface receptors to their effectors [Gillman, AG. 1984, Bray, P., *et. al.* 1986]. They are all heterotrimers, made up of an α-subunit which binds and hydrolyses GTP and a βγ-dimer that serves as a functional monomer [reviewed; Neer, EJ. 1994]. In recent years, numerous members of the heterotrimeric G-protein family have been cloned from vertebrates and invertebrates. To date, twenty α-subunits, five β-subunits and twelve γ-subunits have been identified. Random association of these subunits would produce hundreds of different heterotrimeric proteins, however it appears that there are

preferred combinations of isoforms that associate to form a limited number of distinct complexes [Pronon, AN. and Gautam, N. 1992, Ray, K., *et. al.* 1995, Lee, C., *et. al.* 1995].

In a resting state, G-proteins exist in a holomeric inactive state, with GDP bound to the α-subunit. Ligand stimulation produces a change in conformation of the receptor which possesses seven transmembrane helices. This leads to a decreased affinity of the α-subunit of the G-protein for GDP which consequently dissociates and is replaced by GTP. With GTP bound, the α-subunit is activated and dissociates from the βγ-dimer. This activated state persists until GTP is hydrolysed to GDP by the intrinsic GTPase activity of the α-subunit which re-associates with the βγ-dimer [Neubig, RR., *et. al.* 1994]. Activated G_s-α interacts with and activates adenylyl cyclase.

1.2.3. Adenylyl Cyclases

The functional role of adenylyl cyclases is to synthesise cAMP from ATP in response to activation in response to a number of hormones and neurotransmitters. These enzymes have a complex structure. A short cytoplasmic amino-terminus is followed by six transmembrane spans (M_1), then a large cytoplasmic domain of about 40kDa (C_1), then a second set of six transmembrane domains (M_2) and a second cytoplasmic domain (C_2). Such a structure resembles that of certain channels and ATP dependent transporters, particularly the P glycoprotein and cystic fibrosis transmembrane conductance regulator [reviewed Taussig, R. and Gilman, AG. 1995]. Consequently it has prompted speculation

that the adenylyl cyclases may also serve as channels or transporters but there is no evidence to support this. However, an adenylyl cyclase from *Paramecium* has been reported to be a potassium channel, although its structure is not yet known [Schultz, JE., *et. al.* 1992].

Adenylyl cyclases are expressed at relatively low levels which combined with their liability in detergent containing solutions hindered their purification and characterisation. It was not until an affinity matrix with forskolin was made that purification became possible [Pfeuffer, T. and Metzger, H. 1882]. It became apparent that were at least two distinct classes that differed in their ability to be stimulated by calmodulin [Pfeuffer, E., *et. al.* 1985, Mollner, S. and Pfeuffer, T. 1988, Smigel, MD. 1986]. Sufficient quantities of the calmodulin sensitive form were isolated to sequence and full length cDNAs were subsequently cloned. This Ca^{2+}/calmodulin sensitive form was termed type-I [Krupinski, J., *et. al.* 1989]. Clones for seven additional isoenzymes have since been identified [Feinstein, PG., *et. al.* 1991, Bakalyar, HA. and Reed, RR. 1990, Gao, B. and Gilman, AG. 1991, Yoshimura, M. and Cooper, DMF. 1992, Cali, JJ., *et. al.* 1994]. The overall sequence homology of the different isoforms of adenylyl cyclases is 50%. However two regions in the cytoplasmic domains, $C_{1\alpha}$ and $C_{2\alpha}$, have 93% sequence homology. $C_{1\alpha}$ and $C_{2\alpha}$ are also highly homologous to each other as well as to regions of membrane bound guanylyl cyclases, and are hypothesised to be the sites of catalytic activity [Chinkers, M. and Grabers, DL. 1991]. Furthermore, catalytic activity has been show to require both $C_{1\alpha}$ and $C_{2\alpha}$ and several point mutations within these regions compromise catalytic activity severely [Tang, WJ.,

et. al. 1992]. The amino-terminal and carboxyl-terminal halves of type-I adenylyl cyclase have no catalytic activity when expressed alone but activity is restored when they are expressed concurrently [Tang, WJ., *et. al.* 1991]. Analogously, soluble forms of guanylyl cyclase are heterodimers, each subunit containing a region that is homologous to $C_{1\alpha}$ and $C_{2\alpha}$ and both subunits are required for catalysis [Nakane, M., *et. al.* 1990], suggesting that both domains contribute to the binding site.

The function of the divergent sequences mirrors the wide range of regulatory influences that effect them. All mammalian adenylyl cyclases are activated by the α-subunit of G_s. However, types I, III and VIII are also regulated by nanomolar concentrations of Ca^{2+}/calmodulin [Krupinski, J., *et. al.* 1989, Bakalyar, HA. and Reed, RR. 1990], whereas the other isoforms are insensitive. Furthermore the G-protein βγ-subunit complex has a prominent type-specific regulation on adenylyl cyclases. The G_s-α stimulatory effect on type II and IV enzymes is greatly potentiated by βγ, whereas the activity of Type I is markedly inhibited [Tang, WJ. and Gilman, AG. 1991].

1.2.4. Guanylyl Cyclases

Guanylyl cyclases fall into two families, transmembrane and cytosolic. The transmembrane receptor family possesses a single transmembrane domain, an intracellular protein kinase homology domain and a cyclase catalytic domain. The extracellular, ligand binding region varies from receptor to receptor. The cytosolic forms are made up of two different subunits (α and β), each of which contains a

cyclase catalytic domain [Gerzer, R., *et. al.* 1981], which are related to the $C_{1\alpha}$ and $C_{2\alpha}$ domains of adenylyl cyclases. They also contain bound haem and are activated by nitric oxide and drugs such as nitrovasodilators [Garbers, DL. 1992].

4.2.4.1. Membrane bound guanylyl cyclases

The known peptide ligands for membrane bound guanylyl cyclases are the natriureic peptides (A-type natriureic peptide (ANP), B-type natriureic peptide (BNP) and C-type natriuretic peptide (CNP)) and heat stable enterotoxins / guanylins. Four membrane bound species have been identified, GC-A, GC-B, GC-C and ret-GC and it is suggested that these receptors must at least dimerise to form a single catalytically active site [Garbers, DL. *et. al.* 1994]. In fact, human GC-A has been shown to exist as a tetramer that is sensitive to reducing agents and that the cytoplasmic domain is required for this association [Lowe, DG., 1992]. The protein kinase homology domain (KHD) contains the majority of the conserved amino acids reported as being invariant within the catalytic domain of protein kinases [Hanks, EG., *et. al.* 1988]. An exception is the replacement of an invariant Asp with other amino acids such as Asr, Ser or Asn, a phenomenon which is also seen with the KHD-2 domain of JAKS [Witthuhn, BA., *et. al.* 1994]. No protein kinase activity has ever been shown in either the KHD of guanylyl cyclases or JAKS domain 2 [Witthuhn, BA., *et. al.* 1994]. The function of the KHD in GC-A appears to be that it is required to bind ATP in order to potentiate the signal generated by ANP binding , although no ATPase activity has been detected [Chinkers, M., *et. al.* 1991].

4.2.4.3. Cytosolic guanylyl cyclases

Four isoenzymes of the cytoplasmic cyclase subunits have been identified (α_1, α_2, β_1 and β_2), each of which exists as an $\alpha\beta$-dimer. Studies [Yuen, PST., *et. al.* 1994] have shown that a single point mutation on α_1 destroys all catalytic activity when it is associated with β_1, suggesting that, as with the membrane-bound forms, dimerisation produces a catalytically active site. The mechanism by which NO binding to haem activates soluble guanylyl cyclases is not known. However a third class of haem proteins have been shown to exist, haem-based sensors, which are distinct from the oxygen carriers and electron transporters and contain the FixL proteins [David, M., *et. al.* 1988, Gilles-Gonzalez, MA., *et. al.* 1994]. The FixL proteins are involved in a cascade that leads to nitrogen fixation, their protein kinase catalytic domain is inhibited by oxygen binding to haem, they contain a putative α-helical domain between their haem binding domain and their catalytic region and they normally exist as homodimers [David, M., *et. al.* 1988, Gilles-Gonzalez, MA., *et. al.* 1994]. In these respects they bear some resemblance to soluble guanylyl cyclases and it is thought that that binding of NO to haem has an allosteric effect that is transmitted through the α-helical region [Gilles-Gonzalez, MA., *et. al.* 1994].

1.2.5. cAMP dependent protein kinase

The discovery of cAMP-dependent protein kinase (PKA) provided the first clues about protein phosphorylation and its role in cellular signalling [Krebs, EG., 1986, Walsh, DA., *et. al.* 1968]. It is tightly regulated and maintained in an

inactive state in the absence of cAMP. However, unlike other protein kinases, the activating ligand, cAMP, binds to a distinct regulatory subunit, inducing conformational changes that lead to dissociation of the holoenzyme. The catalytic subunits share extensive sequence homologies with all eukaryotic protein kinases [Hanks, EG., *et. al.* 1988]. Even the closest homologue, in terms of sequence homology, of PKA, cGMP-dependent protein kinase has regulatory and catalytic domains as part of a single polypeptide chain [Takio, K., *et. al.* 1984].

The major function of the regulatory subunits are to bind to and maintain the catalytic subunits in an inactivate state in the absence of cAMP. The binding of cAMP to the regulatory subunits causes the holoenzyme to dissociate into two active catalytic units and a regulatory subunit dimer. Two major classes of regulatory subunits and their corresponding holoenzymes have been shown to exist [Flockhart, DA. and Corbin, JA 1982]. Type I holoenzymes were originally classified by the presence of a high affinity binding site for MgATP in the regulatory subunit (RI) [Lee, DC., *et. al.* 1983]. Type II were distinguished by autophosphorylation of the regulatory subunits (RII) [Hofmann, F., *et. al.* 1975]. More recently the RI and RII subunits have been shown to be encoded by different genes and differ in antigenicity, amino acid sequence and affinity for cAMP analogues.

Isoforms of RI (α and β) and RII (α and β) have also been identified, as well as for the PKA catalytic subunit (α, β and γ) which differ in their subcellular localisation and tissue distribution. RI isoforms are primarily found in the cytosolic fraction of the cell and RII isoforms in the particulate fraction

[Reviewed; McKnight, GS. 1991, Doskeland, SO., *et. al.* 1993]. The α- and β-forms of the catalytic subunit are highly homologous (93% at the amino acid level). They are both widely distributed throughout most tissues, the α-form generally being the predominant species. However, neither of these have so far shown any difference in specificity for proteins they phosphorylate. Distribution of the γ-form, however, is much more restricted and has so far only been identified in primate testes [Beebe, S., *et. al.* 1990] and is only 83% homologous to the α- and β-forms.

1.2.5.1. cAMP response elements

Activated PKA modulates the function of nuclear factors that bind to DNA sequences present in the promoter region of cAMP-inducible genes. Most of these genes contain one or more cAMP response elements (CREs). The consensus CRE is constituted by the palindromic sequence TGACGTCA [Borrelli, E., *et. al.* 1992]. The first protein found to bind to a CRE was CRE-binding protein (CREB) [Hoeffler, JP., 1988]. Following the discovery of CREB, a number of other binding proteins have been identified which can be classified into a number of groups. They all belong to the basic region / leucine zipper (bZip) transcription class of proteins, in which the DNA-binding domain is composed of a conserved region of about 30 amino acids, rich in basic residues [Landschultz, WH., *et. al.* 1988]. Immediately C-terminal to this region is a region with a heptad leucine repeat, which forms an amphipathic α-helix with the leucines aligned along one ridge. Two of these helices can associate in a coiled-coil conformation

[Landschultz, WH., *et. al.* 1988], allowing dimerisation of the CRE-binding factor, thus forming a Y-shaped structure, the arms of which represent the DNA-binding domains [Vinson, CR., *et. al.* 1989, O'Neil, KT., *et. al.* 1990].

The CRE-binding factors can be divided into activators and repressors. Examples of activators are CREB, CREMτ and ATF-1 [Meyer, TE. and Habener, JF. [1993] and repressors, CREMα, CREMβ and CREMγ [Laoide, BM., *et. al.* 1993]. Phosphorylation by PKA, in the case of transcriptional activators, leads to DNA binding and transcriptional activation [Gonzalez, GA. and Montminy, MR. 1989, de Groot, RP., *et. al.* 1993]. Conversely, dephosphorylation by protein phosphatase-1 leads to transcriptional attenuation of a CRE-driven gene [Nichols, M., *et. al.* 1992]. Transcriptional repressors are also phosphorylated by PKA and consequently bind to the CRE. However they lack twoglutamine-rich domains, found in the transcriptional activators, which are essential for transcriptional activation [Foulkes, NS., *et. al.* 1991].

1.2.5.2. Protein kinase A anchoring proteins

Phosphorylation of target substrates by PKA mediates certain hormonal responses by altering the biological activity of key enzymes and structural proteins. PKA is a multifunctional kinase with broad substrate specificity and yet it can trigger discrete physiological responses even in the same cell [Reviewed; Scott, JD. 1991]. For example, phosphorylation of membrane-bound neurotransmitter receptor channels modulates the flow of ions into the cell [Wang, LY., *et. al.* 1991], while phosphorylation of nuclear transcription factors alters the

activity of certain genes [Meyer, TE. and Habener, JF. 1993]. Work performed by Barsony and Marx using microwave fixing techniques has shown that specific hormones can increase cAMP concentrations in subcellular compartments in epithelial and fibroblast cell lines [Barsony, J. and Marx, SJ. 1990]. For example, isoprenaline and prostaglandin E_2 promote cAMP accumulation close to the plasma membrane, whereas calcitonin causes perinuclear accumulation of cAMP. Prolonged treatment with forskolin causes nuclear accumulation of cAMP. One hypothesis to account for the selectivity of PKA action is individual effectors activate particular pools of the kinase which are compartmentalised to intracellular sites which are close to preferred substrates [Harper, JF., *et. al.* 1985, Scott, JD. and Carr, DW. 1992].

Localisation of PKA is determined by the regulatory (R) subunits, of which there are two forms, RI being cytosolic and RII particulate. Up to 75% of the cellular pool of RII is associated with the plasma membrane, cytoskeletal components, endoplasmic reticulum or nuclei [Corbin, JD., *et. al.* 1975, Leiser, M., *et. al.* 1986, Nigg, EA., *et. al.* 1985, Nigg, EA., *et. al.* 1985a, Joachim, S. and Schwock, G. 1990]. Type II PKA compartmentalisation is determined by association of RII with specific A-kinase anchoring proteins (AKAPs) [Lohmann, SM., *et. al.* 1984, Leiser, M., *et. al.* 1986, Bregman, DB., *et. al.* 1989, Carr, DW., *et. al.* 1992]. A number of AKAPs have been identified, each localising PKA to specific subcellular regions and often showing tissue specific expression. They are named simple by virtue of their molecular weights. AKAP100, which is predominantly expressed in cardiac and skeletal muscle and localises RII to the

sarcoplasmic reticulum [McCartney, S., *et. al.* 1995]. AKAP79, which is expressed to the highest levels in the cerebral cortex and localises to the postsynaptic densities [Carr, DW., *et. al.* 1992]. AKAP95 is found in the nucleus of most tissues and is involved in targeting RII for cAMP responsive nuclear events [Coghlan, VM., *et. al.* 1994]. AKAP75 associates with the dendritic microtubules of the cytoskeleton in neuronal tissue [Glantz, SB., Li, Y. and Rubin, CS. 1993] and AKAP150 is found associated with the microtubules in the neurones of the cerebral cortex and hippocampus and various other neurones throughout the forebrain.

RII dimerisation is required for AKAP binding [Scott, JD., *et. al.* 1990]. More specifically, the first 5 amino acids of each RII unit, especially the isoleucines at positions 3 and 5, have been shown to be required for the interaction [Hausken, ZE., *et. al.* 1994]. The site of interaction for the RII subunit on the AKAP consists of an amphipathic helix of 14-18 amino acids which must be maintained in the correct conformation to bind [Carr, DW., *et. al.* 1992].

1.2.6. Action of cGMP

The mechanisms of action of cGMP are three-fold. Firstly it serves to regulate cGMP-gated ion channels, secondly, it activates cGMP-dependent protein kinase (PKG) and thirdly, it regulates a number of phosphodiesterases. Regulation of phosphodiesterases will be discussed in section 1.3.

1.2.6.1. Regulation of cGMP-gated ion channels

Light stimulation of the vertebrate rod photoreceptor cell leads to cGMP hydrolysis with the consequent closing of a plasma membrane cGMP-gated cation channel. The net effect of which is transient hyperpolarisation of the cell and a neural response. A similar cGMP-gated ion channel exists in cone photoreceptor cells, although it is encoded by a different gene [Kaupp, UB., *et. al.* 1989, Bönigk, W., *et. al.* 1993]. In the olfactory sensory system, a channel with a high affinity for cGMP and a 74% amino acid homology to the retinal cGMP-gated channel has been described [Kaupp, UB., 1991]. The mechanism of cGMP regulation of photoreceptor ion channels is discussed further in section 1.3.7.

1.2.6.2. Activation of cGMP dependent protein kinases

Currently, two major types of vertebrate cGMP dependent protein kinase, the soluble type I (PKG-I) and the membrane bound type II (PKG-II) have been recognised. PKG-I has been shown to exist in two isoforms designated α and β [Lincoln, TM., *et. al.* 1988, Wolfe, L., *et. al.* 1989]. The protein sequences of both forms being almost identical in their cGMP binding and catalytic regions but only 36% homology in their N-terminal ends and they have since been identified as splice products of a single gene [reviewed, Butt, E., *et. al.* 1993]. PKG-I exists as a homodimer, whereas PKG-II exists as a monomer. The dimerisation domain of PKG-I is in the N-terminal region, a region that also contains binding sites for cGMP and autophosphorylation sites (Ser-50, Ser 72, Thr-58, Thr-84 in PKG-Iα), the function of which is to increase the rate of cGMP dissociation from the high

affinity cGMP binding site, thus down-regulating activity following stimulation [Hofmann, F., *et. al.* 1985].

Not only do the PKG isoforms differ in their monomeric or dimeric composition but they also have a very specific tissue distribution. The highest concentration of PKG-I are in cerebella Purkinje cells, smooth muscle cells and platelets, whereas PKG-II is predominantly located in the epithelial brush border of the small intestine [deJonge, HR., 1981, reviewed Butt, E., *et. al.* 1993].

1.3. CYCLIC NUCLEOTIDE PHOSPHODIESTERASES

1.3.1. General background

Cyclic nucleotide phosphodiesterases (PDEs) provide the sole means of removing cAMP and cGMP from cells by hydrolysing the 3'-phosphate diester bond to give the corresponding 5'-nucleoside monophosphate. This terminates PKA activation as cAMP can no longer bind to and activate PKA. A number of highly distinct PDEs exist within the cell. These are currently categorised into eight families by virtue of their substrate specificity, regarding cAMP and cGMP, their sensitivity to inhibitors and their sequence homology (Table 1.1.). PDE1 isoforms hydrolyse both cAMP and cGMP is stimulated by Ca^{2+} / calmodulin, for which is there is a distinct recognition site [Wu, Z., *et. al.* 1992]. PDE2 isoforms hydrolyse both cAMP and cAMP but their activity is stimulated by micromolar concentrations of cGMP, due to binding of cGMP to a distinct regulatory site [Stroop, SD. and Beavo, JA. 1992, Mercy, P-F., et. al. 1995, Pyne, NJ., et. al. 1986]. PDE3s also hydrolyse both cAMP and cGMP, but here the activity is

Table 1.1. Summary of PDE families and their properties

Family Name	Number of Genes	K_m cAMP	K_m cGMP	Inhibitors (K_i)	References
PDE1	3	21-35μM	1.2-5μM	nicardipine (1-3μM) IMBX (6-7μM)	Wu, Z., *et. al.* 1992
PDE2	1	36μM (-cGMP) 20μM (+cGMP)	11μM	EHNA (1-5μM) IBMX (20μM +cGMP) (40μM -cGMP)	Stroop, SD. and Beavo, JA. 1992. Mercy, P-F., *et. al.* 1995. Pyne, NJ., *et. al.* 1986.
PDE3	2	0.1-0.8μM	0.1-0.8μM	cilostamide (0.05μM) milrinone (0.5μM) IBMX (2μM) cGMP (0.1μM)	Manganiello, VC., *et. al.* 1995
PDE4	4	1-5μM	310μM	Rolipram (1-2μM) RO2074 (9μM) IBMX (15μM)	Bolger, G. 1994. Lobban, M., *et. al.* 1994 Table 1.3.
PDE5	2	500μM	4-5μM	Zaprinast (0.3μM) dipyridamole (0.8μM) IBMX (8μM)	Francis, SH., *et. al.* 1990
PDE6	3	2mM	60μM	IBMX	Yamazaki, A., 1992. Pfister, C., *et. al.* 1993.
PDE7	1	0.2μM		None	Michaeli, T., *et. al.* 1993.
PDE8	0	0.1μM	1.8μM	zaprinast (23μM) IBMX (26μM)	Mukai, J., *et. al.* 1994.

inhibited by micromolar concentrations of cGMP [Manganiello, VC., *et. al.* 1995]. PDE4s are cAMP specific and insensitive to cGMP or Ca^{2-} / calmodulin. They are, however, specifically inhibited by the drug rolipram [Bolger, G. 1994]. PDE5 and PDE6 both specifically hydrolyse cGMP but differ in structure and tissue distribution, PDE6 is found only in photoreceptor cells [Yamazaki, A., 1992, Pfister, C., *et. al.* 1993, Michaeli, T., *et. al.* 1993]. PDE7 specifically hydrolyses cAMP but is insensitive to all known PDE inhibitors, including the general PDE inhibitor isobutylmethylxanthine (IBMX) [Michaeli, T., *et. al.* 1993]. PDE8 is a recently discovered PDE that does not fit with any of the above groups in that it is insensitive to Ca^{2-}/calmodulin and cGMP but will hydrolyse both cAMP and cGMP and is insensitive to specific inhibitors of PDE1, PDE2, PDE3, PDE4 and PDE5. Although a species suggested as PDE8 has been suggested, no cDNA has yet been identified [Mukai, J., *et. al.* 1994].

A further level of complexity exists for the majority of the PDE families. This is determined by, in most cases, multiple genes in each family apart from PDE2, PDE7 and PDE8 and multiple splice variants of the genes in all cases but PDE7 and PDE8. These variants show differences in tissue and subcellular distribution, susceptibility to phosphorylation and sensitivity to inhibitors. Each of these factors will be discussed in sections 1.3.2., 1.3.3. ,1.3.4., 1.3.5., 1.3.6., 1.3.7., 1.3.8. and 1.3.9.

1.3.1.1. Homology

Mammalian PDEs all possess a common structural pattern. They all contain a conserved domain of about 270 amino acids which displays ~25-40% homology between PDE families and at least 70% within a PDE family. This domain is usually found in the C-terminal portion of the enzyme, the extreme C-terminal and the N-terminal regions are often extremely divergent [Charbonneau, H. 1990]. This conserved region represents the catalytic domain of PDEs [Stroop, S. and Beavo, JA. 1992, Stroop, SD, *et. al.* 1989].

1.3.1.2. Nomenclature

Due to the large and complex gene structure of PDEs and the continuing discovery of new genes and slice variants, nomenclature became rather confused. Consequently a standard system has been devised and is outlined in figure 1.3.1.

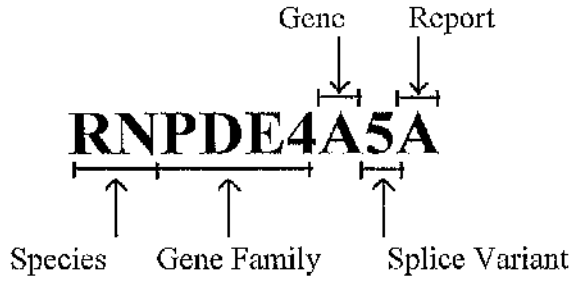

Figure 1.3.1. PDE Nomenclature

Example shows a type 4 PDE from rat. It denotes gene A of the PDE4 family and splice variant 5 of that gene.

1.3.2. PDE1 Calcium/calmodulin stimulated PDE

Initial studies with PDE from rat brain showed that the PDE activity could be activated by a protein factor and calcium [Appleman, MM., *et. al.* 1985], this protein factor later being named calmodulin [Cheung, WY., 1967, 1970, 1971, Kakiuchi, S. and Yamazaki, R., 1970, Kakiuchi, S., *et. al.* 1970, Teo, TS., *et. al.* 1973]. It is evident today that CaM-PDEs exist as distinct isoenzymes, encoded by three different genes, PDE1A (~61kDa subunit), PDE1B (~63kDa subunit) and PDE1C (~75kDa subunit).

Initial experiments that were performed on brain CaM-PDEs showed that two species could be found, these being 60kDa and 63kDa [Sharma, RK., *et. al.* 1980], which were then established to be subunits of different isoenzymes by a series of experiments [Wang, JH., *et. al.* 1980]. The PDE1C gene was identified in brain and testes [Shenolikar, S., *et. al.* 1985, Rossi, P., *et. al.* 1988]. Each of the PDE1 genes have been shown to be alternatively spliced. For example, PDE1A has two splice variants, PDE1A1 (~59kDa) found in the heart and PDE1A2 (~61kDa) found in the brain. These two genes are identical in sequence apart from their extreme N-termini which contain unique sequences [Taira, M., *et. al.* 1993, Beltman, J., *et. al.* 1993]. Additionally, structurally related PDE1B splice variants have been identified by RNase protection assays in brain, kidney and adrenal medulla [Bentley, JK., *et. al.* 1992, Repaske, DR., *et. al.* 1992, Sonnenberg, WK., *et. al.* 1993].

PDE1s are found in virtually all other mammalian tissues at relatively low levels, with the exception of human peripheral blood lymphocytes and monocytes

[Thompson, WJ, *et. al.* 1980]. Levels can be so low that a few tissues were originally determined not to contain PDE1s, mainly due to high levels of other PDE activities. However, with the development of better separation techniques such as anion exchange chromatography, the PDE1 activity was identified in these tissues, e.g. sperm [Wasco, WM. and Orr, GA., 1984]. Mammalian brain is the richest source of CaM-PDEs, where it is enriched in certain regions, particularly the large pyramidal cells of the cerebral cortex, the pyramidal cells of the hippocampus and olfactory nucleus and Purkinje cells of the cerebellum [Kincaid, RL., *et. al.* 1987]. Mammalian heart is the tissue where CaM-PDEs are next most abundant, although ten fold less than brain [La Porte, DC., *et. al.* 1979]. Most of the CaM-PDE isoforms are cytosolic, although a fraction of brain enzyme is found to membrane associated and indeed, PDE1C in rat sperm displays 100% membrane association [Wasco, WM. and Orr, GA., 1984, Chaudhry, PS. and Cassilas, ER. 1988].

The N-terminal region of isoforms from all three PDE1 genes contain a domain that is predicted to form a basic amphipathic helix which is homologous to the Ca^{2+}/CaM binding domain of other proteins [Novac, JP., *et. al.* 1991]. Although species from all three genes are activated by Ca^{2+}/CaM, their affinities for Ca^{2+}/CaM varies. For example the affinities of the 61kDa PDE1A and the 63kDa PDE1B form are almost identical but the 59kDa PDE1A form, which differs from the 61kDa PDE1A form only in the N-terminal region, has a much higher affinity [Charbonneau, H., *et. al.* 1991]. The activation of PDE1s over basal level by Ca^{2+}/CaM is of the order of 6-20 fold. However, large variations in these

figures have been published. This may have been due to impure preparations of the PDEs, but is more likely to have been as a result of proteolysis, to which PDE1s are extremely sensitive. Proteolysis often results in a CaM independent activated form [Ho, HC., *et. al.* 1976].

Further regulation of PDE1s comes from protein phosphorylation, various isoforms are phosphorylated by PKA [Sharma, RK, and Wang, JH. 1985] and others by Ca^{2+}/CaM dependent protein kinase-II [Sharma, RK, and Wang, JH. 1986, Zhang, GY., *et. al.* 1990, Hashimoto, Y., *et. al.* 1989]. The effect of the phosphorylation by both enzymes is to decrease the affinity of the enzyme for Ca^{2+}/CaM, thus down regulating its activity. Phosphorylation by PKA can be blocked by Ca^{2+}/CaM [Sharma, RK, and Wang, JH. 1985]. Both phosphorylations can be removed by the action of Ca^{2+}/CaM-stimulated phosphatase [Zhang, GY., *et. al.* 1990], consequently both the phosphorylation and dephosphorylation reactions are controlled by second messengers.

1.3.3. cGMP stimulated PDEs (PDE2)

PDE2s, or cGMP-stimulated PDEs (cGS-PDEs) were initially described in experiments done on rat liver supernatant [Beavo, JA., *et. al.* 1970] and in the crude particulate fractions from several tissues, particularly brain [Beavo, JA., *et. al.* 1971]. The purified bovine cardiac PDE2 has been shown to exist as a homodimer with subunits of ~105kDa and has been completely sequenced [Trong, HL., *et. al.* 1990]. Only one gene has been identified for PDE2 and yet, both particulate and soluble forms are found [Pyne, NJ. *et. al.* 1986]. However, peptide

maps generated from purified bovine brain and liver cytosolic PDE2s [Pyne, NJ. *et. al.* 1986, Tanaka, T., *et. al.* 1991, Murashima, S., *et. al.* 1990], RNase protection assays [Sonnenberg, WK., *et. al.* 1991] and sequence analysis of rat brain PDE2 [Epstein, P., *et. al.* 1994] are consistent with generation of brain and cardiac membrane associated PDE2 isoforms by alternative splicing.

PDE2s hydrolyse both cAMP and cGMP with positively co-operative kinetics, thus at saturating levels of cyclic nucleotides, the hydrolysis of one can be stimulated by the other [Moss, J., *et. al.* 1977]. After treatment with chymotrypsin, a PDE2 fragment of ~36kDa, which did not exhibit positively co-operative kinetics with respect to cAMP, was separated from a 60kDa N-terminal cGMP-binding fragment [Stroop, SD, *et. al.* 1989, Stroop, S. and Beavo, JA. 1991, Stroop, S. and Beavo, JA. 1992]. These studies were performed by photolabelling with high specific activity [^{32}P]cGMP and ultraviolet irradiation, demonstrating that the intact enzyme was labelled in a biphasic manner, with labelling affinities of about 1μM and 30μM. However, the two unique photolabelled sites could be separated by the proteolysis with chymotrypsin [Stroop, SD, *et. al.* 1989]. Binding to the 36kDa fragment could be abolished by pre-treatment with cAMP prior to photolabelling and since PDE2s hydrolyse cAMP as well as they do cGMP, this was thought to be the catalytic C-terminal region, which was later confirmed by sequencing. This demonstrated the existence of two functional domains, one C-terminal and catalytic and the other N-terminal and regulatory. The N-terminal region possesses a sequence of about 400 amino acids which contains a tandem repeat homologous to one found in the retinal rod

PDE5 and represents a putative cGMP binding domain [Stroop, S. and Beavo, JA., 1992]. A region between the catalytic domain and the non-catalytic cGMP-binding site has been identified as a bridge or hinge region [Stroop, SD, *et. al.* 1989] and it has been identified as a dynamic intermediate in the activation of PDE2 by cGMP, the allosteric changes being transmitted to the catalytic region via the this bridge.

1.3.4. cGMP-inhibited PDEs (PDE3)

Properties and characteristics of PDE3s have been studied with highly purified as well as partially purified preparations from a number of sources. The catalytic properties and inhibitor sensitivities of the highly purified preparations of PDE3s are very similar. Essentially they are considered to be cAMP specific, since, although the K_m values for cAMP and cGMP are similar, in the 0.1-0.8μM range, the V_{max} for cAMP being 10-20 fold higher than for cGMP [Degerman, E., *et. al.* 1995, Rascon, A., *et. al.* 1992, Pyne, N., *et. al.* 1987, and reviewed Manganiello, VC. *et. al.* 1995]. Thus cGMP is hydrolysed only at a very low rate. Another characteristic that defines PDE3s is their sensitivity to inhibition by certain drugs that augment myocardial contractility, inhibit platelet aggregation and relax smooth muscle. Examples of such drugs are cilostamide, milrinone and OPC3911, with IC_{50} values of <0.1μM, 0.5μM and 0.1μM respectively [reviewed Manganiello, VC. *et. al.* 1995].

cDNAs encoding two subfamilies of PDE3s have been identified (PDE3A and PDE3B) and cloned from rat and human adipose and cardiac sources, with

multiple species of RPDE3B being cloned [Taira, M., *et. al.* 1993]. The domain structure of these PDEs is similar to that of all other PDEs, with homologous C-terminal regions, containing the putative catalytic domain and N-terminal regulatory domains that contain hydrophobic, putative membrane association domains [Taira, M., *et. al.* 1993]. Within the putative catalytic region is an insertion of 44 amino acids that is not found in any of the other PDE families. This insertion differs in sequence between PDE3A and PDE3B [Meacci, E., *et. al.* 1992, Taira, M., *et. al.* 1993]. This region has been termed the PDE3 insertion.

Incubation of intact adipocytes, hepatocytes or platelets with agents that activate adenylyl cyclase and elevate cAMP leads to the activation of PDE3 [Manganiello, VC., *et. al.* 1995a, Beltman, J., *et. al.* 1993]. This activation is thought to be important in feedback regulation of cAMP levels and PKA activation state. Several studies indicate that activation is as a consequence of PKA phosphorylation of PDE3 [Kilgour, E., *et. al.* 1989, Degerman, E., *et. al.* 1990, Smith, CJ., *et. al.* 1991]. It has been proposed that at least two phosphorylation sites exist in rat liver dense-vesicle PDE3, one which effects activity and the other that does not affect activity but prevents the activating phosphorylation from occurring [Kilgour, E., *et. al.* 1989]. In frog ventricle, however, a PDE3, that is membrane associated, is inhibited by glucagon via a pertussis toxin-sensitive G-protein [Brechler, V., *et. al.* 1992], clearly indicating defined functions for different PDE3 species

Incubation* of rat adipocytes results in rapid phosphorylation and activation of PDE3B. The result of which is a reduction in cAMP, PKA activity, hormone-

*with insulin

stimulated lipase activity and lipolysis [Degerman, E., *et. al.* 1995,]. The insulin sensitive kinase responsible has been partially purified and its action has been shown to be blocked by wortmannin, suggesting that insulin activation of phosphotidylinositol-3-kinase (PI3-K) is an important upstream event in the activation of the adipocyte PDE3B [Rahn, T., *et. al.* 1994]. The role of phosphorylation has been confirmed by incubating adipocytes with okadaic acid, a protein phosphatase inhibitor, resulting in activation of the kinase [Shibita, H., *et. al.* 1991

1.3.5. cAMP-specific phosphodiesterases (PDE4)

1.3.5.1. Introduction

The cAMP specific PDE4 family are a diverse family of proteins that are important regulators of intracellular signalling and have been shown exhibit an extremely complex gene structure [Bolger, G. 1994]. They are encoded by four genes, PDE4A, PDE4B, PDE4C and PDE4D, each of which displays alternative splicing to generate multiple proteins from each gene [Bolger, G. 1994]. The family is distinguished by its high and specific affinity for cAMP and its sensitivity to specific inhibitors that include the antidepressant drug rolipram [Beavo, JA., *et. al.* 1994, Conti, M., *et. al.* 1991, Beavo, JA. and Reifsnyder, DH. 1990, Thompson, WJ. 1991]. PDE4s are the closest mammalian homologues to the *dunce* gene of *Drosophila melanogaster*, which was isolated as a mutation effecting learning and memory [Qiu, Y. *et. al.* 1991, Qiu, Y. and Davis, R. 1993]. Each of the genes encode putative catalytic regions that have a high degree of

homology and are identical within the splice variants any particular gene [Bolger, G. 1994]. The N-terminal regions, however, are extremely divergent, even amongst closely related splice variants, although, two conserved regions are found within the N-terminal regions and have been termed UCR-1 and UCR-2 [Bolger, G., *et. al.* 1993]. These may have a regulatory role and will be discussed later.

A variety of approaches have been used to clone members of the PDE4 family. The first approach was to use the cDNA of the *Drosophila melanogaster dunce* gene to screen mammalian cDNA libraries [Davis, RL., *et. al.* 1989, Henkel-Tiggs, J. and Davis, RL. 1990]. A second approach was to isolate cDNAs that could suppress the heat shock-sensitive phenotype of *Saccharomyces cerevisiae* with mutations in the RAS-cAMP pathway. Activating mutations of this pathway produce their phenotype by elevating cAMP levels and the introduction of a PDE into these cells can lower the cAMP levels sufficiently to restore heat shock resistance. PDEs from rat and humans have been isolated by this approach [Colicelli, J., *et. al.* 1989, Colicelli, J., *et. al.* 1991, Michaeli, T., *et. al.* 1993]. PCR has also been employed, with oligonucleotide primers designed to amplify DNA sequences with homology to both *dunce* and previously isolated PDE4s [Bolger, G., *et. al.* 1994a]. A number of rat and human genes have been isolated and each shows a one to one homology, in that each rat gene is more closely related to its human counterpart than to any of the other rat genes PDE4s [Bolger, G., *et. al.* 1994a].

Comparison of the amino acid sequences of *Drosophila dunce* and human PDE4s demonstrates regions of strong conservation of within their coding regions.

Three regions of homology are seen, one of these is the putative catalytic region [Jin, SLC., *et. al.* 1992] which is 90% homologous in all PDE4 genes, and the other two are UCR-1 and UCR-2. UCR-1 and UCR-2 appear to be distinct features of the PDE4 family, as these regions are strongly conserved between organisms as evolutionary diverse as *Drosophila melanogaster* and humans [Figure 1.3.2.] but have no close homologues in any other sequence in the GenBank or EMBL databases [Bolger, G., *et. al.* 1993]. UCR-1 and UCR-2 are distinct in that they are separated by a region of low homology and given the strong evolutionary conservation, they may encode distinct structural domains that have an essential function [Bolger, G., *et. al.* 1993, Bolger, G., 1994]. Indeed, parallels may be drawn to the regulatory domains of other PDE families, such as the cGMP binding domain of PDE1s and the Ca^{2+}/calmodulin binding domain of PDE2s which are also N-terminal and strongly conserved between each PDE of the family.

1.3.5.2. PDE4A

The gene for PDE4A is localised on chromosome 19, the same chromosome but a different locus to PDE4C and on a different chromosome to the PDE4B and PDE4D genes [Milatovich, A., *et. al.* 1994, Horton, Y., *et. al.* 1995]. The structure of the gene is extremely complex, containing in excess of 14 exons and is found between the genes for TYK2 and the LDL receptor [Olsen, A., Sullivan, M. and Houslay, MD. unpublished data]. In rat, it is now known that the PDE4A gene encodes three splice variants, the shortest of which is RD1

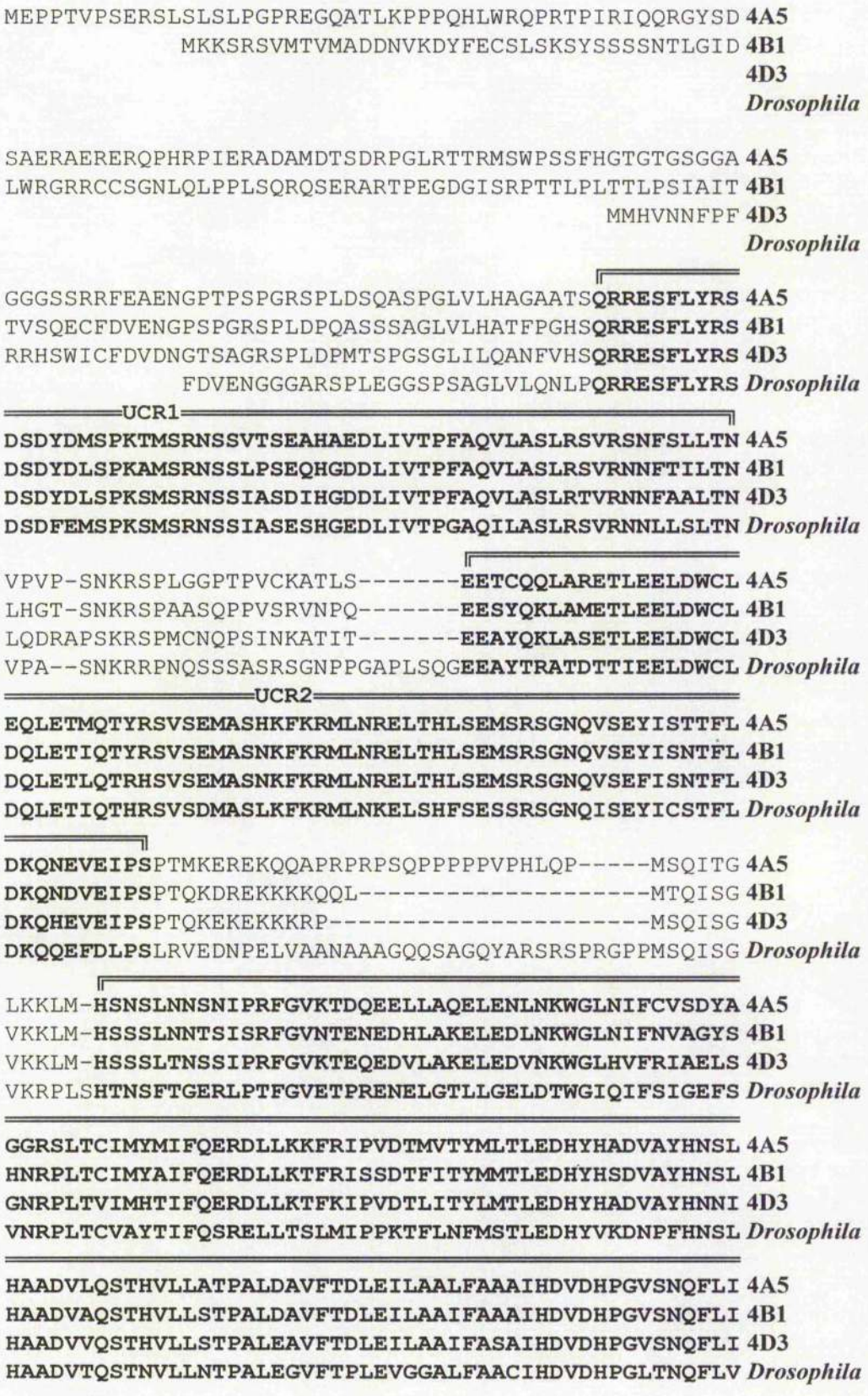
MEPPTVPSERSLSLSLPGPREGQATLKPPPQHLWRQPRTPIRIQQRGYSD 4A5
MKKSRSVMTVMADDNVKDYFECSLSKSYSSSSNTLGID 4B1
4D3
Drosophila
SAERAERERQPHRPIERADAMDTSDRPGLRTTRMSWPSSFHGTGTGSGGA 4A5
LWRGRRCCSGNLQLPPLSQRQSERARTPEGDGISRPTTLPLTTLPSIAIT 4B1
MMHVNNFPF 4D3
Drosophila
GGGSSRRFEAENGPTPSPGRSPLDSQASPGLVLHAGAATSQRRESFLYRS 4A5
TVSQECFDVENGPSPGRSPLDPQASSSAGLVLHATFPGHSQRRESFLYRS 4B1
RRHSWICFDVDNGTSAGRSPLDPMTSPGSGLILQANFVHSQRRESFLYRS 4D3
FDVENGGGARSPLEGGSPSAGLVLQNLPQRRESFLYRS Drosophila
UCR1
DSDYDMSPKTMSRNSSVTSEAHAEDLIVTPFAQVLASLRSVRSNFSLLTN 4A5
DSDYDLSPKAMSRNSSLPSEQHGDDLIVTPFAQVLASLRSVRNNFTILTN 4B1
DSDYDLSPKSMSRNSSIASDIHGDDLIVTPFAQVLASLRTVRNNFAALTN 4D3
DSDFEMSPKSMSRNSSIASESHGEDLIVTPGAQILASLRSVRNNLLSLTN Drosophila
VPVP-SNKRSPLGGPTPVCKATLS-------EETCQQLARETLEELDWCL 4A5
LHGT-SNKRSPAASQPPVSRVNPQ-------EESYQKLAMETLEELDWCL 4B1
LQDRAPSKRSPMCNQPSINKATIT-------EEAYQKLASETLEELDWCL 4D3
VPA--SNKRRPNQSSSASRSGNPPGAPLSQGEEAYTRATDTTIEELDWCL Drosophila
UCR2
EQLETMQTYRSVSEMASHKFKRMLNRELTHLSEMSRSGNQVSEYISTTFL 4A5
DQLETIQTYRSVSEMASNKFKRMLNRELTHLSEMSRSGNQVSEYISNTFL 4B1
DQLETLQTRHSVSEMASNKFKRMLNRELTHLSEMSRSGNQVSEFISNTFL 4D3
DQLETIQTHRSVSDMASLKFKRMLNKELSHFSESSRSGNQISEYICSTFL Drosophila
DKQNEVEIPSPTMKEREKQQAPRPRPSQPPPPPVPHLQP-----MSQITG 4A5
DKQNDVEIPSPTQKDREKKKKQQL----------MTQISG 4B1
DKQHEVEIPSPTQKEKEKKKRP----------MSQISG 4D3
DKQQEFDLPSLRVEDNPELVAANAAAGQQSAGQYARSRSPRGPPMSQISG Drosophila
LKKLM-HSNSLNNSNIPRFGVKTDQEELLAQELENLNKWGLNIFCVSDYA 4A5
VKKLM-HSSSLNNTSISRFGVNTENEDHLAKELEDLNKWGLNIFNVAGYS 4B1
VKKLM-HSSSLTNSSIPRFGVKTEQEDVLAKELEDVNKWGLHVFRIAELS 4D3
VKRPLSHTNSFTGERLPTFGVETPRENELGTLLGELDTWGIQIFSIGEFS Drosophila
GGRSLTCIMYMIFQERDLLKKFRIPVDTMVTYMLTLEDHYHADVAYHNSL 4A5
HNRPLTCIMYAIFQERDLLKTFRISSDTFITYMMTLEDHYHSDVAYHNSL 4B1
GNRPLTVIMHTIFQERDLLKTFKIPVDTLITYLMTLEDHYHADVAYHNNI 4D3
VNRPLTCVAYTIFQSRELLTSLMIPPKTFLNFMSTLEDHYVKDNPFHNSL Drosophila
HAADVLQSTHVLLATPALDAVFTDLEILAALFAAAIHDVDHPGVSNQFLI 4A5
HAADVAQSTHVLLSTPALDAVFTDLEILAAIFAAAIHDVDHPGVSNQFLI 4B1
HAADVVQSTHVLLSTPALEAVFTDLEILAAIFASAIHDVDHPGVSNQFLI 4D3
HAADVTQSTNVLLNTPALEGVFTPLEVGGALFAACIHDVDHPGLTNQFLV Drosophila

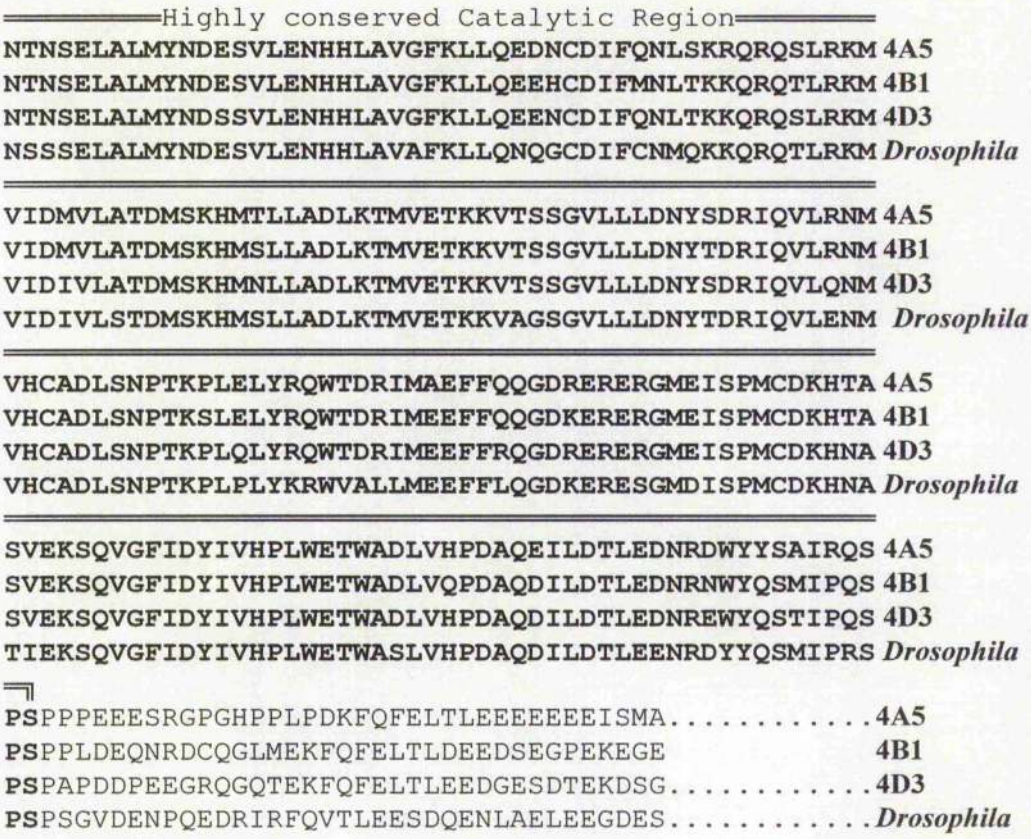

Figure 1.3.2. Homology between PDE4 genes.

Shows the sequence homology between four distinct PDE4 forms, the human PDE4A species, PDE46 (HSPDE**4A5**), the human PDE4B species, PDE4**B1**, the human PDE4D species, PDE43 (HSPDE**4D3**), and the *Drosophila melanogaster* dunce gene, *dnc*. The C-termini of these sequences have been truncated here and exons one and two of *dnc* are not shown. The upstream conserved regions, UCR1 and UCR2 are indicated and are in bold text, also in bold is a homologous region, C-terminal to the UCR regions which contains the putitive catalytic region. PDE4C is not shown due to concerns about clones that are 5' truncated (section 1.3.5.4.)

(RNPDE4A1A) which lacks the UCR-1 region and the N-terminal portion of UCR-2 [Davis, RL., *et. al.* 1989]. Whether this has significance to the function of RD1 remains to be seen. The longer species are rpde6 (RNPDE4A5) [Bolger, G., *et. al.* 1994a, McPhee, I., *et. al.* 1995] and rPDE39 (RNPDE4A8) [Bolger, G., *et. al.* 1996]. A schematic diagram of their structure is given in Figure 1.3.3. Initially RD2 (RNPDE4A2) and RD3 (RNPDE4A3) [Davis, RL., *et. al.* 1989] were suggested as splice variants, but these are now considered to be attributable to cloning artefacts or errors in sequencing [Bolger, G., *et. al.* 1993, Bolger, G., *et. al.* 1994a].

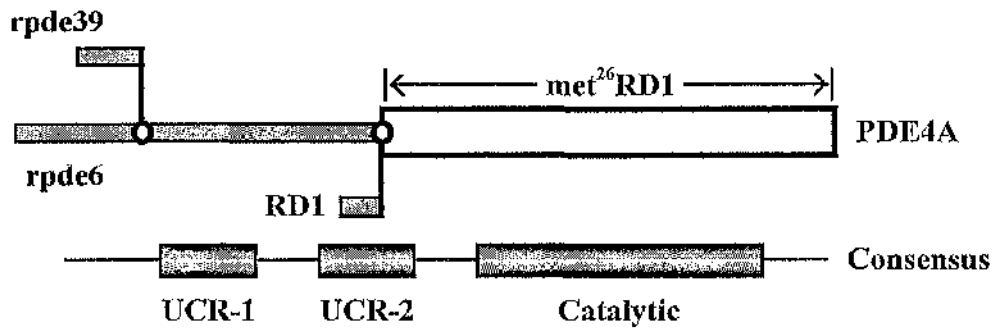

Figure 1.3.3. Splice variant diagram for rat PDE4A.

Shows splice variants of the PDE4A gene from rat, rpde6, rpde39 and RD1. met^{26}RD1 is an engineered truncation that lacks any N-terminal splice regions The empty rectangle represents the core C-terminal catalytic region that is identical in each of the PDEs. The shaded areas represent alternatively spliced regions and the empty circles splice junctions.

In humans, three PDE4A splice variants have been isolated to date. Only one of these hPDE46 (HSPDE4A5), the human homologue of rpde6, is a catalytically active species [Bolger, G., *et. al.* 1993, Bolger, G., *et. al.* 1996]. Two other clones have been identified which possess both unique N- and C-terminal regions. The unique C-terminal regions, however, leads to the foreshortening of the putative catalytic region, producing proteins which fail to exhibit any catalytic activity [Horton, Y., *et. al.* 1995, Bolger, G., *et. al.* 1993]. The function of these inactive species has yet to be determined. To date, no human homologues of RD1 or rPDE39 have been identified.

The expression patterns of the rat PDE4A splice variants appear to be profoundly different. RD1 is found exclusively in the brain [Bolger, G. 1994, Davis, RL., *et. al.* 1989, Bolger, G., 1994a, Shakur, Y., *et. al.* 1995], rPDE39 is found in testes [Bolger, G., *et. al.* 1996] and hepatocytes [Zeng, L. and Houslay, MD., unpublished data] and rpde6 is expressed in a number of different tissues, although the highest levels of expression are in the brain [Bolger, G. 1994a]. Although both RD1 and rpde6 are expressed in brain, their distribution throughout regions of the brain is profoundly different (table 1.2.). It can be seen that while RD1 is distributed through all regions of the brain, rpde6 is not expressed in either the brain stem or cerebellum. This differential expression pattern presumably reflects cell specific differences in alternative splicing and perhaps the presence of distinct promoters.

On a subcellular level, RD1 is found associated exclusively with membranes, particularly the plasma membrane, golgi apparatus and intracellular

vesicles [Shakur, Y., *et. al.* 1995]. rpde6 is found distributed between the cytosol (74%), membrane (13%) and low speed pellet (13%) [McPhee, I., *et. al.* 1995]. rPDE39, like rpde6, is found distributed between the membrane (15%) and cytosol (85%) but unlike rpde6, is not found associated with the low speed pellet [Bolger, G., *et. al.* 1996]. If however, the artificially truncated PDE4A, met^{26}RD1 (figure 1.3.2), which lacks any splice regions and is catalytically active, is expressed in COS cells it is rendered entirely cytosolic [Shakur, Y., *et. al.* 1993]. This would imply that the subcellular distribution of the rat PDE4As is determined by their N-terminal splice region since, in each case, their C-termini are identical.

Table 1.2. Distribution of rpde6 and RD1 in brain regions

Relative distribution (percentage PDE4 activity ± SD) of these two splice variants was determined by immunoblotting [McPhee, I., *et. al.* 1995].

Region	rpde6 Cytosol	rpde6 Membrane	RD1 Membrane
Brain Stem	0	0	4±2
Cerebellum	0	0	10±1
Cortex	35±5	27±4	25±3
Hippocampus	10±3	14±3	17±2
Hypothalamus	20±3	25±4	8±1
Mid-Brain	5±2	6±2	16±2
Pituitary	0	0	0
Striatum	30±4	28±4	20±3

Evidence to support this theory has come from studying the membrane association of RD1 which was shown to be determined by a sequence of amino acids within the N-terminal splice region [Scotland, G. and Houslay, MD., 1995]. Analysis of the N-terminal structure was done by ^{1}H-NMR and four structural components were identified; an N-terminal amphipathic helical domain, followed by a highly mobile hinge region, then a distorted helical region made up of seven residues, three of which are tryptophans that form a well ordered hydrophobic domain and finally a further helical region [Smith, KJ., *et. al.* 1996]. Given this structure it is unlikely that it could insert into membranes, nor could it form an integral transmembrane protein since met^{26}RD1 is only 26 amino acids shorter and is entirely cytosolic. It is more likely, therefore, that it associates with a membrane bound anchoring protein

To investigate which regions of the N-terminal 23 amino acids of RD1 confer membrane association, an in-frame chimera of these was made by fusing it to the N-terminus of a bacterial enzyme, chloramphenicol acetyl transferase (CAT). When CAT alone was expressed in COS cells, it was entirely cytosolic. Expression of the fusion protein, however, was entirely membrane-associated [Scotland, G. and Houslay, MD., 1995]. Deletion analysis of the structural domains of the N-terminus was also done using these CAT-chimeras and it was shown that the membrane association was determined by the distinct tryptophan-rich domain that forms a compact distorted helical structure [Smith, KJ., *et. al.* 1996]. Given the structure of this domain, hydrophobic interaction might explain why RD1 could not be washed off membranes by using high salt but could be

solubilised with very low concentrations of the detergent Triton X-100 [McPhee, I., *et. al.* 1995].

No homology between the N-terminal regions of rpde6 and rPDE39 to RD1 is apparent. The membrane association of these proteins would therefore seem likely to be conferred by a different mechanism, the nature of which remains to be investigated.

Another function of the N-terminal regions is their control of catalytic activity. met^{26}RD1 encodes a highly active cytosolic PDE when expressed in COS cells [Shakur, Y., *et. al.* 1995]. However, determination of the activities of the other splice variants, relative to met^{26}RD1 gave values* of 0.5, 0.15 and 0.15 for RD1, rpde6 and rPDE39 respectively [McPhee, I., *et. al.* 1995, Bolger, G., *et. al.* 1996, Shakur, Y., *et. al.* 1995]. The splice regions therefore attenuate the PDE activity, the mechanism of which is not known.

Clearly the PDE4A N-terminal splice regions regulate subcellular localisation, catalytic activity and are expressed in a tissue specific manner. Exactly what elements within the N-terminal region of rpde6 and rPDE39 define the localisation remain to be determined as does the physiological function of localising PDEs to distinct subcellular regions.

1.3.5.3. PDE4B

As with the PDE4A gene, a number of splice variants of the PDE4B gene have been identified, although it is still not clear how many of these represent endogenously expressed species. At the time this thesis commenced, the most

* Values are V_{max} relative to the V_{max} for met^{26}RD1.

likely candidates for full length clones were DPD (RNPDE4B1) [Colicelli, J., *et. al.* 1989] and rPDE4 (RNPDE4B2A) [Swinnen, JV., *et. al.* 1991]. A human equivalent of rPDE4, HSPDE4B2A, has been cloned [McLaughlin, MM., *et. al.* 1993] However, the discovery of a human homologue of DPD, TM72 (HSPDE4B1) which is extended at the N-terminus has supported the hypothesis that both PDE4B1 clones are not full length [Bolger, G., *et. al.* 1993]. Absolute identity of sequence is seen between rPDE4 and the current DPD clone, except for an N-terminal extension of 48 amino acids in rPDE4 [Monaco, L., *et. al.* 1994]. More recently, a further human clone has been identified, PDE4B3 [Owens, R. and Houslay, MD. personal communication], which is identical to DPD along DPD's entire length. However, like PDE4B2, PDE4B3 has an N-terminal extension. This data would indicate that the point at which DPD was proposed to start represents a splice junction, onto which unique N-terminal domains are added, as seen in each of the human clones.

The distribution of rPDE4 and DPD has been well characterised in rat brain [Lobban, M., *et. al.* 1994]. It should be noted that at the time of this work, DPD was considered full length. The species characterised by Lobban [Lobban, M., *et. al.* 1994] might now be considered either to be a proteolytic degradation product, possibly truncated rPDE4, or an as yet unidentified splice variant. DPD and rPDE4 display very different subcellular localisations, DPD being entirely cytosolic and rPDE4 entirely membrane associated, indicating that the N-terminal region of rPDE4 is responsible for the membrane attachment [Lobban, M., *et. al.* 1994]. Distribution of the two isoforms throughout various brain regions does

however reveal differences in their expression [Lobban, M., *et. al.* 1994]. The pituitary contained no immunoreactive material for either DPD or rPDE4, the cerebellum, brain stem and mid brain contained no DPD but expressed rPDE4 whereas the striatum, hypothalamus, hippocampus and cortex expressed both species. This does not however rule out the possibility that DPD represents proteolysed rPDE4 since the preparations from cerebellum, brain stem and mid brain may simply have been less proteolysed. It is intriguing that DPD was found to contribute 13-35% of the total PDE4 activity in brain cytosol and rPDE4, 40-50% of the PDE4 activity in the membranes in all brain regions apart from the mid-brain where it only represented 20% [Lobban, M., *et. al.* 1994]. This means that PDE4Bs, regardless of the species, must play a significant role in cAMP metabolism in the brain.

The rat PDE4B mRNAs expressed in the Sertoli cell are derived from the assembly of 11 exons, exons 5-10 encoding the catalytic region [Monaco, L., *et. al.* 1994]. This leaves the remaining six exons to code for 'regulatory' regions that have the potential for alternative splicing. Furthermore, Monaco and colleagues [Monaco, L., *et. al.* 1994] report that rPDE4 mRNA is likely to be expressed in brain containing additional 5'-exons, since the 5'-untranslated sequence has nine AUG codons in three reading frames. However, each of these is followed by stop codons, determining the presence of short open reading frames which have been hypothesised to reduce the translatability of the mRNA, slowing the translation rate [Kozac, M. 1991].

Clearly the debate is still open as to the exact nature of PDE4Bs and longer, alternatively spliced species may still be found.

1.3.5.4. PDE4C

In contrast to the other PDE4 genes, little is known about the PDE4C gene. Until very recently no full length clones had been identified for PDE4C, although two partial coding sequences were identified in the rat, rPDE1 (RNPDE4C1A) [Swinnen, JV., *et. al.* 1989] and rPDE36 (RNPDE4C1B) [Bolger, G., *et. al.* 1994a] and one partial human clone, DPDE1 (HSPDE4C1), [Bolger, G., *et. al.* 1993]. Recently a full length human clone has been reported [Engels, P. *et. al.* 1995], which, unlike the other PDE4 genes, is not expressed at all in the immune system [Engels, P. *et. al.* 1995] and in stark contrast to the rat, is detected in the brain. Rat PDE4C is detected only to extremely low levels in the brain, perhaps indicating a species specific expression pattern.

1.3.5.5. PDE4D

The PDE4D gene is perhaps the best characterised, with the greatest number of splice variants identified of any of the other PDE4 genes, with five human variants identified. Each of these splice variants possess identical C-terminal catalytic regions and have uniquely spliced N-terminal domains [Nemoz, G., *et. al.* 1995, Bolger, G., *et. al.* 1996a] (Figure 1.3.4.). The structure can be seen to be remarkably similar to the PDE4 gene, as with the case of RD1 (RNPDE4A1), there are two PDE4D splice variants, PDE4D1 and PDE4D2, which have the UCR-1 region spliced out [Bolger, G., *et. al.* 1993], the functional

significance of which is not known. The only difference between these two genes is an insertion of 79 amino acids in the N-terminal region of PDE4D1, the function of which is not known. Three further splice variants have been identified, PDE4D3 [Sette, C., *et. al.* 1994, Baecker, PG., *et. al.* 1994], PDE4D4 [Bolger, G., *et. al.* 1993] and PDE4D5 [Bolger, G., *et. al.* 1996a].

Each of the PDE4D splice variants shows different tissue and subcellular distributions. At a subcellular level, PDE4D1 and PDE4D2 are entirely cytosolic, whilst the other splice variants show a distribution of 20-30% associated with the membrane, a further 10% with the low speed pellet and the remainder in the cytoplasm [Bolger, G., *et. al.* 1996a]. This is not dissimilar to the PDE4A gene and

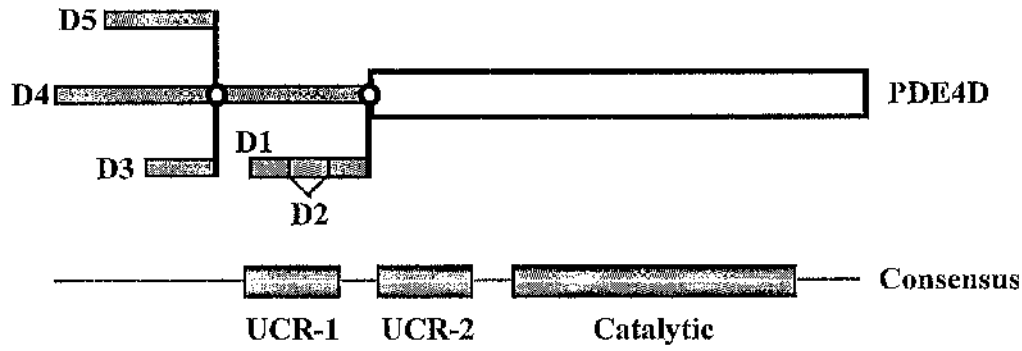

Figure 1.3.4. PDE4D splice variants.

Shows splice variants of the human PDE4D gene. The empty rectangle represents the core, catalytic region common to all species. The shaded areas are unique, alternatively spliced, regions and the circles splice junctions

again, suggests that this differential distribution is conferred by the N-terminal splice regions.

A functional attribute of one of these PDE4D splice variants is that PKA can phosphorylate PDE4D3 within its N-terminal region [Sette, *et. al.* 1994]. No phosphorylation has been reported with the other PDE4D splice variants. This phosphorylation also occurred in intact cells expressing three isoforms as a result of incubation with dibutyryl cAMP. Two effects of this phosphorylation are seen. Firstly, there is an increase in enzyme activity which may be of importance in regulating cAMP levels that have been increased through hormonal activation. For example, thyroid stimulating hormone (TSH) stimulation of rat thyroid FRTL cells causes and elevation of cAMP levels and results in a PKA mediated phosphorylation of PDE4D3. Secondly, sensitivity to PDE4 specific inhibitors, RS-25334 and RS-33793 is dramatically increased, 100 and 330 fold respectively [Avarez, R., *et. al.* 1995]. There are two consensus sites for PKA mediated phosphorylation of PDE4D3, Ser^{13} and Ser^{54}, both of which are phosphorylated, but it has been suggested that only Ser^{54} is involved in activation of the enzyme. Ser^{54} lies within UCR-1 [Sette, C. and Conti, M. 1995], perhaps this indicating one of the functions of the evolutionary conserved regions. UCR-1 however lies in a region that is shared by PDE4D3, PDE4D4, PDE4D5 and none of these have been found to be phosphorylated by PKA [Sette, C. and Conti, M. 1996], as well as PDE4A, PDE4B and PDE4C which preliminary reports [Sette, C. and Conti, M. 1996] show cannot be activated by PKA dependent phosphorylation of Ser^{54}. This might imply that Ser^{54} maybe phosphorylated in all species but the kinases

maybe different in each case, perhaps a function determined by the unique regions within the species.

It is evident that the PDE4D gene encodes a number of different splice variants that are differentially regulated by virtue of their N-terminal domains. One splice variant has been shown to be regulated by phosphorylation, however details of their subcellular distribution remains to be determined.

1.3.5.6. Therapeutic use of PDE4 inhibitors

The initial therapeutic possibilities of PDE4 inhibitors goes back 20 years to the discovery of a compound called rolipram [Schwabe, U., *et. al.* 1976]. Several studies on partially purified PDE4 preparations from smooth muscle and heart indicated that it serves as a competitive, non-stereo-selective PDE4 inhibitor (low μM) [Reeves, ML., *et. al.* 1987, Torphy, TJ. and Cieslinski, LB 1990]. Recent work, however, has demonstrated that rolipram has an IC_{50} in the sub μM range [Souness, JE. and Scott, LC. 1993, Souness, JE., *et. al.* 1995, Alvarez, R., *et. al.* 1995]. Rolipram has been shown to serve as an antidepressant. This may reflect the high concentration of PDE4 isoforms in brain and consistent with this role for PDE4s in CNS function, the PDE4 related *dunce* PDE influences learning and memory in *Drosophila melanogaster* [Davis, RL., *et. al.* 1989] and cAMP exerts similar influences in mouse.

More recently the therapeutic focus of PDE4 inhibitors has focused on their inhibitory effects on the functions of several immunocompetent / inflammatory cells [Reviewed, Palfreyman, MN. and Souness, JE. 1996] and a number of more potent compounds than rolipram have been identified (Table 1.3.). A great deal of interest has focused on the anti-asthma potential of PDE4 inhibitors and their ability to potently suppress tumour necrosis factor-alpha (TNFα) production from mononuclear phagocytes. This has enabled studies into their potential treatment for a number of other disorders which are associated with over secretion of TNFα [Schade, FU. and Schudt, C. 1993]. Examples are auto-immune diseases such as arthritis and multiple sclerosis [Tracey, KJ. and Cerami, A. 1993, Feuerstein, GZ., *et. al.* 1994], viral diseases such as AIDS and bacterial or parasitic infections like septic shock and cerebral ischaemia [Sekut, L. *et. al.* 1995, reviewed Souness, JE. and Rao, S. 1996]. Indeed PDE4 inhibitors have also been shown to alleviate arthritis in animal models [Sekut, L. *et. al.* 1995]. This considerable potential for PDE4 inhibitors has been hampered by the side effects of the drugs, mainly nausea and vomiting [Palfreyman, MN. and Souness, JE. 1996].

The IC_{50} of rolipram for PDE4 usually lies within the range of 0.1-2μM, as measured for crude subcellular fractions [Souness, JE., *et. al.* 1996], partially purified preparations [Reeves, ML., *et. al.* 1987], or recombinant protein expressed in mammalian cells [Livi, GP., *et. al.* 1990]. Little variation was seen between each of the PDE4 genes, although rolipram was reported to be 10-fold less potent against PDE4C [Bolger, G., *et. al.* 1993], but this perhaps relates to the

Table 1.3. Potencies of PDE4 inhibitors against crude monocyte PDE4.

measured at 1μM cAMP [Souness, JE. and Rao, S., 1996]

Compound	IC_{50} (μM)
Rolipram	0.3
WAY PDA 641	0.3
Ro 20-1724	2.4
Ibudilast	1.3
Denbufylline	0.2
RP 73401	0.0012
CDP 840	0.007
Trequinsin	0.4

discrepancy over the nature of the full length PDE4C species. The only other varaitions that have been seen are that cytosolic rpde6 (RNPDE4A5) was 10-fold more sensitive to rolipram compared to the membrane associated form. Also, the phosphorylated form of PDE4D3 was 60-300 fold more sensitive to the PDE4 inhibitors, RS-25334 and RS-33793, than the dephosphorylated form [Alvarez, R., *et. al.* 1995], whereas the potency of trequensin was uneffected. Studies with brain membrane and cytosol fractions have reported high-affinity rolipram binding, with a K_D ~2nM [Schneider, HH., *et. al.* 1986]. High-affinity rolipram binding displays stereoselectivity, with the R-(-)-enantiomer being 10-20 fold more potent than the S-(+)-enantiomer [Schneider, HH., *et. al.* 1986, Schmiechen, R., *et. al.* 1990]. This

high-affinity binding stereoselectivity contrasts with the only slight stereoselectivity of the binding reported in the low μM range. Evidence has been provided for a high-affinity rolipram-binding site (HARBS) on HSPDE4A and HSPDE4B [Torphy, TJ., *et. al.* 1992, McLaughlin, MM., *et. al.* 1993]. Studies on recombinant PDE4 suggest that the HARBS is distinct from the catalytic region for two reasons. (1) The affinity of rolipram for the HARBS on HSPDE4A is approximately 100-fold greater than for inhibition of catalytic activity [Torphy, TJ., *et. al.* 1992]. (2) The rank order of potency of structurally dissimilar compounds in displacing [^{3}H]-rolipram from the high-affinity site does not correlate with their inhibition of cAMP hydrolysis [Torphy, TJ., *et. al.* 1992].

The physiological effects of PDE4 inhibitors are divided according to whether they are caused by inhibitor binding to the HARBS or are as a result of inhibition of catalytic activity. For example an excellent correlation between suppression of histamine-induced bronchoconstriction and PDE4 inhibitor displacement of [^{3}H]-rolipram from the high-affinity site was seen in brain membranes [Harris, AL., *et. al.* 1989]. However, in human monocytes, PDE inhibitor suppression of lipopolysaccharide induced TNFα release and potentiation of PGE_2-induced cAMP accumulation correlated poorly with HARBS binding and a much better relationship is observed with inhibition of monocyte PDE4 [Souness, JE., *et. al.* 1996].

Pharmaceutical companies are now paying a great deal of attention to developing compounds which specifically inhibit PDE4 but have lower affinities for the HARBS. An example is SB 207499 which is equipotent with rolipram in

eliciting functional responses in several inflammatory cells but is far less effective at stimulating acid production in parietal cells, thus reducing nausea [Barnette, MS., *et. al.* 1994]. The reason for this may be that this compound is 3-fold more potent than rolipram at inhibiting HSPDE4A but 28-fold less effect at dissociating [^{3}H]-rolipram from the high-affinity site.

1.3.6. cGMP specific phosphodiesterases (PDE5)

PDE5s contain two distinct binding sites for cGMP. One of these is the catalytic site where cGMP is enzymatically cleaved to 5'-GMP but the other site exhibits no catalytic activity at all. In this respect, they resemble PDE2s, PDE3s and PDE6s. PDE5 differs from the others, however, in its almost complete inability to hydrolyse cAMP, cGMP is hydrolysed at a rate that is ~100 times faster than cAMP. Binding of cGMP to the non-catalytic site of PDE5 induces a conformational change in an N-terminal domain of about 142 amino acids, the result of which is that Ser-92 becomes a target for phosphorylation by PKG [Fransis, SH., *et. al.* 1990, Thomas, MK., *et. al.* 1990, Thomas, MK., *et. al.* 1990a]. The functional significance of these cGMP induced changes has yet to be worked out.

Zn^{2-} has been shown [Francis, SH., *et. al.* 1994] to support PDE5 catalytic activity, through a specific, high affinity interaction with the enzyme. PDE5 contains at least two sites for Zn^{2+} binding and two Zn^{2+} binding consensus motifs, that resemble those found in thermolysin, have been identified in the primary sequence of the catalytic domain. These sites are conserved in the

catalytic domains of all mammalian PDEs [Francis, SH., *et. al.* 1994]. The role of these Zn^{2+} binding domains in catalysis remains to be determined, although it seems likely that they are required for catalysis [Francis, SH., *et. al.* 1994].

PDE5 was first identified in the lung [Hamet, P. and Coquil, J-F. 1978, Fransis, SH., *et. al.* 1980] and platelets [Hamet, P. and Coquil, J-F. 1978, Hamet, P., *et. al.* 1984]. Since then it has also been identified in a number of other tissues, including rat spleen [Coquil, J-F. 1983], vascular smooth muscle [Hamet, P., *et. al.* 1984, Coquil, J-F. 1983] and sea urchin sperm [Fransis, SH., *et. al.* 1980]. The subunit molecular weight of PDE5 is ~93kDa and the native species, ~178kDa, suggesting that PDE5 exists as a homodimer [Fransis, SH. and Corbin, JD. 1988, Thomas, MK., *et. al.* 1988, Thomas, MK., *et. al.* 1988a].

1.3.7. Photoreceptor cGMP specific phosphodiesterases (PDE6)

Visual excitation in the vertebrate rod photoreceptor cell involves a light activated cGMP enzyme cascade in the outer rod segment. Absorption of a photon by the receptor, rhodopsin, leads to activation of PDE6, via a G-protein, transducin. The effect is a rapid and transient decrease in cellular cGMP levels which results in the closure of a Na^{+} channel, normal kept open by cGMP, and the membrane becomes hyperpolarised [Fresenko, EE., *et. al.* 1985].

PDE6 is a latent enzyme complex which is composed of three subunits, PDE6-α, PDE6-β and PDE6-γ in the ratio of 1:1:2 respectively [Tuteja, N., *et. al.* 1988, Baehr, W., *et. al.* 1979] . PDE6-α and PDE6-β contain separate catalytic sites that are inhibited by the binding of PDE6-γ. Transducin is activated, like all

G-proteins, by the exchange of GDP for GTP on its α-subunit and dissociation of the α-subunit from its βγ-counterparts. The α-subunit then releases the catalytic constraint of the PDE6-γ subunit on catalytic activity of the PDE6-α and PDE6-β subunits and cGMP is hydrolysed.

The catalytic, PDE6-α and PDE6-β, subunits show a 72% sequence homology, each possessing putative catalytic domains within their C-terminal regions that show a degree of homology to all other PDEs [Li, T., *et. al.* 1990]. Additionally two N-terminal, non-catalytic, cGMP-binding sites, with dissociation constants of 0.2-2μM for cGMP are also present on PDE6-α and PDE6-β [Li, T., *et. al.* 1990]. These binding sites are involved in allosteric modulation of activity [Stroop, S. and Beavo, JA., 1992]. The PDE6-γ subunit is a highly conserved protein through all vertebrate species [Takemoto, IJ., *et. al.* 1984]. Its role in the inhibition of activity of the other two subunits was originally suggested by experiments that used trypsin to degrade the γ-subunit and consequently activating the α- and β-subunits [Miki, N., *et. al.* 1975]. The ability of the α-subunit of transducin to interact with the PDE6-γ subunit is reported to be further regulated by the binding of cGMP to the non-catalytic sites of PDE6-α and β [Arshavsky, VY., *et. al.* 1992].

1.3.8. IBMX Insensitive phosphodiesterases (PDE7)

The PDE7 gene was cloned from a human glioblastoma cell line [Michaeli, T., *et. al.* 1993] by a method similar to that used to clone DPD [Colicelli, J., *et. al.* 1989], which utilised a yeast *ras2*^{val19} temperature sensitive mutation to raise

intracellular cAMP levels. The method used to identify PDE7 simply deleted the two endogenous *Saccharomyces cerevisiae* PDEs, *PDE1 and PDE2* instead of the $ras2^{val19}$ mutation.

The human PDE7 cloned (HCP-1) showed considerable homology to other cAMP PDEs, including the putative catalytic region. High levels of PDE7 RNA have been found in human skeletal muscle and lower levels of expression have been detected in a number of tissues, including brain and heart [Michaeli, T., *et. al.* 1993]. Biochemical analysis demonstrated that PDE7 has a very high affinity for cAMP (0.2μM) and is not affected by Ca^{2+}/CaM or cGMP, in which respect it resembles the PDE4 family. However, it is not susceptible to inhibition by IBMX or any known PDE4 inhibitors. HCP1 does not appear to be full length so it is possible that the pharmacological properties may be altered with the discovery of a full length clone. This is unlikely to change its designation since the sequence is distinct from any other PDE family, so it is likely that PDE7 will remain as a distinct family of PDE isoenzymes.

1.3.9. PDE8

PDE8 has been suggested [Mukai, J., *et. al.* 1994] as the most recently discovered PDE isoenzyme family. However, beyond its separation and biochemical characterisation, no further data is available, so its acceptance as a separate family has yet to be confirmed. PDE8 was isolated by Mukai [Mukai, J., *et. al.* 1994] by a process of Mono-Q anion exchange chromatography on cytosolic rat brain cerebrum. A unique peak of activity was detected that was

insensitive to Ca^{2+}/CaM or cGMP and would hydrolyse cAMP and cGMP with K_m values of 0.1μM and 1.8μM respectively. PDE1, PDE2, PDE3, PDE4 and PDE5 inhibitors had no effect on the activity unless at high concentrations where they become non-specific. It would appear therefore that Mukai and colleagues have identified a PDE with novel characteristics, however, no further characterisation has been published to date.

1.4. PROTEIN-PROTEIN INTERACTIONS

Many signalling processes are controlled by sending amplified signals to targets. Often these signals are maintained in macromolecular form, rather than being passed to small molecules such as cAMP. Such signal transducers generally affect a small number of target molecules and usually have their catalytic function separated from their binding regions, which can bring substrates to catalytic centres, link the signal transducers to upstream proteins and localise protein complexes to particular subcellular regions. The binding regions are often modular ones that are constructed with a common core recognition ability, coupled to a fine specificity control. A number of protein-protein interaction domains are known, Src homology (SH2 and SH3) domains [Koch, CA., *et. al.* 1991], pleckstrin homology (PH) domains [Mayer, BJ., *et. al.* 1993], WW domains [Bork, P. and Sudol, M., 1994] and phosphotyrosine binding (PTB) domains [Kavanaugh, WM. and Williams, LT., 1994]. Each of these have a few common features in that they are all modular domains that maintain their structure and binding abilities in

isolation and have closely apposed N- and C-termini so that can be 'plugged in' to the surface of proteins.

1.4.1. phosphotyrosine binding (PTB) domains

PTB domains are regions of about 100-150 residues in the insulin receptor substrates 1 and 2 (IRS 1 and IRS 2) and in the adapter protein Shc [Kavanaugh, WM. and Williams, LT., 1994]. These proteins bind to autophosphorylation sites on the insulin and epidermal growth factor (EGF) receptors, respectively. The amino acid sequences of the IRS 1 and IRS 2PTB domains are closely related to each other, but have no identifiable similarity to the sequence of the PTB domain from Shc [Kavanaugh, WM. and Williams, LT., 1994]. They have, however, been shown by NMR [Zhou, MM., *et. al.* 1996] and crystallographic [Eck, MJ., *et. al.* 1996] studies to have closely related three dimensional structures. Both the IRS and Shc PTBs recognise the sequence NPxY where Y represents a phosphorylated tyrosine [Wolf, G., *et. al.* 1995], which bears no resemblance to the seqences recognised by SH2 domains [See below]

1.4.2. WW domains

WW domains are protein motifs of about 40 amino acids, first identified in the Yes associated protein (YAP) and dystrophin and since then in a number of other proteins [Bork, P. and Sudol, M., 1994, Sudol, M., *et. al.* 1995]. The domain contained four well conserved aromatic residues, two of which were tryptophans, hence the name WW domain [Bork, P. and Sudol, M., 1994]. Initial studies showed that the YAP WW domain bound to a proline-rich sequence within the

SH3 domain of Yes [Sudol, M., 1994]. The proline-rich sequences that WW domains bind to have the sequence PPPPY [Chen, HI. and Sudol, M., 1995]. This sequence has been shown not bind to SH3 domains, which also recognise proline-rich sequences [Section 1.4.6.] and is consequently reported to be a distinct motif [Chen, HI. and Sudol, M., 1995].

1.4.3. Pleckstrin homology (PH) domains

PH domains are units of about 100 amino acids that were first identified in the pleckstrin protein [Haslam, R., *et. al.* 1993, Mayer, BJ., *et. al.* 1993] which has two such units. The sequence homology between PH domains from different proteins, like PTB domains, is low [Musacchio, A., *et. al.* 1994] but the structural similarity, as determined by NMR, is high both between PH domains and with PTB domains [Downing, AK, *et. al.* 1994]. PH domains have been shown to bind to phosphoinositides [Ferguson, Km., *et. al.* 1995, Hyvönen, M., *et. al.* 1995], so although PTB and PH domains share similar structure, they have evolved distinct mechanisims for phospholigand recognition.

1.4.4. Src-homology domains

Tyrosine kinase activity, exhibited by receptors and oncogenes, can stimulate cell growth and proliferation. One means of achieving this is through the activation of MAP kinase via a sequence of phosphorylation and recruitment effects. The specific recruitment effects involved depend upon defined protein-protein interactions and insight into the molecular basis that defined them came initially from studies done on sequence homology of various Src family tyrosine

kinases. These studies identified three regions called Src homology 1 (SH1), Src homolgy 2 (SH2) and Src homology3 (SH3). SH1 represented the catalytic ATP-binding domain, whereas SH2 and SH3 reflected distinct globular domains that could mediate protein-protein interactions and were essential for Src to function [Koch, CA., *et. al.* 1991].

SH2 and SH3 domains have little in common. They are both true protein domains, as far as they form compact globular domains and maintain their structure in isolation. The have closely apposed N- and C-termini so that they can be 'plugged-in' to the surface of proteins. Both are found in a wide variety of proteins; protein kinases, lipid kinases, protein phosphatases, phospholipases, Ras-controlling proteins and transcription factors. They are also found in adapter proteins such as Crk and Grb2 which have no enzymatic function but simply serve to complex proteins. SH3 domains are also found in cytoskeletal elements where they mediate the action of signal transduction pathways on cellular architecture and cell movement [Koch, CA., *et. al.* 1991, Mayer, BJ. and Baltimore, D. 1993, Pawson, T. and Schlessinger, J. 1993, Musacchio, A., *et. al.* 1994].

1.4.5. SH2 domains

Cellular response to growth and differentiation factors involves dimerisation and autophosphorylation of the receptor protein tyrosine kinase (RTK). In response to autophosphorylation, a number of proteins become associated with the RTK. It was shown that these proteins contain SH2 domains and that they would not associate with unphosphorylated receptor [Mayer, BJ. and

Baltimore, D. 1993]. Indeed, SH2 domains specifically bind to phosphorylated tyrosyl residues in proteins. The binding of SH2 domains to phosphorylated tyrosine residues can potentially have two effects. It may alter the subcellular localisation of a protein, thus bringing it closer to its substrate, or it may alter the conformation of either the SH2 domain-containing protein itself or the protein containing the P-Tyr, or another protein in the complex, thus modulating their activities to transduce a signal.

An example of activation by subcellular localisation is the RTK-mediated Ras activation pathway [Pawson, T. and Schlessinger, J. 1993]. Ras is a GTPase which is found associated with the plasma membrane. Ras is activated by the guanine nucleotide exchange factor SOS, which, even in quiescent cells is found in the cytoplasm, associated with an adapter protein Grb2. Grb2 has no catalytic function, it is composed simply of two SH3 domains and one SH2 domain, association with SOS is via its SH3 domains. Activation and autophosphorylation of the epidermal growth factor receptor creates binding sites for the SH2 domain of Grb2, the consequence of which is the localisation of the Grb2-SOS complex to the plasma membrane. Once at the plasma membrane, SOS is close to its substrate Ras, which is subsequently activated. SOS has been shown to be active in both the cytoplasm and at the plasma membrane so transduction of the signal from the receptor to Ras is entirely dependent on the recruitment of SOS to the plasma membrane via Grb2 and its SH2 domain [Li, N., *et. al.* 1993].

If the only requirement for SH2 interaction was phosphotyrosine then there would be no cellular control over which protein interacts with what so SH2

domains contain a further recognition site, usually for the three amino acids which are immediately carboxyl to the phosphorylated tyrosine residue (P-Tyr) and it is these residues that confer specificity. For example phosphotidylinositol 3'-kinase (PI3K) contains two SH2 domains and the consensus sequence for binding of these domains is P-Tyr-(Val/Met)-X-Met. If the platelet derived growth factor (PDGF) receptor is mutated at these sites then PI3K no longer binds to it. However the binding of Grb2, which has a different specificity, to the PDGF receptor is unaffected [Cantly, LC., *et. al.* 1991, Kazlauskas, A., *et. al.* 1992, Pawson, T. and Schlessinger, J. 1993].

A systematic approach was used to determine the optimal peptide ligand for specific SH2 domains. This involved the generation of an eight amino acid phosphotyrosyl peptide library that was randomised at positions P-Tyr-(+1)(+2)(+3) [Songyang, Z., *et. al.* 1993, Songyang, Z., *et. al.* 1994]. Of the 22 SH2 domains that were tested, each selected specific peptide sequences, apart from the SH2 domains from src family tyrosine kinases which all selected the sequence YEEI (table 1.4.). These specificities are not absolute however, there may be more than one SH2 domain within a cell with a high affinity for a particular ligand. Consequently, *in vivo*, the ability of an SH2 domain to engage a particular phosphoprotein may depend on the local concentration of proteins as well as the modulating effect of other domains found on interacting proteins.

Little is known about the allosteric activation via with SH2 domains. Syp phosphatase is activated 50-fold upon binding of its SH2 domain to phosphopeptides [Sugimoto, S., *et. al.* 1994]. How this activation is transmitted to

the catalytic domain is unclear since very little conformation change occurs in the SH2 domain itself upon binding [Lee, C., *et. al.* 1994]. One possible explanation for this is that in a non-activated state, *i.e.* absence of P-Tyr, the SH2 domain interacts with another region of the protein. The best example of this occurring is in the case of Src, where a P-Tyr in the carboxyl tail of Src itself loops back to bind the SH2 domain and negatively regulate the kinase [Superti-Furga, G., *et. al.* 1993].

1.4.6. SH3 domains

A key step in deciphering the basis of the interaction of SH3 domains came with the discovery of two SH3 binding peptides, 3BP1 and 3BP2, by screening an cDNA expression library with the SH3 domain of Abl [Cicchetti, P., *et. al.* 1992]. The location of the possible binding regions of 3BP1 and 3BP2 was narrowed down to regions of ~10 amino acids that were rich in prolines [Ren, R., *et. al.* 1993] and since then a number of *in vivo* ligands have been identified and their binding regions mapped to proline-rich peptide sequences [Finan, P., *et. al.* 1994, Musacchio, A., *et. al.* 1994]. Of all the Proline-rich peptides identified to date, the basic core requirement for SH3 domain interaction is PxxP. However, a preference is displayed for arginine residues within 5 amino acids of the proline and often, further, nearby prolines aid interaction [Ren, R., *et. al.* 1993, Yu, H., *et. al.* 1994, Feng, S., *et. al.* 1994]. More specifically, the Src SH3 domain is reported to prefer the proline-rich sequence RXLPPLRPΦ, where X represents any amino acid except cysteine and Φ represents a hydrophobic residue [Yu, H., *et. al.* 1994].

Table 1.4. Peptide ligands for SH2 domains

Shows the preferred amino acids at positions +1, +2 and +3 from the phosphorylated tyrosyl residue (pY) for a number of SH2 domains. [Songyang, Z., *et. al.* 1993].

Domain	pY	pY+1	pY+2	pY+3
Src Family SH2	pY	EDT	END	IVML
Abl SH2	pY	ETM	NED	PVL
Crk SH2	pY	DK	HFN	PLR
p85 N-SH2	pY	MVIE	X	M
p85 C-SH2	pY	X	X	M
Phospholipase Cγ C-SH2	pY	VI	IL	PIV
Phospholipase Cγ N-SH2	pY	LIV	ED	LIV
Csk SH2	pY	TAS	KRQN	MIV R
Grb2 SH2	pY	QYV	N	YQV

This peptide falls into class I sequences, classified by the presence of an RXL motif. A second class of ligands class II, exist that lack this motif [Yu, H., *et. al.* 1994, Alexandropoulos, K., *et. al.* 1995]. A more extensive characterisation of peptide ligands has recently been performed for various SH3 domains using a phage display library [Sparks, AB., *et. al.* 1996], the results are summarised in table 1.5. A criticism of these studies may be that all the binding studies were performed using short peptides which does not account for any three dimensional structural contribution. A three dimensional requirement for a left-handed polyproline type II helix is, however, reported [Yu, H., *et. al.* 1994]. Additional prolines, N- and C-terminal to the basic PxxP motif are reported to greatly stabilise such a structure [Yu, H., *et. al.* 1994] and it has been recently reported that the binding surface of Nef for the SH3 domain of Hck, a trosine protein kinase, consists of a non-contiguous amino acid sequence [Grzesiek, S., *et. al.* 1996]. [Lee, C.H., *et. al.* 1996]

The importance of SH3 domains in cellular signalling was first highlighted by the mutation of the SH3 domain of v-Crk, which abolished its transforming potential. Additionally, the mutation of the SH3 domains of the non-receptor tyrosine kinases, Abl and Src, activates the transforming potential of the proto-oncogene products [reviewed Cohen, GB., *et. al.* 1995]. Thus, SH3 domains may serve to organise protein complexes within the cell, bringing substrates to enzymes and regulate enzymic activities within the cell.

Table 1.5. Proline-rich peptide ligand consensus for various SH3 domains identified by phage display library screening [Sparks, AB., *et. al.* 1996].

'X' represents any amino acid, '+' basic, 'Ψ' aliphatic and 'Φ' aromatic.

SH3 Domain	Ligand Consensus													
Src	L	X	X	R	P	L	**P**	X	Ψ	**P**				
Yes	Ψ	X	X	R	P	L	**P**	X	L	**P**				
Cortactin			+	P	P	Ψ	**P**	X	K	**P**	X	W	L	
Crk						Ψ	**P**	Ψ	L	**P**	Ψ	K		
Grb2 N-term		Φ	D	X	P	L	**P**	X	L	**P**				
PLCγ				P	P	V	**P**	P	R	**P**	X	X	T	L

Compartmentalisation plays an important role in the regulation of signal transduction processes. Many of the signalling proteins that localise to the plasma membrane or cytoskeleton contain SH3 domains, suggesting that SH3 domains mediate localisation to these regions [Mayer, BJ. and Baltimore, D. 1993] Using micro-injection, it was shown that the SH3 domain of phospholipase C γ is responsible for targeting it to cytoskeletal microfilaments , while both the SH3 domains of Grb2, but not its SH2 domain are required for its localisation to membrane ruffles [Bar-Sagi, D., *et. al.* 1993]. There are also many examples of SH3 domains influencing signalling pathways involving G-proteins, such as the Grb2-SOS complex modulating Ras GTPase activity (section 1.4.1.) and the interaction of the C-terminal SH3 domain of Grb2 with Vav, a hematopoietic-specific guanine-nucleotide exchange factor [Ye, Z-S. and Baltimore, D. 1995].

1.4.3. Interactions between SH2 and SH3 domains

Given the fact that SH2 and SH3 domains are found together on a number of proteins, it is not surprising to discover evidence that their activities may be coordinated. For example Src kinase can be negatively regulated by interactions between its SH2 domain and a P-Tyr on its C-terminal tail [Superti-Furga, G., *et. al.* 1993]. This inhibition, however, requires a functional Src SH3 domain since mutation of the SH3 domain activates the kinase by making the SH2 domain more accessible to exogenous substrate [Superti-Furga, G., *et. al.* 1993]. Additionally, a phosphoprotein, p68, has been identified that will independently interact with both isolated Src SH3 and isolated Src SH2. However, a much higher affinity for

binding is seen with the tandem SH2-SH3 module [Fumagelli, S., *et. al.* 1994, Taylor, SJ. and Shalloway, D., 1994]. A similar synergism is observed in the binding of the 110kDA actin filament-associated protein to Src's SH2 and SH3 domains [Flynn, DC., *et. al.* 1993]. Structural evidence to support SH2-SH3 co-operativity was provided by crystallography of a fragment of Lck, a Src family tyrosine kinase, which contained the SH2 and SH3 domains [Eck, MJ., *et. al.* 1994]. The fragment crystallised as a dimer with extensive intermolecular SH2-SH3 contacts. Interestingly, an SH2 proline was found to lie in the SH3 domain binding pocket in an orientation similar to that of PXXP peptide. Eck also crystallised the SH2-SH3 fragment in the presence of a phosphorylated peptide that corresponds to the C-terminal tail of Lck. As expected, the phosphorylated tyrosine residue bound in an orientation similar to that observed in SH2 complexes, however the rest of the peptide did not. It was found to lie in the crease of the intermolecular SH2-SH3 interface. While there is no evidence for the existence of Src or Lck as dimers, the possibility that Src might explain why functional SH2 and SH3 domains on Src are required for the negative regulatory effect of the tyrosine phosphorylated C-terminal tail of Src.

1.5. PERSPECTIVES

In this thesis I describe a series of experiments aimed at trying to determine the rapid activation of PDE4B species in adipocytes by insulin and to define the interaction of PDE4 species with SH3 domains.

Chapter 2

Materials and Methods

2.0. SOURCES OF REAGENTS

2.0.1 PDE clones

Clones for rpde6 rpde39, hpde46, HSPDE4D1, HSPDE4D2, HSPDE4D3, HSPDE4D4 and HSPDE4D5 were all kindly donated by Graeme Bolger, Department of Medicine & Ocologic Science, Huntsman Cancer Institute, University of Utah, Salt Lake City, UT 84148, USA [McPhee, I., *et. al.* 1995, Bolger, G., *et. al.* 1996, Bolger, G. and Houslay, MD., unpublished data]. RD1 was a gift from Ron Davis [Davis, RL., *et. al.* 1989]. met^{26}RD1 was generated in this laboratory by Yasmin Shakur [Shakur, Y., *et. al.* 1993].

2.0.2. SH3-GST fusion protein clones

The Src SH3-GST, SH2-GST, SH2SH3-GST and full length Src-GST fusion protein clones were obtained from Margaret Frame, Beatson Institute for Cancer Research, Garscube Estate, Glasgow, G61 1BD, Scotland. The Lck SH3-GST, Csk SH3-GST, Grb2 SH3-SH2-SH3-GST and Crk SH3-GST fusion proteins were obtained from Siegmund Fisher, Laboratory of Molecular and Cellular Oncology, Cochin Institute for Molecular Genetics, National Institute of Health & Medical Research, Cochin Hospital, Paris, France. The Lyn SH3-GST, Fyn SH3-GST and Abl SH3-GST fusion proteins were kind gifts from David Baltimore, Department of Biology, Massachusetts Institute of Technology, MA 02139, USA. The cortactin SH3-GST fusion protein was given to us by Nancy McGee and Thomas Parsons, UVA Medical Centre, Charlottesville, VA 22908, USA.

2.0.3. Cell lines

All cell lines used in these studies were originally obtained from ECACC, Department of Cell Resources, Centre for Applied Microbiology and Research, Porton Down, Salisbury, Wiltshire. SP4 ODJ.

2.1. POLYACRYLAMIDE GEL ELECTROPHORESIS

2.1.1. Buffers

2.1.1.1. Resolving gel buffer (Buffer A):

2M	Tris/HCl, pH 8.8
0.4% (w/v)	SDS

2.1.1.2. Stacking gel buffer (Buffer B):

0.5M	Tris/HCl, pH 6.8
0.4% (w/v)	SDS

2.1.1.3. Acrylamide mix:

30% (w/v)	acrylamide : N,N'methylenebisacrylamide
	29:1 (3.3% cross-linking, Bio-Rad)

2.1.1.4. Resolving gel (8%):

13.9ml	distilled water
7.8ml	Buffer A
8mls	acrylamide mix
300µl	10% ammonium persulphate
18µl	N,N,N',N'-tetramethylethylenediamine
	(TEMED)

2.1.1.5. Stacking gel:

6.8ml	distilled water

1.35ml	Buffer B
1.7ml	acrylamide mix
100µl	10% ammonium persulphate
10µl	TEMED

2.1.1.6. Laemmli buffer (2x): [Laemmli, UK. (1970) Nature 227. 680-685]

2.5ml	1M Tris/HCl, pH 6.8
5ml	glycerol
8ml	10% (w/v) SDS
3.5ml	distilled water
0.007% (w/v)	bromophenol blue
1ml	ß-mercaptoethanol (added prior to use)

2.1.1.7. Electrode buffer:

192mM	Glycine
25mM	Tris
0.15 (w/v)	SDS

2.1.2. Preparation of Samples

Samples containing no more than 400µg of protein were added to an equal volume of 2x Laemmli buffer and boiled for five minutes.

2.1.3. Protein Molecular Weight Markers

Prestained protein molecular weight markers (Bio-Rad) containing the following proteins; myosin H chain (200kDa), phosphorylase B (97.4kDa), BSA (68kDa), ovalbumin (43kDa), carbonic anhydrase (29kDa), ß-lactalbumin (18.4

kDa) and lysozyme (14.3kDa) were used. Its should be noted that the apparent molecular weights varied from batch to batch and the sizes of the proteins are indicated on any particular figure.

2.1.4. Casting and Running of the Gel

Following assembly of the gel apparatus, the resolving gel was poured between the plates and 2ml of water was layered on top. When the gel had set, about 30 minutes, the water was removed, a comb inserted and the stacking gel poured. When the stacking gel had set, the comb was removed and the gel placed in a tank containing electrode buffer. The samples were loaded into the wells and the gels were run at 60mA per gel until the bromophenol blue reached the bottom of the gel.

2.1.5. Staining and Drying

Gels were fixed in 0.25% Coomassie Blue (Brilliant Blue R250) in 5:1:4, water : acetic acid : methanol for 1 hour at room temperature. Destaining was performed with 5:1:4, water : acetic acid : methanol at room temperature until the background was sufficiently reduced. Gels were dried onto Whatman 3MM paper under vacuum at 60^{O}C for 2hrs.

2.1.6. Non-denaturing polyacrylamide gel electrophoresis

2.1.6.1. Resolving Gel:

10% (w/v)	Acrylamide (of which 2% N,N'methylenebisacrylamide)
375mM	Tris / HCl, pH 8.9

0.5mM	Potassium persulphate
5µg/ml	Riboflavin
0.1% (v/v)	TEMED

2.1.6.2. Stacking Gel:

4% (w/v)	Acrylamide (of which 20% N,N'methylenebisacrylamide)
60mM	Tris / Phosphate, pH 6.8
0.5mM	Potassium persulphate
5µg/ml	Riboflavin
0.1% (v/v)	TEMED

2.1.6.3. Anode Buffer:

60mM	Tris / HCl, pH 7.5

2.1.6.4. Cathode Buffer:

46mM	Glycine
40mM	Tris / HCl, pH 8.9

2.1.6.5. Elution Buffer:

20mM	Tris / HCl, pH 7.4
0.1mM	Ethyleneglycol-bis (β-aminoethyl ether)-N,N,N',N'-Tetra-acetic acid (EGTA)
50mM	Sodium Chloride
50mM	β-Mercaptoethanol

0.1% (v/v)	Protease inhibitor cocktail (PMSF 40mg/ml, benzamidine 156mg/ml, apoprotinin 1mg/ml, antipain 1mg/ml, leupeptin 1mg/ml, pepstatin 1mg/ml, dissolved in DMSO)

2.1.6.6. Casting and running of the gels

A tube gel apparatus was used with an internal diameter of 5mm. Each gel was composed of 1.6ml resolving gel and 0.7ml stacking gel. All constituents of the gels, including the apparatus and buffers were cooled to 4°C prior to casting the gels. The gels were photo-polymerised at 4°C and set after about 10 minutes. Samples to be loaded onto the gels were supplemented with 10% (v/v) cathode buffer which had 25% (v/v) glycerol and 12.5 µg/ml amaranth dye added. Gels were run at 110 volts while the samples were in the stacking gel and 160 volts once they had entered the resolving gel. Electrophoresis was terminated when the dye reached the bottom of the gel.

2.1.6.7. Elution of samples

The gel was removed from the glass tube by filling a syringe with cathode buffer and applying pressure to the top of the gel. The gel was then wrapped in cling-film, snap frozen in a dry-ice methanol bath and sliced into a number of slices, approximately 1mm thick using a sharp scalpel. Each of the slices were then placed in separate vials, 200µl of elution buffer added and incubated at 4°C overnight.

2.2. WESTERN (IMMUNO) BLOTTING *

2.2.1. Buffers

2.2.1.1. Blotting buffer:

192mM	glycine
25mM	Tris
20% (v/v)	methanol
80% (v/v)	water

2.2.1.2. Tris buffered saline (TBS):

0.5M	NaCl
20mM	Tris/HCl, pH 7.4

2.2.2. Transfer to Nitrocellulose

The SDS polyacrylamide gel was placed in a cassette on top of a piece of nitrocellulose paper (Schleicher & Schuell), bound by two pieces of Whatman 3MM paper and two pieces of sponge. The cassette was soaked in blotting buffer, being careful to exclude any bubbles and was loaded into the transfer tank with the nitrocellulose side of the cassette towards the positive electrode. The tank was filled with blotting buffer and the proteins transferred for 2 hours at 1amp.

2.2.3. Immuno-detection using ECL from Amersham

The nitrocellulose was blocked using 5% Marvel in 100ml of TBS for at least 2hrs with gentle shaking. The nitrocellulose was washed 2x 5mins with TBS + 0.1% Nonidet P40 (NP40) and 2x 5mins in TBS. First, antibody specific to the

* Towbin, H., Staehelin, T. and Gordon, J. (1979) PNAS 76, 4350-4355. Burnette, WN. (1981) Anal. Biochem. 112, 195-203.

protein of interest was added in 10ml of TBS + 1% Marvel, sealed in a polythene bag and incubated at room temperature with vigorous shaking for 2hrs. After washing as described above, a second, horse radish peroxidase (HRP) conjugated, antibody directed against the 1st antibody added; 40µl in 100ml TBS + 1% Marvel. This was then incubated for 1hr at room temperature with gentle shaking and washed 4x 5mins with 100ml TBS.

The nitrocellulose was incubated with ECL (Amersham) reagents as per manufacturers instructions. X-ray film (Fuji) was exposed to the nitrocellulose for 5secs to 10mins depending on the intensity of the signal. The film was then developed.

2.3. TRANSFORMATION OF BACTERIA

2.3.1. Medium and buffers

2.3.1.1. L-broth:

170mM	NaCl
0.5% (w/v)	Bacto-Yeast Extract
1% (w/v)	Bacto-Tryptone
pH 7.5	

2.3.1.2. LB-Agar:

170mM	NaCl
0.5% (w/v)	Bacto-Yeast Extract
1% (w/v)	Bacto-Tryptone
2% (w/v)	Agar

2.3.1.3. Transformation buffer 1:

100mM	RbCl
50mM	$MnCl.4H_2O$
30mM	Potassium acetate
10mM	$CaCl_2.2H_2O$
15% (w/v)	redistilled glycerol

pH 5.8, adjusted with 0.2M acetic acid. Filter sterilise through a 0.22μ filter.

2.3.1.4. Transformation buffer 2:

10mM	RbCl
10mM	3-[N-Morpholino]propane sulphonic acid (MOPS)
75mM	$CaCl_2.2H_2O$
15% (w/v)	redistilled glycerol

pH 6.8, adjusted with 0.2M NaOH. Filter sterilise through a 0.22μ filter.

2.3.2. Preparation of Competent *E.coli* JM109

A 10ml culture of JM109 *E.coli* in L-broth was inoculated from a glycerol stock and grown overnight at 37°C with constant shaking. A 500ml L-broth culture was inoculated with 3mls of the overnight culture and grown at 37°C, shaking at 200rpm until the optical density at 550nm was between 0.5 and 0.55. The culture was divided equally between two sterile 250ml centrifuge bottles and cooled on ice for 30 minutes. They were then centrifuged at 2500rpm (950g) in a JA14 rotor for 15 minutes and each pellet resuspended in 20ml of ice-cold

transformation buffer 1. The cells were incubated on ice for a further 15 minutes before centrifugation at 2500rpm for 10 minutes. The supernatant was removed and the cell pellets gently resuspended in 3.5ml of transformation buffer 2. When the cells were completely resuspended, they were pooled and again incubated on ice for 15 minutes. The competent cells were then snap-frozen in 250µl aliquots and stored at -80°C.

2.3.3. Transformation

An aliquot of competent cells was removed from storage in the -80°C freezer and allowed to thaw slowly on ice. For each transformation to be performed, a 50µl aliquot of competent cells was transferred to a sterile Eppendorf tube. To each 50µl, approximately 100ng of DNA was added and incubated on ice for 15mins. The cells were then heat shocked for 90 seconds at 42°C and incubated on ice for a further 1 minute. 1ml of L-broth was then added and the transformed cells were incubated at 37°C for 30-60 minutes with shaking. 100µl of the bacteria were then plated on a 10cm agar plate containing selection medium. Transformed colonies were picked and glycerol stocks made (section 2.3.4.)

2.3.4. Glycerol stocks

Single colonies were picked and used to seed a 10ml L-broth culture which was grown overnight at 37°C. To 750µl of the overnight culture, 250µl of 80% glycerol in L-broth was added and vortexed. The glycerol stock was stored at -80°C.

2.4. GLUTATHIONE-S-TRANSFERASE-FUSION PROTEIN INDUCTION

A scraping taken from a frozen glycerol stock was used to seed a 10ml L-broth culture supplemented with ampicillin (50µg/ml) which was grown over night at 37°C. This was used to inoculate a 500ml L-broth culture containing ampicillin which was grown for 2hrs at 37°C with constant shaking. Expression of the fusion protein was induced by adding 500µl of 100mM isopropyl-ß-D-thiogalactopyranoside (IPTG, Boeringer Mannheim) and the culture was incubated for a further 5 hours at 37°C. The bacteria were harvested by centrifugation and resuspended in 20ml of PBS containing a protease inhibitor cocktail (PMSF 40mg/ml, benzamidine 156mg/ml, apoprotinin 1mg/ml, antipain 1mg/ml, leupeptin 1mg/ml, pepstatin 1mg/ml, 1000x dissolved in DMSO). They were then frozen at -20°C in 1ml aliquots.

2.5. PULL DOWN ASSAY FOR PHOSPHODIESTERASE-SH3 INTERACTION*

2.5.1 Buffers

2.5.1.1. Phosphate buffered saline (PBS)

KCl	2.7mM
NaCl	137mM
Na_2HPO_4	4mM
NaH_2PO_4	0.15mM, pH 7.4

* Methed adapted from Haefner, R., *et. al.* 1995

2.5.2. Interactions using phosphodiesterase from transfected COS7 cells

An aliquot of the bacteria which had been induced to express the fusion protein of interest were thawed and lysed by sonication. The debris was pelleted by centrifuging for 1 min at 16,000g in a bench top centrifuge. For every 1ml of supernatant, which on average yielded 400-800μg of fusion protein, 100μl of glutathione sepharose 4B beads (Pharmacia Biotech) equilibrated in PBS were added and incubated end over end for 1hr at room temperature. The beads were washed three times with 1ml of PBS over 15 minutes, resuspended as a 50% slurry and assayed for protein concentration.

As a routine, volumes of slurry containing 400μg of beads were pelleted and the supernatants removed. To each of the pellets, an amount of cytosolic PDE, from pSV.SPORT-PDE transfected COS7 cells, capable of hydrolysing 2000pmol/min of cAMP at 30°C was added and incubated for 10mins at 4°C. The beads were washed as before, the washes being retained for assay. The determination of PDE bound to the immobilised GST fusion proteins was performed by Western blot, using a polyclonal antibody raised against the conserved C-terminal region specific to rat PDE4A, PDE4B, PDE4C, or PDE4D. Bound PDE activity was measured by first releasing the SH3-PDE complex from the agarose beads by incubation with 100μl of 10mM-glutathione in 50mM-TrisHCl buffer pH 8.0 for ten minutes at room temperature. This treatment was repeated a twice more and the supernatants pooled.

2.5.3. Interactions using phosphodiesterases from rat tissue

For preparation of rat tissue cytosols see section 2.11.3.The method used is almost identical to that described for COS cell extracts, however, 100-400μg of brain cytosol were used and the binding performed for 30 minutes at 4°C.

2.6. IMMUNOPRECIPITATION

2.6.1. Buffers

2.6.1.1. Immunoprecipitation Buffer

10mM	Ethylenediaminetetra-acetic acid (EDTA)
100mM	$NaH_2PO_4.2H_2O$
1% (w/v)	Triton X100
50mM	N-2-Hydroxyethylpiperazine-N'-2-ethanesulfonic acid (Hepes), pH 7.2

2.6.1.2. Wash Buffer

10mM	Ethylenediaminetetra-acetic acid (EDTA)
100mM	$NaH_2PO_4.2H_2O$
1% (w/v)	Triton X100
0.1% (w/v)	Sodium dodecyl sulphate (SDS)
50mM	N-2-Hydroxyethylpiperazine-N'-2-ethanesulfonic acid (Hepes), pH 7.2

2.6.2. Procedure

The sample to be immunoprecipitated from was in either TBS, PBS or KHEM buffer. The sample was diluted to 1ml in immunoprecipitation buffer so that at least 50% (v/v) was immunoprecipitation buffer. 20µl of polyclonal antibody were added and incubated end over end at 4°C overnight. 200µl of Pansorbin (Calbiochem) were added and incubated end over end at 4°C for at least 2 hours. The Pansorbin was pelleted by spinning at 14,000g at 4°C in a bench top microfuge for 2 minutes and washed three times with wash buffer and once with PBS.

2.7. PHOSPHODIESTERASE ENZYME ASSAY

Briefly, [^{3}H]-cyclic nucleotide (8 position of the adenine or guanine ring) was hydrolysed to form labelled nucleotide mono-phosphate. The nucleotide mono-phosphate ring was then converted to the corresponding labelled nucleoside by incubation with snake venom which has 5'-nucleotidase activity. The conditions were such that complete conversion took place within the incubation time. Unhydrolysed cyclic nucleotide was separated from the nucleoside by batch binding of the mixture to Dowex-1-chloride. This bound the charged nucleotides but not the uncharged nucleosides.

2.7.1. Buffers

2.7.1.1. Assay buffer:

10mM	$MgCl_2$
20mM	Tris/HCl, pH 7.4

2.7.2. Procedure

A 2x stock solution of cAMP was made by adding 30µl of [^{3}H]-cAMP (1mCi/ml, 41.7µM) to 10ml of 2µM cAMP in assay buffer. The assay volume was 100µl which consisted of 50µl 2x cAMP stock and 50µl of sample, a proportion of which could be replaced by an effector or made up with buffer. All tubes were kept on ice prior to incubation at 30°C. The reaction was stopped usually after 10 minuets by boiling for two minutes. The vials were then cooled on ice and 25µl of 1mg/ml snake venom (Sigma) was added and incubated for a further 10 minutes. After cooling, 400µl of Dowex resin was added and incubated on ice for 15 minutes. The dowex was pelleted by spinning in a bench top centrifuge for 3 minutes and 150µl of the supernatant removed for scintillation counting in 2mls Ecoscint A.

2.7.2. Use of PDE assay to profile PDE families present in various tissues

To determine the contribution of various PDE families to the overall cyclic nucleotide phosphodiesterase content of a tissue, the normal PDE assay, supplemented with various specific inhibitors and additional factors was used, since each of the PDE families has its own specific catalytic and regulatory properties.

2.7.2.1. PDE1

The PDE1 family requires Ca^{2+}/Calmodulin for activity. To measure PDE1 activity, the activity was measured when supplemented with Ethyleneglycol-bis (β-aminoethyl ether)-N,N,N',N'-Tetra-acetic acid (EGTA) (2mM), to chelate the

calcium which inactived the enzyme and with EGTA and an excess of $CaCl_2$ (5mM) and Calmodulin (10U/100µl) which fully activated it. The difference between these values represented the PDE1 activity.

2.7.2.2. PDE2

The PDE2 family is activated by cGMP and inhibited by the drug EHNA. The difference in PDE activity when supplemented with cGMP (10µM), compared to cGMP with EHNA (10µM) represented the PDE2 activity. The addition of cGMP alone was not sufficient since PDE3 is inhibited by cGMP.

2.7.2.3. PDE3 and PDE4

The PDE3 family is specifically inhibited by the drug cilostamide and the PDE4 family by rolipram. Measurement of PDE activity with and without cilostamide (10µM) and with and without rolipram (10µM) present gave the contribution of PDE3 and PDE4 respectively

2.7.2.4. Isobutylmethylxanthine (IBMX) insensitive.

The only other family measured was that that is insensitive to IBMX, a PDE inhibitor that inhibits all PDE families, apart from PDE7. The activity that remained afterr IBMX treatment was used to indicate PDE7 activity, although it had to be considered that IBMX may not have completely inhibited all other PDEs at the concentrations used. The IBMX insensitive fraction was represented as the PDE activity remaining when IBMX (100µM) was added to the PDE assay buffer.

2.8. TISSUE CULTURE

2.8.1. NG108-15 cell line

NG108-15 cells are mouse neuroblastoma, rat glioma cell hybrids, formed by Sendai virus induced fusion of mouse and rat clones.

2.8.1.1. Growth medium for NG108-15 cells:

Growth medium was Dulbecco's Modified Eagle's Medium (DMEM, Sigma D5671). This was supplemented with Penicillin / Streptomycin (100 units/ml, Sigma), 10mM glutamine, 5% (v/v) HAT supplement (Sigma) and 5% controlled process serum replacement type 3 (CPSR, Sigma).

2.8.1.2. Maintenance of NG108-15 cells

Cells were grown in an atmosphere of 95% air and 5% CO_2 at 37°C in 10ml of the medium detailed above. Cells were given fresh medium daily. When the cells reached about 90% confluency the cells were passaged 1:7 to fresh flasks and medium.

2.8.1.3. Passaging NG108-15 cells

The cells were washed in 10ml of PBS prewarmed to 37°C and 2ml of trypsin were added. The cells were then returned to the incubator for 2 minutes or until they detached from the flask. They were then spun for 5 mins at 200g to pellet the cells. The medium was removed and the cells resuspend in 70ml of fresh medium which was distributed to seven new flasks.

2.8.1.4. Differentiation of NG108-15 cells using forskolin

NG108 cells grown to about 80% confluency were passaged 1:9 into medium detailed above but containing 1% (v/v) CPSR. The passage medium contained 10μM forskolin to elevate cAMP levels and induce differentiation. If necessary the cells medium was replaced as the medium changed to a yellow colour. Extreme care was taken while handling the differentiating cells because they did not attach very strongly to the surface of the plate. At 7-8 days after adding forskolin, the cells had completely differentiated.

2.8.2. NCB20 cell line

2.8.2.1. Growth medium for NCB20 cells:

Growth medium was Dulbecco's Modified Eagle's Medium (DMEM, Sigma D5671). This was supplemented with Penicillin / Streptomycin (100 units/ml, Sigma), 10mM glutamine and 10% foetal calf serum (Sigma).

2.8.2.2. Maintenance of NCB20 cells

Cells were grown in an atmosphere of 95% air and 5% CO_2 at 37°C in 10ml of the medium detailed above. When the cells reached about 90% confluency the cells were passaged 1:5 to fresh flasks and medium.

2.8.2.3. Passaging NCB20 cells

The cells were washed in 10ml of PBS prewarmed to 37°C and 2ml of trypsin were added. The cells were then returned to the incubator for 2 minutes or until they detached from the flask. They were then spun for 5 mins at 200g to

pellet the cells. The medium was removed and the cells resuspend in 50ml of fresh medium which was distributed to five new flasks.

2.8.3. COS7 cell line

COS7 cells are a fibroblast-like cell line derived from the African green monkey kidney cells. These cells have been transformed by an origin defective mutant of SV40 which codes for wild type T-antigen. They make an excellent host for transfection with vectors requiring the expression of SV40 T-antigen. They permit replication of any plasmid caontaining an SV40 origin of replication, thus amplifying the expression of any genes encoded by the plasmid.

2.8.3.1. Growth medium for COS7 cells:

Growth medium was Dulbecco's Modified Eagle's Medium (DMEM, Sigma D5671). This was supplemented with Penicillin / Streptomycin (100 units/ml, Sigma), 10mM glutamine and 10% foetal calf serum (Sigma).

2.8.3.2. Maintenance of COS7 cells

Cells were grown in an atmosphere of 95% air and 5% CO_2 at 37°C in 10ml of the medium detailed above. When the cells reached about 90% confluency the cells were passaged 1:5 to fresh flasks and medium.

2.8.3.3. Passaging COS7 cells

The cells were washed in 10ml of PBS (section 2.5.1.1.) prewarmed to 37°C and 2ml of trypsin were added. The cells were then returned to the incubator for 2 minutes or until they detached from the flask. They were then spun for 5

mins at 200g to pellet the cells. The medium was removed and the cells resuspend in 50ml of fresh medium which was distributed to five new flasks.

2.9. COS7 CELL TRANSFECTION

2.9.1. Buffers

2.9.1.1. Transfection medium (make fresh)

Transfection medium was Dulbecco's Modified Eagle's Medium (DMEM, Sigma D5671). This was supplemented with Penicillin / Streptomycin (100 units/ml, Sigma), 10mM glutamine, 10% new-born calf serum (Sigma) and 100μM chloroquine.

2.9.1.2. Tris EDTA buffer (TE):

1mM	Ethylenediaminetetra-acetic acid (EDTA)
10mM	Tris / HCl, pH 7.5

2.9.2. Procedure

Cells were passaged to about 33% confluency 24hrs prior to transfection. 10μg of DNA was diluted to 250μl in TE and 200μl of DEAE Dextran (10mg/ml in PBS) were added. This was incubated for 15 minutes at room temperature. COS7 cell growth medium was aspirated from the cells and 5ml of transfection medium added. The DNA solution was added dropwise to the cells and mixed by swirling. The cells were returned to the incubator for 3-4hrs.

The cells were shocked by first aspirating the transfection medium and 5ml of 10% DMSO in PBS were added for exactly 2 minutes. The DMSO was

aspirated and the cells washed with 10mls of PBS. The cells were returned to normal growth medium, placed in the incubator for three days and split only if necessary. Functional assays were then performed.

Lysis of transfected COS7 cells

KHEM buffer

50mM	KCl
10mM	Ethyleneglycol-bis (β-aminoethyl ether)-N,N,N',N'-Tetra-acetic acid (EGTA)
50mM	N-2-Hydroxyethylpiperazine-N'-2-ethanesulfonic acid (Hepes), pH 7.2
1.92mM	$MgCl_2$
1mM	Dithiothreitol (DTT), added fresh
20μg/ml	Cytochalasin B, added fresh
Protease inhibitors (section 2.4), added fresh	

TEA / KCl

10mM	Triethanolamine (TEA)
150mM	KCl
pH 7.2 with HCl	

Procedure

The culture medium was removed from the cells and 2ml of KHEM added. The cells were incubated at 4°C for 45 minutes. The KHEM was removed and 5ml of TEA / KCl were added and incubated for 10 minutes at 4°C. The TEA / KCl

was removed and the cells washed with 5ml KHEM. 1ml of KHEM was then added and the cells incubated for 2 minute at 4°C. The KHEM was aspirated, the cells scraped from the plate and homogenised with 20 strokes in a glass on glass dounce homogeniser. The homogenate was centrifuged at 650g for 10 minutes to pellet debris. The supernatant was snap-frozen in liquid nitrogen in 100µl aliquots and stored at -80°C or used for membrane and cytosol preparations (section 2.11.3.). Note in preparations where the cytoskeleton was required intact, the cytochalasin was omitted from the KHEM buffer.

2.10. ADIPOCYTE PREPARATION

Adipocytes were prepared from the epididymal fat pads from male Sprague-Dawley rats of weight 200-250g. These rats were provided by the University's animal house.

2.10.1. Buffers

2.10.1.1. Low-phosphate Krebs:

114mM	NaCl
4.7mM	KCl
1.18mM	$MgSO_4.7H_2O$
50µM	KH_2PO_4
25mM	$NaHCO_3$
25mM	HEPES, pH 7.4
3% (w/v)	Bovine serum albumin (BSA) (add fresh)
1M	$CaCl_2$ (add fresh)

2.10.1.2. Incubation buffer:

50µg/ml	Adenosine deaminase
2mg/ml	Collagenase
500µg/ml	Trypsin Inhibitor

Made up in low-phosphate Krebs

2.10.2. Procedure:

Epididymal fat pads were dissected out directly to low phosphate Krebs buffer at 37°C. The pads were finely chopped using scissors and rinsed in a tea-strainer. They were transferred to 10ml of incubation buffer in a siliconised glass vessel and incubated at 37°C for approximately 50 minutes in a shaking water bath. Cells were rinsed through a nylon tea-strainer with low-phosphate Krebs to remove any cells that remain as clumps. Cells were centrifuged at 600rpm (80g) for 2mins to float adipocytes and the buffer below the adipocytes removed. The adipocytes were resuspended in 30ml of low-phosphate Krebs at 37°C and spun again. This was repeated twice more. The cells were finally resuspended at approximately 15% cells in total volume of suspension. Protease inhibitors were added (PMSF 40mg/ml, benzamidine 156mg/ml, apoprotinin 1mg/ml, antipain 1mg/ml, leupeptin 1mg/ml, pepstatin 1mg/ml, 1000x dissolved in DMSO) and the cells gently gassed with 95% 0_2 and 5% CO_2 at 37°C in a shaking water bath for 20 minutes before adding any drugs.

2.11. PREPARATION OF RAT TISSUE FRACTIONS

All rats used were male Sprague-Dawley rats of weight 200-250g, supplied by the University's on site animal house.

2.11.1. Buffers

2.11.1.1. Homogenisation buffer:

1mM	EDTA
10mM	Tris/HCl, pH 7.4
100μM	Dithiothreitol
Protease inhibitor cocktail	

2.11.2. Preparation of a crude homogenate from brain

A brain from a 200-250g male Sprague-Dawley rat was dissected and finely chopped in 20mls of ice-cold homogenisation buffer The chopped brain was washed through a tea-strainer with 50mls of ice-cold homogenisation buffer and homogenised with eight strokes at full speed in a rotary homogeniser using a Teflon pestle and a glass vessel, in 5mls of homogenisation buffer. The homogenate was centrifuged at 650g for 10 minutes to pellet debris. The supernatant was snap-frozen in liquid nitrogen in 100μl aliquots and stored at -80°C or used for membrane and cytosol preparations (section 2.11.3.). A similar method was used for preparing homogenates of heart, lung, liver and testes.

2.11.3. Preparation of brain membrane and cytosol fractions

Rat brain homogenate was centrifuged at 245,000g and 4°C in a Beckman TL-100 centrifuge for 20 minutes. The supernatant constituted the cytosol fraction and was snap-frozen in liquid nitrogen in 100µl aliquots. The pellet or membrane fraction was resuspended in an identical volume to the cytosol fraction, snap-frozen in 100µl aliquots and stored at -80°C. A similar method was used for preparing cytosol and membrane fractions from heart, lung, liver and testes.

2.12. PROTEIN ASSAY

2.12.1. Bradford assay

This method of protein determination is based on the Bradford method.* A standard curve was constructed using 0-20µg bovine serum albumin (BSA). These concentrations of protein were dissolved in 800µl distilled water. To this, 200µl Bio-Rad reagent was added, the tubes were vortexed and the absorbance was read against a blank curvette containing no protein, at a wavelength of 595nm. Protein concentrations of the samples were determined in a similar way, diluting 5µl of the sample in 800µl distilled water, adding Bio-Rad reagent and reading the absorbance in the spectrophotometer as before. All samples were assayed in duplicate. Protein concentrations were determined by plotting the standard curve and fitting a 3rd polynomial curve to the points. The equation of the line was used to determine the protein concentration of the samples.

* Bradford, MM. (1976) Anal. Biochem. **72**, 248-254.

2.13. DNA MANIPULATIONS

2.13.1. Plasmid purification

All plasmids were purified from *E.coli* JM109. Large cultures, 500ml were purified with use of Wizard Maxi-Preps (Promega) and small, 10ml cultures with Wizard Mini-Preps (Promega). In both instances, the manufacturers instructions were followed. Following purification, an extra ethanol precipitation step was used to further increase the purity of the plasmid (Section 2.13.2.).

2.13.2. Ethanol precipitation

To the volume of DNA to be ethanol precipitated, 10% (v/v) 3M sodium acetate was added and 2 volumes of 100% ethanol. The vial was mixed and incubated at -80°C for 30 minutes. The vial was spun at high speed in a microfuge for 10 minutes to pellet the DNA. The supernatant was aspirated and 1ml of 70% ethanol added the DNA was pelleted again by spinning at high speed in a bench-top centrifuge for 5 minutes, the supernatant aspirated and the pellet allowed to air-dry for 5-10 minutes. The DNA was resuspended in TE buffer (section 2.9.1.2) and the purity of the DNA checked by UV absorption at 260nm and 280nm where A_{260}/A_{280}=1.8 for pure plasmid DNA.

2.13.4. Restriction enzyme digests

All restriction enzyme digest were performed on pure plasmid DNA using restriction enzymes supplies by Promega. Incubation were conditions were 37°C for a minimum of 1 hour using the appropriate buffer supplied by Promega. Following digestion DNA was cleaned-up using Wizard Clean-up kit (Promega)

or run on an agarose gel and the required band excised, the DNA then being purified by the use of Wizard PCR purification kit (Promega).

2.13.5. Ligations

Ligations were performed at 37°C overnight using T_4 DNA ligase (Promega), using buffer and conditions as supplied by the manufacturer.

2.13.6. Polymerase chain reaction (PCR)

PCR was performed usually with 30 cycles of replication, a melting temperature of 94°C, an annealing temperature of about 50°C, depending on the primers and an elongation temperature of 72°C. Taq polymerase, Taq buffer, 3M magnesium chloride and dNTPs were all supplied by Promega.

Chapter 3

Regulation of PDE4B

3.1. INTRODUCTION

As discussed in Chapter 1, the PDE4 family is encoded by four genes; PDE4A, PDE4B, PDE4C and PDE4D, each of which have distinct chromosomal locations [Milatovich, A., *et. al.* 1994, Horton, Y., *et. al.* 1995]. For active splice variants within the PDE4 family, there is high homology in their C-terminal regions (figure 1.3.2.), whereas low homology of this region is seen between different PDE families. Within this C-terminal region is the catalytic domain, the sequence similarity presumably reflects the sensitivity of each of the splice variants to the PDE4 inhibitor, rolipram. The N-terminal regions show extremely low levels of homology, both between and within families [Bolger, G., *et. al.* 1994, Conti, M., *et. al.* 1995]. It is these N-terminal domains which regulate the PDEs properties, such as catalytic activity, effector binding and subcellular distribution.

At the time this work commenced, only two PDE4B splice variants were suggested to represent full length clones and work performed by Lobban [Lobban, M., *et. al.* 1994] was the first attempt to characterise them as endogenously expressed species. For the purpose of this chapter, only these will be discussed in the introduction, the implications of recent findings will be considered in the conclusions. The suggested species were DPD (RNPDE4B1) [Colliccelli, J., *et. al.* 1989] and PDE4B2 (RNPDE4B2A) [Swinnen, JV., *et. al.* 1991]. HSPDE4B2A, a human equivalent to RNPDE4B2 has been cloned [McLaughlin, MM., *et. al.* 1993] but no human equivalent to DPD has been identified. DPD was identical to PDE4B2 along its' entire length, the only difference between the two form was an

N-terminal extension of 48 amino acids in PDE4B2 (figure 3.1.1). Therefore, the start point of DPD appears to represent the point of a splice junction.

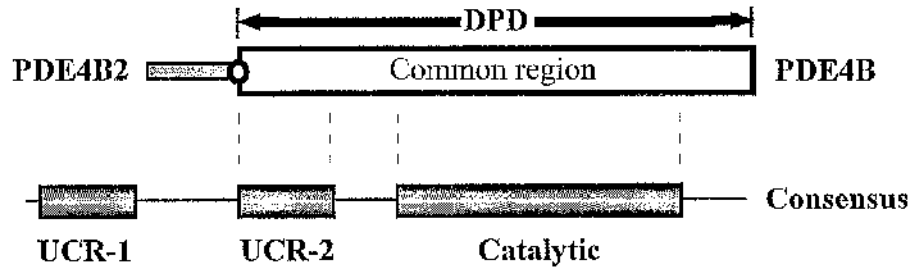

Figure 3.1.1. PDE4B Splice variants

Shows the PDE4B splice variants proposed [Collicelli, J., *et. al.* 1989, Swinnen, JV., *et. al.* 1991]. The common region contains both UCR2 and the catalytic region and represents the entire length of DPD. The empty circle represents the splice junction where an additional N-terminal domain of 48 amino acids is added for PDE4B2.

To determine if the species cloned by Collicelli and Swinnen [Collicelli, J., *et. al.* 1989, Swinnen, JV., *et. al.* 1991] represented endogenously expressed species, their expression was investigated in rat brain using antisera directed to a peptide sequence found in the common C-terminal region, thus recognising both DPD and PDE4B2, and antisera directed to the unique N-terminal region of PDE4B2 [Lobban, M., *et. al.* 1994]. Both DPD and PDE4B2 were reported to be expressed, each with a different subcellular distribution; PDE4B2 was entirely

membrane associated, while DPD was cytosolic. Since the only difference between the two splice variants is a unique 48 amino acid N-terminal domain in PDE4B2, membrane association must be determined by these amino acids.

DPD and PDE4B2 also displayed a very different expression pattern between various regions of the brain, the organ in which they were reported to be expressed to the highest levels [Lobban, M., *et. al.* 1994]. The cerebellum, brain stem and mid brain expressed PDE4B2 but not DPD, the striatum, hypothalamus, hippocampus and cortex expressed both species while the pituitary was shown not to express either species. The most striking finding [Lobban, M., *et. al.* 1994] was that DPD was found to contribute 13-35% of the total PDE4 activity in brain cytosol and PDE4B2, 40-50% of the total PDE4 activity in the membranes. These figures indicated that the two PDE4B enzymes play a significant role in brain cAMP metabolism.

It has been shown that PDE4B mRNAs expressed in the Sertoli cell are derived from the assembly of 11 exons, with exons 5-10 encoding the catalytic region [Monaco, L., *et. al.* 1994]. This means that five exons code for N-terminal regions which have the potential for alternative splicing and a final exon codes for the C-terminal tail (Figure 3.1.2.). Monaco and colleagues further hypothesised that the mRNA of PDE4B2 is likely to be expressed in brain with an additional 5' exon since exon 1b, found in the Sertoli cell is missing in brain. It is possible therefore that either the splice variants DPD and/or PDE4B2 do not represent full length species and that the species detected and characterised [Colliceli, J., *et. al.* 1989, Swinnen, JV., *et. al.* 1991, Lobban, M., *et. al.* 1994] represent proteolytic

products of larger proteins. They may, however, have represented true species and further splice variants may be discovered.

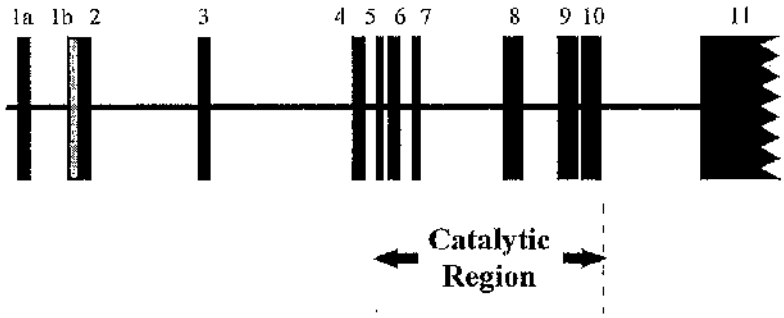

Figure 3.1.2. Proposed gene structure of the PDE4B gene.

Shows the exons as filled boxes, numbered, and the introns as connecting lines of the PDE4B gene. The hatched box represents the coding region derived from the Sertoli cell intron start site, a region which is absent in brain. The box marked 1a represents the upstream exons utilised in brain mRNA. Its presence was inferred by PCR amplification data on brain mRNA and by comparison with the *Drosophila dunce* gene. [From Monaco, *et. al.* 1994].

Insulin is known to reduce cAMP levels in hepatocytes by the activation of phosphodiesterases [Loten, EG. and Sneyd, JGT. 1970]. This is due to the activation of at least three phosphodiesterases. One of these appears to be a PDE4 form, another of these is a PDE3 species that can also be stimulated by glucagon [Heyworth, CM., *et. al.* 1983]. Activation of a PDE3 species by insulin has also been demonstrated in adipocytes and this occurs via a serine phosphorylation [Degerman, E., *et. al.* 1990]. An additional PDE species is also thought to be

activated, althought its identity is not known [Degerman, E., *et. al.* 1990]. Preliminary data in this laboratory had indicated that a PDE4 species from adipocytes could be activated in response to insulin and that this might be a PDE4B form. This chapter describes work which investigates this.

3.2. RESULTS AND DISCUSSION

3.2.1. Detection of DPD by immunoblotting using polyclonal antibodies.

Three batches of antisera, were available that had been made in three separate rabbits, using the same peptide which was chosen to represent the sequence 'A^{508}-T-E-D-K-S-L-I-D-T^{517}' found in the C-terminus of both PDE4B2 and DPD but no other PDE species. The efficiency of these antibodies was tested using DPD expressed in COS cells (figure 3.2.1.). It was evident that each of the three antisera recognised DPD. Both the antisera 653 and 652 recognised a single band with no antigenicity seen with their pre-immune serum, whereas antisera 2296 gave good recognition of DPD but also recognised a lower band of ~38kDa. This 38kDa band was, however, also seen in non-transfected COS cells and was not considered to be a PDE since no PDE activity could be immunoprecipitated from these cells without transfection with a plasmid designed to express DPD.

3.2.2. Immunoblotting for PDE4B in adipocytes and hepatocytes

Work performed previously in the lab showed that DPD was expressed in both hepatocytes and adipocytes. However, difficulties were experienced in this work when immunoblotting adipocytes and hepatocytes with polyclonal antibodies generated from a peptide sequence found in the C-terminal region of

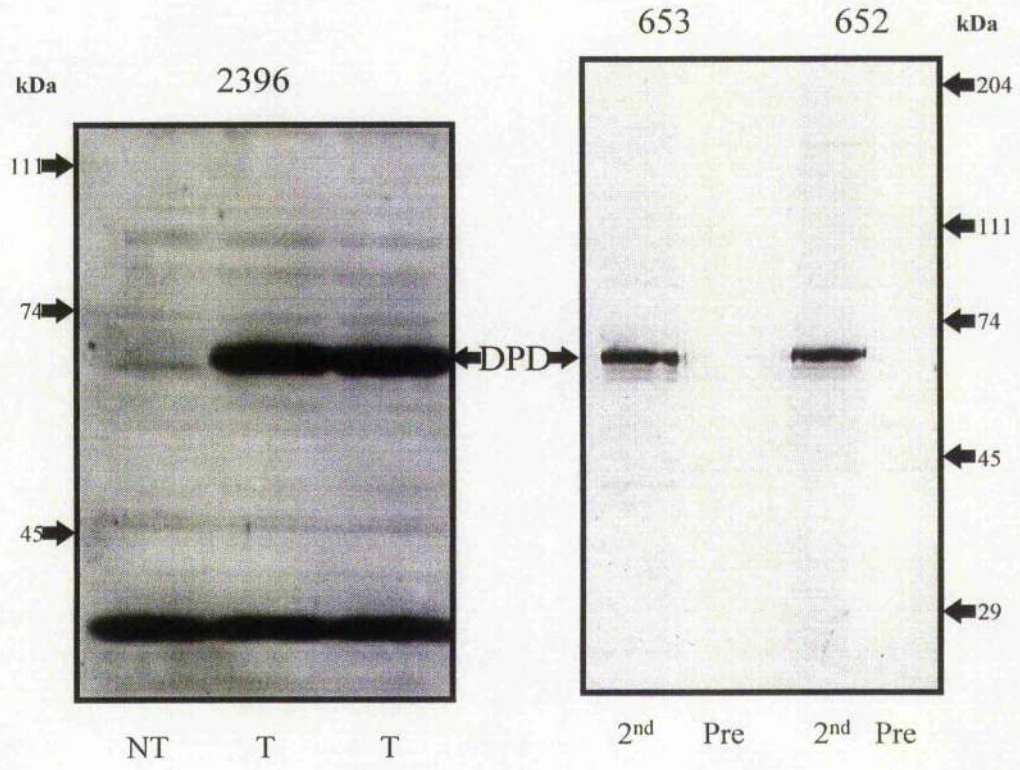

Figure 3.2.1. PDE4B antibodies

Shows the specificity of three polyclonal antisera directed a peptide sequence in the C-terminal region of PDE4B2 and DPD. Antisera 2396 recognised an immunoreactive species of ~59kDa present in COS cells transfected with a plasmid designed to express DPD (lanes 'T') but also detected a non-specific band present in non-transfected COS cells (lane 'NT'). The 2nd bleeds of antisera 652 and 653 recognised the same immunoreactive species of ~59kDa present in COS cells transfected with a plasmid designed to express DPD (lanes '2nd'), with no detection with the pre-immune serum from the rabbits (lanes 'Pre').

both PDE4B2 and DPD. A number of immunoblots on both crude, membrane and cytosol fractions from both adipocytes and hepatocytes, separated on 8% polyacrylamide SDS gels did not detect any immunoreactive species. It was, however, shown that PDE activity could be immunoprecipitated using this antisera (see below) and that the antibody recognised COS cell expressed DPD (see below). Immunoblotting of immunoprecipitated DPD was unsuccessful since the immunoglobulin G (IgG) band of the antisera used to immunoprecipitate DPD co-migrated with DPD. The antisera used for detection was the same as used for immunoprecipitation. Consequently the enzyme-linked second antisera also recognised the immunoprecipitating IgG which was visible as a large band on the blot, masking DPD.

It was known that PDEs were susceptible to proteolysis [Davis, RL. 1990, Conti, M., *et. al.* 1991] and although protease inhibitors were present at all stages of preparing cellular fractions from both rat hepatocytes and epididymal adipocytes, a point of concern was that DPD might have been degraded during the lengthy preparative procedure. In order to try and minimise this problem, both liver and fat pads were dissected directly into boiling 2% SDS in PBS, rapidly minced, homogenised and centrifuged at 650g for 10 minutes to pellet the debris. To the supernatant, an equal volume of Laemmli buffer added the samples subjected to SDS-PAGE and immunoblotted (figure 3.2.2.). Immunoreactive bands, consistent with the size of DPD (59kDa), were seen in both hepatocytes and adipocytes, although levels of detection were weak.

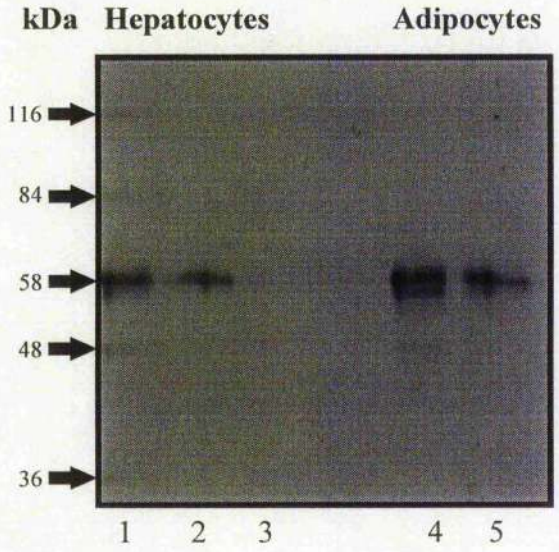

Figure 3.2.2. DPD in adipocytes and hepatocytes

Shows an immunoblot using antisera 653 of rat adipocytes from epididymal fat pads and hepatocytes homogenised directly in boiling 2% SDS. Lane '1' hepatocytes, lane '2' hepatocytes diluted 1:10, lane '3' hepatocytes diluted 1:100, lane '4' adipocytes, lane '5' adipocytes diluted 1:10. The bands seen on the immunoblot are ~59kDa, the same molecular weight as DPD.

3.2.3. Effect of hormones on PDE activity of PDE4B in adipocytes

3.2.3.1. Effect of insulin and isoprenaline

Insulin has been shown to activate a PDE3 in adipocytes [Degerman, E., *et. al.* 1990]. It had been suggested, given the action of insulin in hepatocytes on PDE4 and the lack of correlation between PDE3 phosphorylation and total PDE activation in adipocytes that another PDE was involved in this activation [Beltman, J., *et. al.* 1993]. Preliminary data in the lab also suggested that a PDE4B may be activated by insulin in adipocytes. For this reason the action of insulin on intact rat adipocytes was investigated. Isoprenaline was also used to see if PDE4B was activated in response to elevated cAMP levels.

Intact adipocytes were incubated for 10 minutes with 100nM insulin, 1μM isoprenaline or both together, in the presence of a protease inhibitor cocktail and the protein phosphatase inhibitors okadaic acid [Cohen, P., *et. al.* 1990] and sodium orthovanadate [Swarup, G., *et. al.* 1982]. The phosphatase inhibitors were present to maintain any activation that might have occurred via a phosphorylation. Following incubation, the adipocytes were lysed and PDE4B was immunoprecipitated using antisera 653. The immunoprecipitated PDE4B activity was then measured by PDE assay and it was evident that a two-fold activation was seen with insulin which was shown with a Students *t*-test to be statistically significant ($p<0.05$). This activation was consistent over three experiments (figure 3.2.3.). Although a smaller activation was also seen with isoprenaline, this activation was not statistically significant. Treatment of the adipocytes with isoprenaline and insulin together had no effect on the immunoprecipitated PDE4B

activity. While isoprenaline alone had no significant effect, it clearly attenuated the effect of insulin on the adipocyte PDE4B activity.

The method of activation of PDE4B by insulin was not likely to be via increased production of protein since the time-scale of the experiment was only 10 minutes. Activation must have been either by a phosphorylation or by an allosteric interaction. No phosphotyrosine could be detected on either stimulated or unstimulated adipocyte PDE4B by immunoblotting with an anti-phosphotyrosyl monoclonal antibody, this does not entirely rule out the possibility that a tyrosine phosphorylation occurred but indicates that it is more likely to be either a serine / threonine phosphorylation or another interaction.

3.2.3.2. Time course of activation of PDE4B in adipocytes by insulin.

In order to determine how rapidly the PDE4B from adipocytes was activated by insulin, a time-course was performed (figure 3.2.4.). DPD (PDE4B) could be seen to be activated very rapidly, an increase in activity seen after only one minute and maximal activity at two minutes, after which a gradual reduction of activity occurred. If the activation was via a phosphorylation, then the activation would be expected to be maintained since phosphatase inhibitors were present throughout. However, an independent desensitisation mechanism may be inactivating DPD following activation or, indeed, the activation may not be mediated via a phosphorylation. The activation of DPD did not reflect the activation of the total PDE4 activity which occurred more slowly, peaking at 10

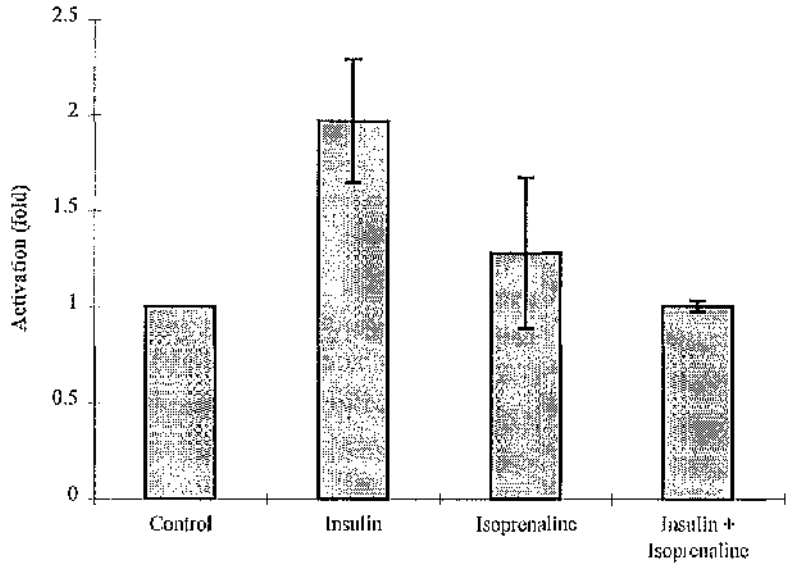

Figure 3.2.3. Effect of insulin and isoprenaline on PDE4B from adipocytes.

Adipocytes prepared from rat epididymal fat pads and equilibrated in low phosphate Krebs buffer for 20mins were treated with insulin (100nM) and isoprenaline (1μM) in the presence of phosphatase inhibitors okadaic acid (1μM) and orthovanadate (100μM) for 10mins. The cells were lysed on ice and PDE4B immunoprecipitated. Graph shows the PDE activity, measured as given in the methods at 1μM cAMP and 30°C, associated with identical protein concentrations of immunoprecipitated enzyme. 'Control' Shows samples incubated with okadaic acid and orthovanadate only. Values are activation over control ± standard error for three separate experiments.

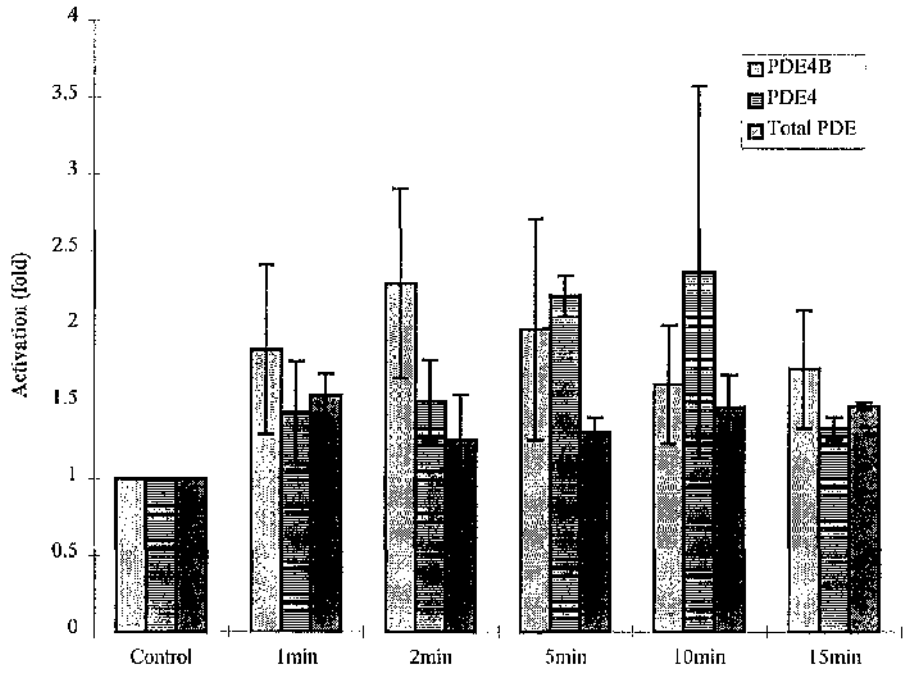

Figure 3.2.4. Time course for insulin activation of PDE4B

Shows the activation of PDE activity, at 1μM cAMP and 30°C of immunoprecipitated PDE4B, all PDE4 activity (measured by adding rolipram (10μM), a PDE4 specific inhibitor, to the PDE assay) and total adipocyte PDE activity. Adipocytes were treated with 100nM insulin at 37°C for the times indicated. Values are expressed as relative to 'control' which represents untreated cells ± standard error for three experiments.

minutes, perhaps indicting that DPD was not the only PDE4 that is regulated by insulin in adipocytes. Very little overall effect of insulin was seen on total PDE activity. However, DPD constituted <2% of the total PDE activity and given that the total PDE activity was very high, the visible effect of insulin on DPD would have been negligible overall. The net effect of insulin on total PDE activity would have been expected to be higher due to the reported effect of insulin on PDE3 [Degerman, E., *et. al.* 1990], the reasons remain unknown.

3.2.4. Difficulties with hormonal activation of DPD

Following the initial set of experiments (above), where insulin was shown to increase the catalytic activity of DPD in intact epididymal fat pads of Sprague Dawley rats, a number of problems were encountered. The most significant of these was the complete loss insulin stimulation of DPD, even though adipocytes were prepared and treated identically to previously. A number of explanations were possible; rats supplied may have been under varying degrees of stress or simply fed state, the adipocytes may not have been supplied with adequate conditions during incubation, or problems with infections in the University's Animal House at the time may have had adverse effects on tissue prepared from the rats.

3.2.4.1. Possible solutions

In order to investigate the change in insulin sensitivity of DPD, the first additional measure that taken was starving the rats overnight in an attempt to regulate their hormonal condition at the time the fat pads were dissected. This had no effect. The next steps were to supplement the incubation medium for the

adipocytes with various nutrients. Throughout a large number of experiments, the incubation medium was supplemented with combinations of glucose (2mM), adenosine (200nM), adenosine deaminase (1U/ml) and (-)-N^6-(2-phenylisopropyl) adenosine (3nM) (PIA) which is an analogue of adenosine that cannot be metabolised. None of these supplements had any effect and the insulin response curve remained completely flat (figure 3.2.5.).

It would appear that after originally demonstrating that DPD could be activated by insulin, it was shown that insulin did not have any effect on DPD from intact adipocytes, thus giving two completely opposed sets of data. Consequently, it was not possible to draw any conclusions about the activation of DPD by insulin. Problems with infection in the University's Animal House continued and it was decided to look for expression of DPD in cell lines in order for its regulation by insulin to be characterised.

3.2.5. Expression of DPD in cell lines

Given that difficulties were incurred in studies with enzyme from Sprague Dawley rats, a series of cell lines were examined for expression of DPD.

3.2.5.1. Expression in 3T3L1 fibroblasts and adipocytes.

The 3T3L1 cells are fibroblasts that can be differentiated in adipocytes. Flasks of 3T3L1 fibroblasts and adipocytes were kindly donated by Gwynn Gould (Department of Biochemistry, University of Glasgow). The cells were scraped from the flasks directly into Laemmli buffer when they had reached 90% confluency and immediately boiled to avoid proteolysis. They were then subjected

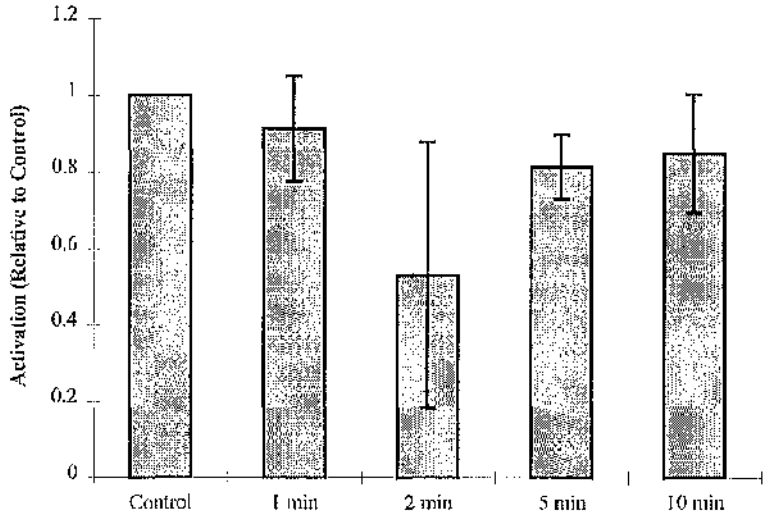

Figure 3.2.5. No activation of DPD by insulin

Adipocytes prepared from rat epididymal fat pads and equilibrated in low phosphate Krebs buffer supplemented with glucose (2mM) and PIA (2nM) for 20mins were treated with insulin (100nM) and isoprenaline (1μM) in the presence of phosphatase inhibitors okadaic acid (1μM) and orthovanadate (100μM) for 10mins. The cells were lysed on ice and PDE4B immunoprecipitated with antisera 653. Graph shows the PDE activity associated with identical amounts of immunoprecipitated enzyme. 'Control' Shows samples incubated with okadaic acid (1μM) and orthovanadate (100μM) only. Values are expressed relative to control ± standard error for three experiments.

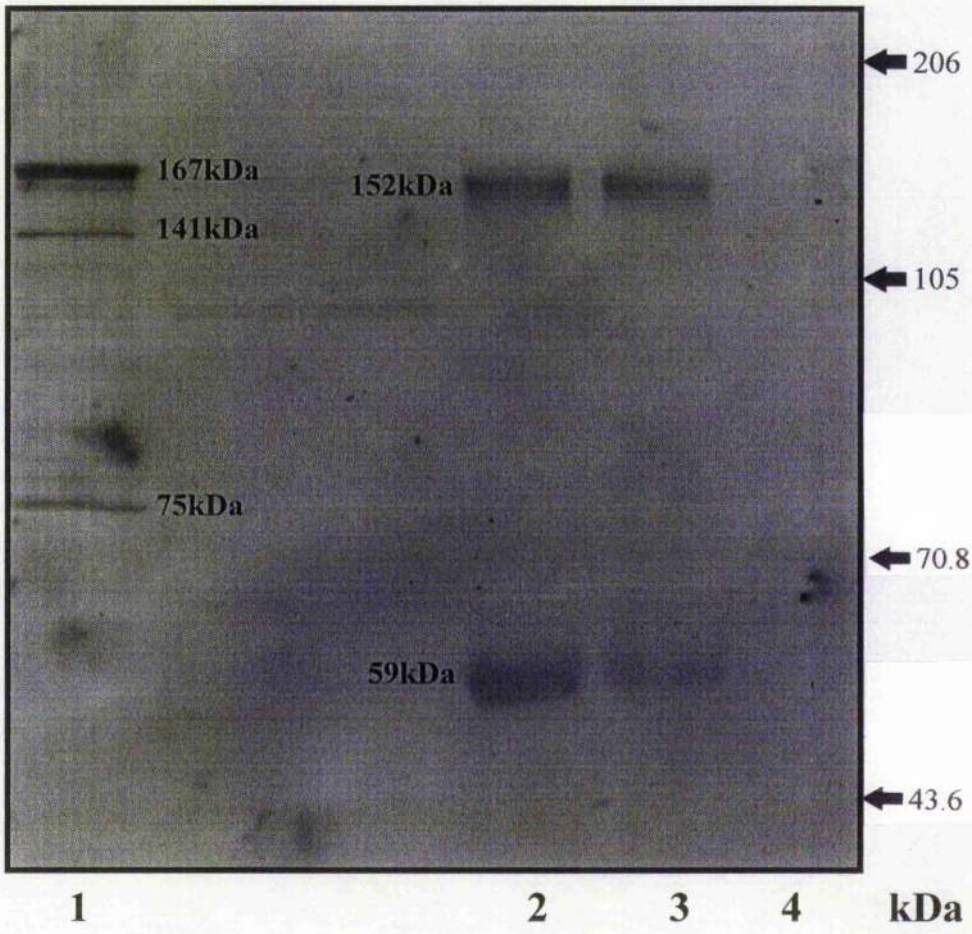

Figure 3.2.6. Immunoblot with anti-PDE4B on 3T3L1 fibroblasts and adipocytes

Cells from a single 90% confluent flask of either 3T3L1 fibroblasts (lanes '2' and '3') or 3T3L1 adipocytes (lane 4) were scraped into 300µl of Laemmli buffer and boiled for 5mins. 50µl were then loaded onto an 8% polyacrylamide gel which was probed with antisera 653. Lane '1' represents 200µg of a crude homogenised Sprague Dawleyrat brain preparation used as a positive control.

to SDS-PAGE and immunoblotted with antisera 653 (figure 3.2.6.). The 3T3L1 fibroblasts showed species of ~59kDa and 152kDa, the 59kDa species was likely to be DPD since it had the same apparent molecular weight. 3T3L1 adipocytes, however, showed no such immunoreactive species, perhaps indicating that expression of DPD was changed with differentiation of this cell line. The nature of the additional species that also seen in the fibroblasts with an apparent molecular weight of about 150-153kDa was not determined since no attempt was made to immunoprecipitate PDE activity with antisera 653 from 3T3L1 fibroblasts. Rat brain was used as a positive control on this immunoblot since it was reported to express DPD to high levels (13-35% cytosolic PDE4 activity) [Lobban, M., *et. al.* 1994] and intriguingly, no species corresponding to the reported size of 59kDa for DPD was seen. Three bands were however visualised, each with much larger molecular weights than expected for DPD, ~75, ~141 and ~167kDa. These sizes were consistent through four separate immunoblots. It is possible that the smaller band of 75kDa may have been PDE4B2, although the reported apparent molecular weight is 64kDa [Lobban, M., *et. al.* 1994]. Possible explanations for these inconsistencies will be discussed in the following sections.

3.2.5.2. Expression in NCB20 and NG108 cell lines.

Cells from NCB20s and NG108s, a mouse neuroblastoma rat glioma hybrid cell line, were scraped directly from the flask into Laemmli buffer and boiled to avoid any potential proteolysis. Three immunoreactive bands were seen (figure 3.2.7.) for each of the cell lines. One of these corresponded to the apparent molecular weight of DPD (59kDa), the other two were much larger in size, being

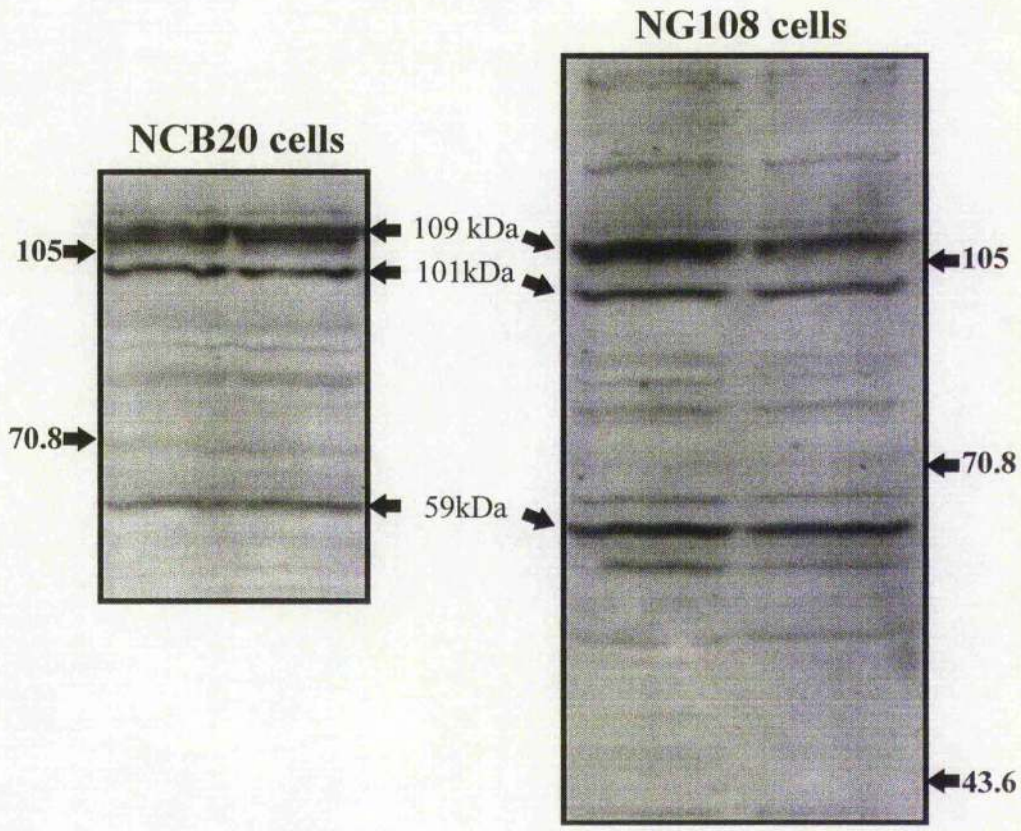

Figure 3.2.7. Immunoblots for PDE4B with NG108 and NCB20 cell lines.

Cells from a single 90% confluent flask of either NG108 or NCB20 cells were scraped into 300µl of Laemmli buffer and boiled for 5mins. 50µl were then loaded onto an 8% polyacrylamide gel which was probed with a antisera 653 to recognise PDE4B species.

approximately 101kDa and 109kDa. Evidently these were different in size to those seen in either rat brain or 3T3L1 fibroblasts.

3.2.5.3. Evidence for multiple splice variants?

It was obvious that a number of immunoreactive species were being detected by immunoblotting various cell lines with antisera directed to a peptide sequence within the C-terminal region of PDE4B species. One might hypothesise that these are 'real' splice variants of the PDE4B gene, perhaps generated by alternative splicing of the 5'region of the gene, as predicted by Monaco [Monaco, L., *et. al.* 1994] (see introduction and conclusions). Perhaps the most striking finding was the lack of any immunoreactive band from rat brain that would represent either DPD or PDE4B2 but instead the existence of three much larger species. These suggestions will be discussed in view of more recently published data on the nature of PDE4B splice variants in the conclusions at the end of this chapter.

3.2.6. Dose response to rolipram of Immunoprecipitated PDE4B from NG108 cells.

In order to ascertain whether or not the species recognised by the anti-PDE4B antisera, 653, were PDE4 species, they were immunoprecipitated from NG108 cells and a dose response to rolipram, the PDE4 specific inhibitor, performed (figure 3.2.8.). It was evident that the immunoprecipitated PDE activity was extremely sensitive to rolipram, a specific PDE4 inhibitor, as the IC_{50} was approximately 0.1μM, which was lower than the figure published for PDE4B, 1μM. Although figure 3.2.8. represents only a single experiment and to obtain an

accurate IC_{50}, the range of rolipram concentrations needed to be lowered, a number of further experiments on material immunoprecipitated from NG108 cells showed the PDE activity immunoprecipitated by the PDE4B antibody to be completely inhibited by rolipram at 10μM, a concentration at which rolipram inhibits all PDE4s but no other PDE family [Reeves, ML., *et. al.* 1987, Torphy, TJ. and Cieslinski, LB. 1990, Souness, JE. and Scott, LC. 1993].

3.2.7. Separation of the PDE4 species expressed in NG108 cells by non-denaturing polyacrylamide gel electrophoresis.

It has been demonstrated that NG108 cells expressed a PDE activity that was recognised by the PDE4B antisera 653 and was sensitive to the PDE4 inhibitor, rolipram. However, it was not know if this activity was solely as a result of the species of 59kDa that corresponded to DPD on immunoblots or if this activity was also contributed to by the other two much larger species of about 101 and 109kDa. In an attempt to resolve these activities, cytosolic fractions from NG108 cells were subjected to non-denaturing PAGE as described in methods. Each non-denaturing gel was snap-frozen, sliced into thin slices and the PDE activity eluted overnight at 4°C. The PDE activity eluted from each of the slices was measured with and without the PDE4 inhibitor rolipram (figure 3.2.9.). Unfortunately, using the given conditions, no PDE species migrated very far into the gel and consequently the activities were not resolved. In order to get around this problem, either the gel would have had to be run for a much longer period of time, perhaps with a different dye as indicator or the acrylamide concentrations

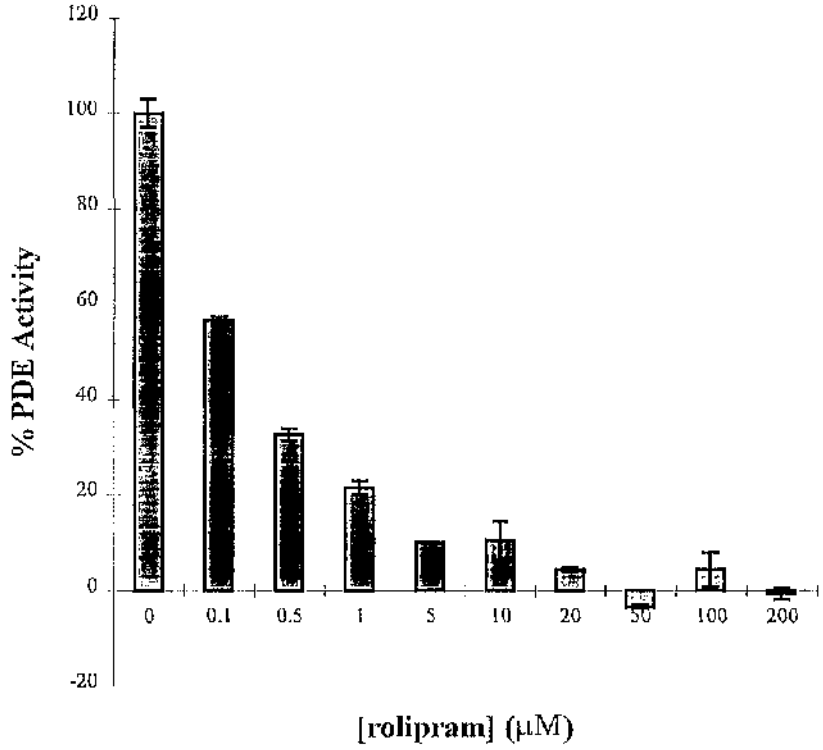

Figure 3.2.8. Dose response of NG108 PDE4B to rolipram

Shows a single experiment with PDE4B immunoprecipitated from NG108 cells on which a PDE assay was performed for 10 minutes at 30°C at 1μM cAMP, in the presence of varying concentrations of the PDE4 specific inhibitor rolipram. Values are % of activity with no added rolipram ± standard error triplicate values within the experiment.

could have been changed to get better resolution. The pH was at its maximal limits for such a gel so changing the pH was not a feasible solution.

Immunoblotting of the two peaks that were rich in PDE4 activity demonstrated that the peak that ran the farthest into the gel contained all three species detected by PDE4B antisera 653 on SDS-PAGE. It also contained rpde6 and RD1, which are PDE4A species so the experiment failed to resolve the three immunoreactive species detected by antisera 653 into fractions that would enable their biochemical characterisation.

3.3. CONCLUSIONS

A number of difficulties were experienced with PDE4B., Recent data, however, casts some light onto these. A human homologue to DPD has been identified, TM72 (HSPDE4B1). However, this is greatly extended at its N-terminus and is still not reported to be a full length clone (figure 3.3.1.) [Bolger, G., *et. al.* 1993]. A further species was then identified that, like TM72 and PDE4B2 (RNPDE4B2), was identical to DPD apart from a unique N-terminal extension, PDE4B3 [Owens, R., and Houslay, MD., personal communication]. This data indicates that the point at which DPD was reported to start represents a common splice junction in PDE4Bs and it would seem likely that the species identified as DPD on immunoblots in this thesis was either a proteolytic fragment of larger species or PDE4B2. The human B1 and B3 clones identified have apparent molecular weights of 103kDa and 102kDa respectively, on immunoblots [Huston, E. and Houslay, MD., unpublished data]. These sizes are not too

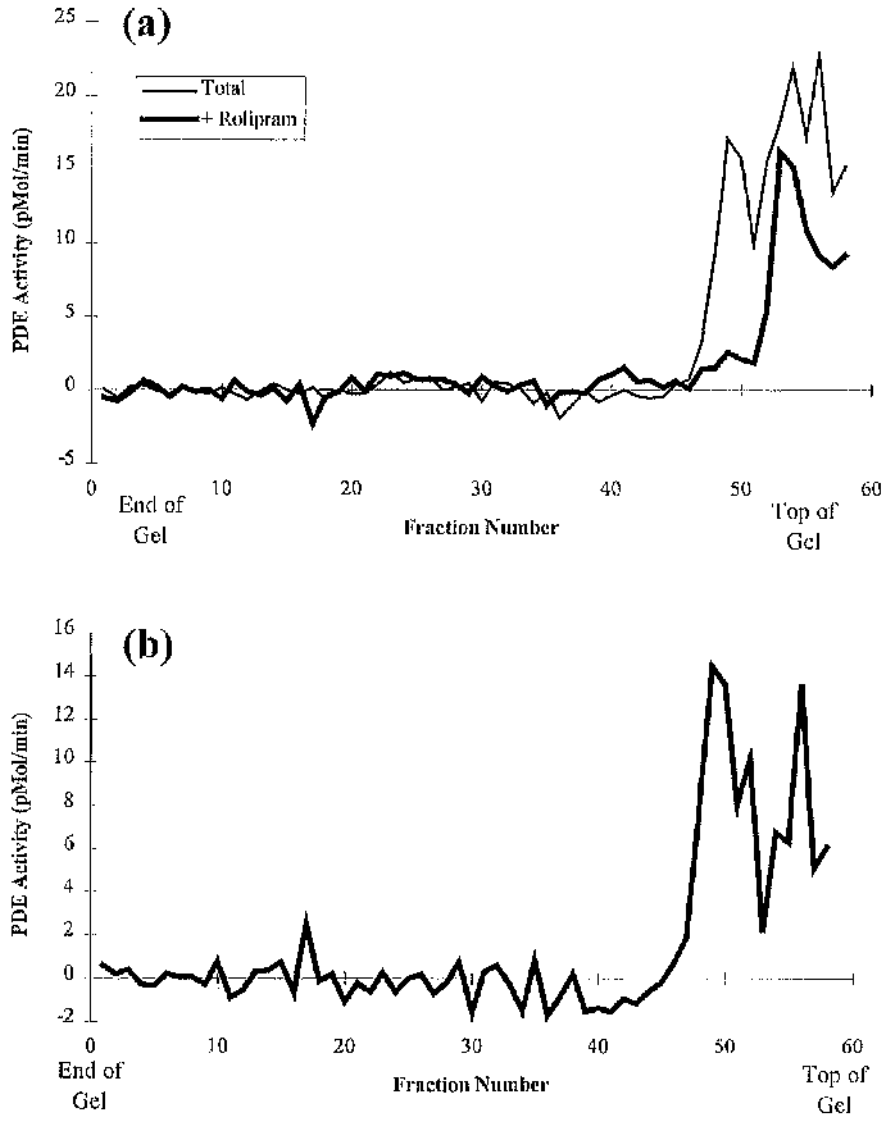

Figure 3.2.9. Non-denaturing PAGE of PDEs expressed in NG108 cells

Panel (a) shows the PDE activity of the slices of the gel ± rolipram. 600μg of cytosol from NG108 cells were loaded onto the gel which was run until the dye-front (Amaranth) reached the bottom of the gel. The PDE activity was elute from the gel slices prior to assay. Panel (b) shows the PDE4 activity of the slices, represented as the total PDE activity minus the activity with 10μM rolipram.

dissimilar to the bands seen in NG108 and NCB20cells of 101kDa and 109kDa. On this basis, the species detected may have represented true rat PDE4B splice variants.

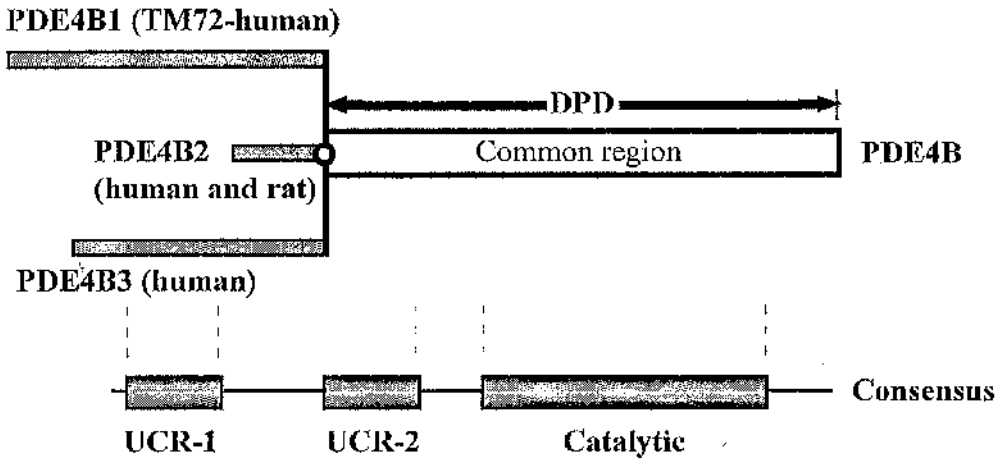

Figure 3.3.1. Schematic representation of human PDE4B species

Shows the current PDE4B species from rat and human. The rat splice variant DPD is identical to all species from the common splice junction (empty circle). Variable domains are shown as shaded rectangles. The positions of UCR1, UCR2 and the putative catalytic region are indicated.

The work of Lobban [Lobban, M., *et. al.* 1994] only detected low MW species in immunoblots of rat brain. However, it should be noted that PDE4B2 was found entirely membrane associated and DPD cytosolic, implicating the region of PDE4B2 that is not found in DPD as being responsible for membrane attachment. In the work performed by Lobban, PDE4B2 was detected by two separate antisera, one directed to a peptide found in its unique N-terminal region

and one made with a peptide in the C-terminal region common in all PDE4B splice variants. DPD was however only detected by the C-terminal antisera, which also recognised PDE4B2. It is possible therefore that the species characterised as DPD was a proteolysed form of PDE4B2. The fact that DPD was cytosolic and PDE4B2 membrane associated can be explained simply by the fact that the N-terminal region of PDE4B2, determining membrane association was clipped off, leaving a fully active cytosolic PDE4B species.

The activation of PDE4B by insulin remains questionable, due to the conflicting data given. A possible mechanism to explain the properties seen is that insulin has been shown to activate the MAP kinase cascade [reviewed White, MF. and Kahn, CR. 1994] which may have led to the phosphorylation and consequent activation of PDE4B within the time scale given. Isoprenaline elevates cAMP levels [Keely, SL. 1979], activating PKA, one of the targets for which is Raf. Phosphorylation of Raf by PKA inactivates it and since Raf is required for the insulin activation of the MAPK cascade [Denton, RM. and Tavare, JM. 1995, White, MF. and Kahn, CR. 1994], this might explain why isoprenaline attenuated the activation of PDE4B by insulin. However, insulin activation of PDE4B was not consistent.

Due to the difficulties experienced at the time, study of PDE4B was abandoned and the following chapters investigate the role of the unique N-terminal splice regions of other PDE4 species in regulating subcellular distribution and protein-protein interactions.

Chapter 4

SH3 Domain Interaction of PDE4A

4.1. INTRODUCTION

The PDE4 family is encoded by four genes, PDE4A, PDE4B, PDE4C and PDE4D. The PDE4A gene lies between the genes for TYK2 and the LDL receptor on chromosome 19 and is extremely complex, having in excess of 14 exons [Olsen, A., Sullivan, M. and Houslay, MD. unpublished data]. Alternative splicing of the PDE4A gene leads, predominantly, to 5' domain swaps, which produces a number of splice variants, each with unique N-terminal domains [Bolger, G. *et. al.* 1994, Conti, M., *et. al.* 1995]. In the rat, there are three splice variants of the PDE4A gene, RD1 [Davis, RL., *et. al.* 1989], rpde6 [Bolger, G., *et. al.* 1994a, McPhee, I., *et. al.* 1995] and rpde39 [Bolger, G., *et. al.* 1996], Figure 4.1.1. In humans three PDE4A splice variants have been isolated to date. Of these, only one, hPDE46, the human homologue of rpde6, has been characterised [Bolger, G., *et. al.* 1993, Bolger, G., *et. al.* 1996]. All active PDE4A splice variants do however have identical 'core'-catalytic units, a phenomenon which is displayed by each of the PDE4 genes. There are however two additional splice variants that possess unique N- and C- terminal regions. These, however, encode catalytically inactive species due to alternative splicing, leading to premature truncation within the putative catalytic region [Horton, Y., *et. al.* 1995, Bolger, G., *et. al.* 1993]. The functional significance of these proteins with no phosphodiesterase activity has yet to be determined.

Each of the rat PDE4A splice variants has a profoundly different expression pattern. RD1 is found exclusively in the brain [Bolger, G. 1994, Davis, RL., *et. al.* 1989, Bolger, G., 1994a, Shakur, Y., *et. al.* 1995], rpde39 is found in

the testes [Bolger, G., *et. al.* 1996] and hepatocytes [Zeng, L. and Houslay, MD., unpublished data] and rpde6 is expressed at its' highest level the brain [Bolger, G., 1994a]. Even though rpde6 and RD1 are both expressed in brain, their expression patterns differ throughout the brain regions [Bolger, G., 1994a, Shakur, Y., *et. al.* 1995, Section 1.3.5.2.], which might imply that they have unique functional roles.

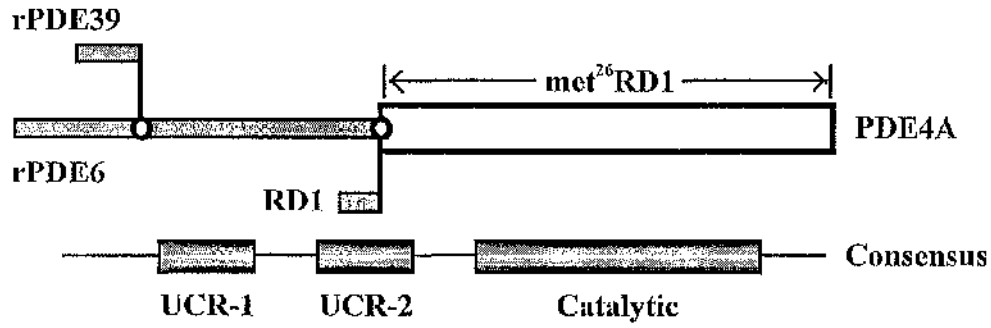

Figure 4.1.1. Splice variant diagram for rat PDE4A.

Shows splice variants of the PDE4A gene from rat, rpde6, rpde39 and RD1. met^{26}RD1 is an engineered truncation that lacks any N-terminal splice region. The empty rectangle represents the core C-terminal catalytic region that is identical in each of the rat PDE4As. The shaded areas represent alternatively spliced regions and the empty circles splice junctions. The positions of UCR1, UCR2 and the putative catalytic region are indicated.

Each of the rat PDE4A splice variants have unique subcellular distributions. RD1 is found to be 100% membrane associated when found in brain [Shakur, Y., *et. al.* 1995] and when transiently expressed in both COS1 and COS7 cells [McPhee, I., *et. al.* 1995, Shakur, Y., *et. al.* 1993]. met^{26}RD1, however, is

found as a fully active enzyme which is expressed 100% in the cytosol [McPhee, I., *et. al.* 1995]. This has led to the proposal that the membrane association of RD1 is conferred by its N-terminal splice region [Scotland, G. and Houslay, M.D. 1995]. This was confirmed by the generation of a chimera of the N-terminal region of RD1 fused to the N-terminus of a cytosolic bacterial enzyme, chloramphenicol acetyl transferase (CAT). This chimera was found to be 100% membrane associated when expressed in COS cells [Scotland, G. and Houslay, M.D. 1995].

The subcellular distribution of rpde6 and rpde39, however, is not as clear cut. In contrast with RD1, which is 100% membrane associated, rpde39 is approximately 15% associated with the membrane fraction and the remainder found in the cytosolic fraction [Bolger, G., *et. al.* 1996]. Similarly, rpde6 is found distributed between the cytosol, membrane (P2 pellet) and also the low speed pellet (P1 pellet); 74%, 13% and 13% respectively [McPhee, I., *et. al.* 1995]. RD1, can be removed from the membrane by washing with very low concentrations of the detergent Triton X-100 [Scotland, G. and Houslay, M.D. 1995]. However, rpde6 and rpde39 cannot be removed by using a combination of 1M NaCl and 4% Triton X-100 [McPhee, I., *et. al.* 1995, Bolger, G., *et. al.* 1996]. It would be expected that any association with integral membrane proteins would be disrupted under such conditions. This might imply that rpde6 and rpde39 are associated with cytoskeletal structures that are associated with membranes and that such remnants are not disrupted by high salt and detergent [Slusarewicz, P., *et. al.* 1994, Jackson, SP., *et. al.* 1994]. There is no sequence homology between the N-terminal region of rpde6 or rpde39 and the membrane targeting domain of RD1 [McPhee, I., *et. al.*

1995], which suggests that there is a fundamental difference in the method of membrane association between RD1 and rpde6/39.

The extreme N-terminal sequence of rpde6 which is unique to that of rpde39 (figure 4.1.1.) contains a number or proline rich peptide sequences (figure 4.1.2.).

ME**P**P**A**A**P**S**E**RSLSLSL**P**G**P**REGQATLK**PPP**QHLWRG**P**R**T**P

IRIQQRGY**P**DSAERSETERS**P**H**R**P**I**ER**A**DAVDTGDR**P**GLRT

Figure 4.1.2. The unique N-terminal region of rpde6.

Prolines are indicated by large bold text and argenines by bold text. Consensus sequences for binding to SH3 domains are underlined.

These proline-rich sequences fit with consensus CLASS II Src homology domain 3 (SH3) binding sites [Alexandropoulos, K., *et. al.* 1995]. SH3 domains or Src homology domain 3, are distinct globular units of proteins that mediate interaction with proteins containing proline-rich sequences. SH3 domains are found in many proteins, including tyrosyl kinases, adapter proteins and cytoskeletal elements [reviewed Cohen, GB., *et. al.* 1995]. They function to recruit proteins to form functional complexes and to compartmentalise cellular signalling [Mayer, BJ. and Baltimore, D. 1993, Mayer, BJ., *et. al.* 1993, Booker, GW., *et. al.* 1993, Guruprasad, L., *et. al.* 1995, Pawson, T. and Gish, GD. 1992].

In this chapter the potential of rpde6 to interact with SH3 domains is investigated. A protocol using SH3 domains fused to glutathione-S-transferase (GST) was adopted. This protocol involved the production of the fusion protein in bacteria. Once the bacteria were lysed, the fusion protein was purified on sepharose beads that had glutathione chemically linked to them. The beads, with the SH3-GST fusion protein complexed to them, could then be incubated with rpde6 and binding measured by immunodetection or enzyme assay. This method has been used by a number of other investigators [Haefner, R., *et. al.* 1995, Ramos-Morales, F., *et. al.* 1994, Alexandropoulos, K., *et. al.* 1995]. It allows rapid and effective purification of the SH3 domain (Section 2.5.).

4.2. RESULTS AND DISCUSSION

4.2.1. Expression of glutathione-S-transferase-SH3 fusion proteins in E.coli.

Glutathione-S-transferase (GST) fusion proteins were expressed to high levels in E.coli JM109 bacteria using an isopropyl-ß-D-thiogalactopyranoside (IPTG) sensitive promoter as described in section 2.4. Expression was induced with 100μM IPTG for 4-6 hours at 37°C. Figure 4.2.1a shows typical examples of such an induction. The fusion proteins were expressed to levels higher than any of the endogenous bacterial proteins. Figure 4.2.1b shows an example of how the fusion protein was purified from the bacterial extract with the glutathione sepharose beads.

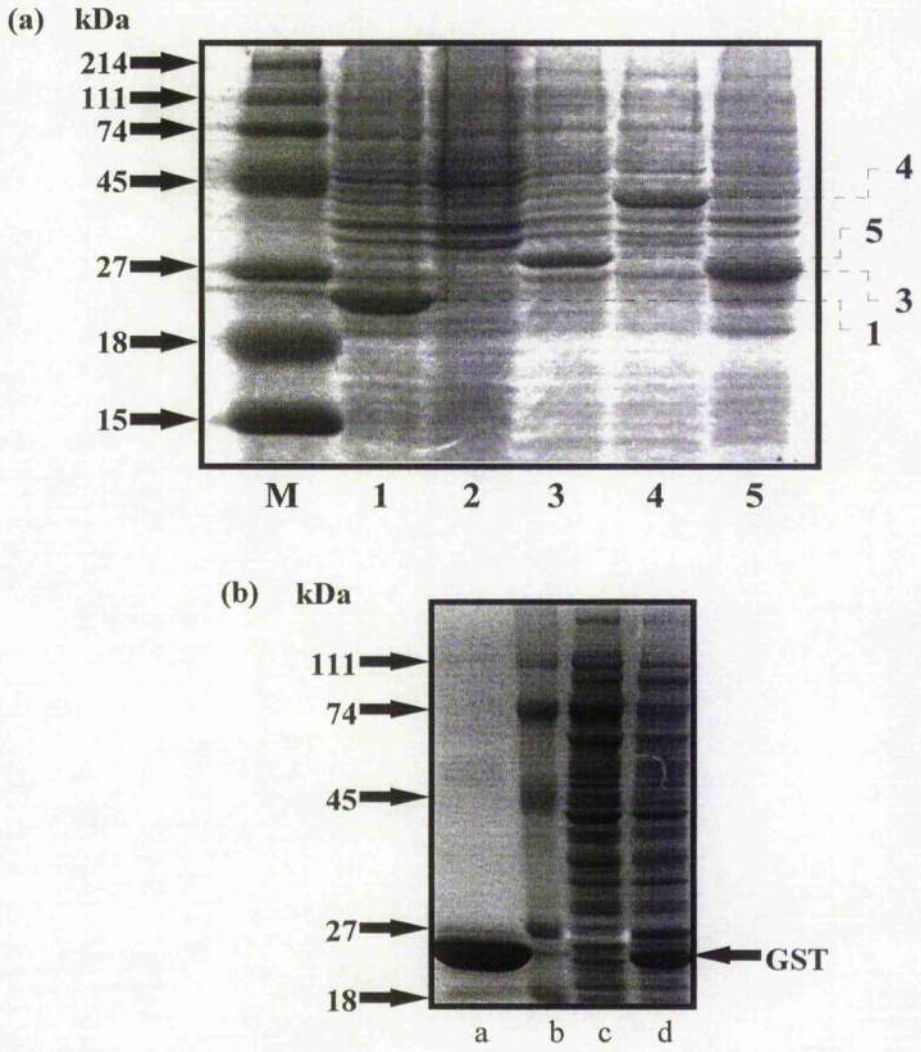

Figure 4.2.1. Induction of GST fusion proteins

Panel (a) shows the induction of GST fusion proteins in E.coli JM109 by 100μM IPTG at 37°C for 5hrs. The fusion proteins can be seen as the bands, indicated with the numbers of their lane. Lane 'M' markers; '1' GST (~25kDa); '2' Not induced; '3' Src SH3-GST (~30kDa); '4' Src SH2-SH3-GST (~40kDa); '5' Fyn SH3-GST (~29kDa). The gel is a 12% polyacrylamide gel stained with Coomassie Blue. Panel (b) shows the purification of GST. Lane (a) Purified GST on glutathione beads, (b) Markers, Bacteria not induced (c) and induced (d) to express GST.

4.2.2. rpde6 binds to the SH3 domain of v-Src.

Using rpde6 from the cytosolic fraction of transfected COS7 cells, preliminary results showed, using a PDE4A-specific polyclonal antisera for detection, that rpde6 can associate with the SH3 domain of v-Src (figure 4.2.2. lane 8). This binding was specific in that rpde6 did not bind to either glutathione beads alone or to glutathione beads with native GST bound to them (figure 4.2.2 lanes 4 and 6). It was therefore evident that the prerequisite for rpde6 to bind was the presence of the SH3 domain of v-Src. Furthermore, washing the GST-Src SH3 beads, with rpde6 attached, with 0.5% Triton X-100 and 0.5M sodium chloride only produced a small reduction in the amount of rpde6 bound, 5-22% as measured by densitometry scanning of four such immunoblots. This is characteristic of the rpde6 that is found associated with pellet fraction of brain and transfected COS cells which could not be removed with either high salt or detergent either [McPhee, I., *et. al.* 1995]. This might suggest that the method of attachment is via an SH3 interaction.

4.2.2.1. All of the cytosolic rpde6 expressed in COS cells will bind to Src SH3

When cytosolic rpde6 from COS cells was presented to the SH3 domains for binding, a number of other COS cell cytosolic proteins will have been present also. Within these will have been proteins that contain SH3 domains that rpde6 could potentially interact with and a number of proteins that potentially could have interacted with the SH3 domain of Src. Thus when cytosolic rpde6 is presented with the Src SH3 domain a degree of competition will have existed for

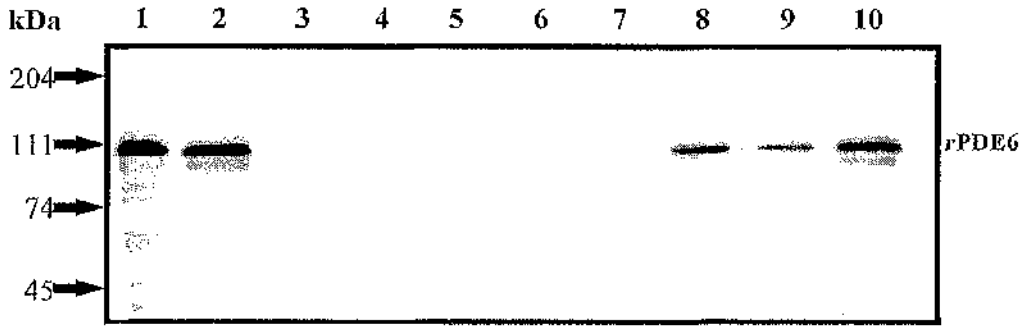

Figure 4.2.2. Binding of rpde6 to the v-Src SH3 domain expressed as a GST fusion protein.

This shows a typical immunoblot using a rat PDE4A specific anti-peptide antiserum that recognises the C-terminus of rpde6. It demonstrates the binding of rpde6 to the SH3 domain of v-Src expressed as a fusion protein. Track 1, membranes (25μg) from rpde6 expressing COS7 cells; track 2, cytosol (25μg) from expressing COS7 cells; track 3, washed glutathione agarose beads after exposure to rpde6; track 4, as track 3 but washed with 0.5M-NaCl + 0.5%-Triton X-100; track 5, blank ; track 6, washed glutathione agarose beads with attached GST (100μg) after exposure to rpde6; track 7, as track 6 but washed with 0.5M-NaCl + 0.5%-Triton X-100; track 8, washed glutathione agarose beads with attached GST-v-Src-SH3 (100μg) after exposure to rpde6; track 9, as track 8 but washed with 0.5M-NaCl + 0.5%-Triton X-100; track 10, supernatant from the GST-v-Src-SH3 glutathione agarose beads after exposure to rpde6.

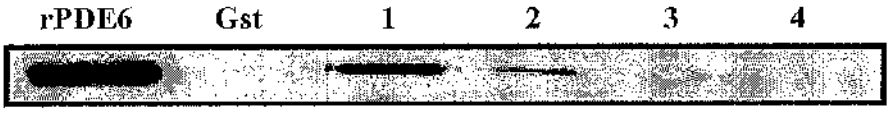

Figure 4.2.3. All of the cytosolic rpde6 from COS cells will bind Src SH3.

Demonstrates that the GST-v-Src-SH3 fusion protein can adsorb all of the rpde6. Here is shown an immunoblot using a rat PDE4A specific antiserum. 'rpde6' shows soluble COS7-cell expressed rpde6; 'Gst' shows GST-containing agarose beads (400μg) exposed to rpde6 and then pelleted and washed; in tracks 1, 2 and 3 are the results of probing agarose beads with attached GST-v-Src-SH3 domain (400μg each) which had been exposed to soluble rpde6, harvested and washed. In this experiment GST-v-Src-SH3 agarose was added to rpde6 and the beads isolated (track 1) as well as a supernatant which was treated again with beads to yield a further pellet (track 2) which was repeated again to yield a pellet (track 3) and a final, clear supernatant (track 4). The band seen was approximately 111kDa. This data represents a typical experiment of one done at least three times

binding. However, figure 4.2.3 shows that all of the cytosolic COS cell rpde6 had the potential to bind to the SH3 domain of Src. This was done by presenting 25μg of cytosolic COS cell rpde6 with three consecutive batches of 400μg Src SH3-GST immobilised on glutathione beads. In order to compare affinities of different SH3 domains for rpde6, quantities of SH3 domain were used such that only a proportion of the rpde6 interacted, in all future experiments.

4.2.3. Measurement of binding by phosphodiesterase enzyme assay

In section 4.2.2., rpde6 was found to interact with the SH3 domain of Src using immunoblotting as the detection method. However, it was not known if rpde6 catalytic activity was affected by binding to the SH3 domain of Src. Measurement of the PDE activity that associated with the SH3 domain of Src required the development of a method to measure PDE activity associated with the GST-Src SH3 beads.

4.2.3.1. Measurement of the proportion of rpde6 that bound to the Src SH3 domain by PDE assay

A method was devised that involved binding 25μg of COS cell cytosol expressing rpde6 to 100μg of the Src SH3 domain, identically to the method for binding used for assay by immunoblotting. After washing of the beads, instead of resuspending the beads in Laemmli buffer for SDS-PAGE, they were resuspended in 100μl of PDE assay buffer. 15-25μl of the resuspended beads were then added directly to a PDE assay which was performed as described in methods. Table 4.1. shows a typical PDE assay. Only about 3% of the rpde6 activity added to the

Table 4.1. Measurement of rpde6 binding to Src-SH3-GST by PDE assay

Shows the proportion of PDE activity that associated with 100μg of the SH3 domain of Src, relative to the quantity of 25μg of rpde6 transfected COS cell cytosol added. Values are expressed as pmols cAMP hydrolysed per minute per 25μg cytosol ± standard error for a single experiment.

	pmols/min/25μg	**% of added**
PDE activity added to SH3 beads	1870 ± 120	100
PDE activity bound to SH3 beads	60 ± 14	3.2
PDE activity recovered *i.e.* unbound	494 ± 1.3	26.4
PDE activity unaccounted for	1316	70.4

beads actually bound to the SH3 domain. Furthermore, if the PDE activity of the supernatant, *i.e.* the fraction containing the PDE that did not become associated, was measured, then discrepancies in the activity figures were found. 3% bound, 26% recovered in the supernatant, which meant that approximately 70% of the activity added was apparently 'lost'.

Possible explanations were that either rpde6 was inactivated upon binding to the src SH3 domain, a large proportion of the PDE activity was loosely associated with the beads after binding but removed in the washes or that the PDE bound to the immobilised SH3 domain, formed a pellet in the assay tube which prevented it from getting access to the substrate.

4.2.3.2. Determination of activity lost in washes

It was reasoned that, if the PDE activity 'lost' when bindings were performed with GST alone was considered as the activity lost through washing and this accounted for in the binding to Src-SH3-GST, the activity bound, unbound and lost should have added up to the total presented for binding. Unless, that is, rpde6 was inactivated upon binding or another factor was contributing to the error. table 4.2. shows that, although a considerable amount of activity was lost in washing GST, considerably more was lost in the washing of Src-SH3-GST beads, indicating that this was not the only factor contributing. A second experiment to confirm this was simply not to wash the beads at all, assuming that a similar quantity of non-specific binding occurred with GST alone, binding could be measured as GST subtracted from Src (table 4.3.). While neither figures added up, GST alone was only missing 9% but about 23% of the activity added was still

Table 4.2. Measurement of PDE activity lost in washing in the binding of rpde6 to Src-SH3-GST

Shows the proportion of PDE activity that associated with 100μg of the SH3 domain of Src and GST alone, relative to the quantity of 25μg of rpde6 transfected COS cell cytosol added. Values are expressed as pmols cAMP hydrolysed per minute per 25μg cytosol ± standard error for a single experiment.

	pmols/min/25μg	% of added
Activity added	1293 ± 38	100
Activity bound to Src SH3	25 ± 2	2
Activity bound to GST	3.5 ± 3	0
Activity in Src SH3 supernatant	195 ± 30	15
Activity in GST supernatant	785 ± 18	61
Activity 'lost' in Src SH3	1073	83
Activity lost in GST washes	504	39
Actual activity 'lost' in Src SH3	569	44

Table 4.3. Assessment of activity lost when no washes were used

Shows the proportion of PDE activity that associated with 100μg of the SH3 domain of Src and GST alone, relative to the quantity of 25μg of rpde6 transfected COS cell cytosol added, when the beads are not washed to remove non-specifically bound PDE. Values are expressed as pmols cAMP hydrolysed per minute per 25μg cytosol ± standard error for a single experiment.

	GST		Src SH3	
	pmol/min/25μg	**% Added**	**pmol/min/25μg**	**% Added**
Activity added	2059 ± 32	100	2059 ± 32	100
Activity on beads	301 ± 10	14	353 ± 6	17
Activity unbound	1603 ± 61	77	1255 ± 55	61
Activity missing	155	9	451	22

missing with Src SH3 domain. These results might have indicated that, perhaps, rpde6 was inactivated upon binding. However, one further possibility existed, and that was, with the rpde6-SH3-GST complex linked to SH3 beads, it formed a pellet at the bottom of the vials very rapidly, which might have prevented catalysis simply by hindering access to substrate.

4.2.3.3. PDE assay following release of fusion protein complex from beads

A simple way of preventing the problem of the beads settling to the bottom of the vial in the PDE assay was to release the GST-SH3-rpde6 complex from the glutathione-sepharose beads using glutathione. One potential problem was that any bound PDE was diluted considerably. In order to compensate for the lower PDE activity, the incubation time of the PDE assay was increased to 30 minutes over which period it still remained linear. Such a procedure was also used to assay the activity contained within various washes, where PDE was also very dilute. Table 4.4 shows a typical experiment. Using this procedure, it was shown that the PDE activity, both bound and unbound, added up to the total presented for binding. This demonstrated that rpde6 was not inactivated upon binding to the SH3 domain of Src. Thus the major factors which had led to discrepancies in the assay was due to bead immobilisation preventing the enzyme from having free access to substrate and activity being lost in the washes.

4.2.4. Time course for binding of rpde6 to the SH3 domain of v-Src

Binding of rpde6 to the SH3 domain of v-Src was shown to be a rapid event, even at 4°C. It can be seen from figure 4.2.4. that maximal binding

Table 4.4. PDE assay with GST-SH3 complex released from beads

Shows the proportion of PDE activity that associated with 100μg of the SH3 domain of Src and GST alone, as a percentage the activity in 25μg of rpde6 transfected COS cell cytosol added. Shows activity released from the beads with 3 washes of 100μl of 10mM glutathione in 10mM Tris, pH 8.0, that that was not released from the beads and the activity that remained in the supernatant or was washed of the beads following binding. Values are expressed as pmols cAMP hydrolysed per minute per 25μg cytosol ± standard error for a single experiment.

	GST	**GST-Src SH3**
Activity left on beads	0.8	1
Activity released from beads	0.9 ± 0.05	6.2 ± 0.07
Activity in supernatant (including washes)	92.8 ± 9.1	88.3 ± 6.8

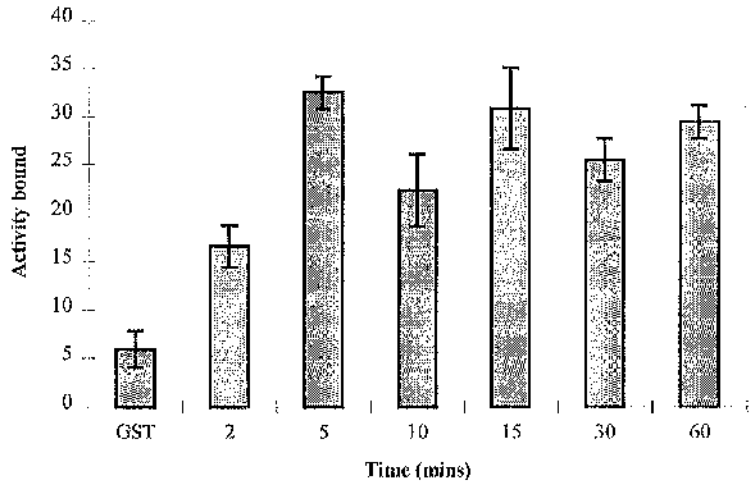

Figure 4.2.4. Time course for the binding of rpde6 to the Src SH3 domain.

In this experiment conditions were chosen (25μg rpde6 transfected COS7-cell cytosol; 200μg v-Src-SH3-GST fusion protein) such that not all of the rpde6 protein would become bound to the GST-v-Src-SH3 fusion protein and the time-course of binding followed by following PDE activity. Binding was done at 4°C Values are given as pmols cAMP hydrolysed/min/25μg of rpde6 added ± standard error. This shows a typical experiment of one done three times.

occurred within five minutes. This demonstrated that not only could the competition for binding be overcome but that this could occur rapidly, perhaps giving some indication as to the affinity of rpde6 for the Src SH3 domain. Previously bindings had been performed for 60 minutes at 4°C but, in light of this data, it was decided that all subsequent bindings be performed for only 10 minutes.

4.2.6. The relationship between binding and amount of SH3 domain used was linear

In previous experiments, only 3-7% of the rpde6 added bound to the SH3 domain. If, however, the quantity of SH3 domain was increased then the proportion of rpde6 that bound increased with a linear fashion (figure 4.2.5.), demonstrating that if the amount of SH3 domain were increased still further, then was likely that all of the rpde6 could be bound, confirming data given in section 4.2.2.1., where all the rpde6 bound to four sequential batches of the Src SH3 domain.

4.2.5. Kinetic properties of rpde6 when bound to Src SH3

It has been demonstrated that the activity of rpde6 was not altered upon binding to the SH3 domain of Src. It has, however, been shown that the IC_{50} for rolipram at (10μM cAMP substrate) differed by an order of magnitude between the membrane-bound and cytosolic forms of rpde6, namely 1.2μM and 0.16μM respectively [McPhee, I., *et. al.* 1995]. Experiments were performed to investigate if the K_m or rolipram inhibition of rpde6 were altered upon binding to SH3 domains.

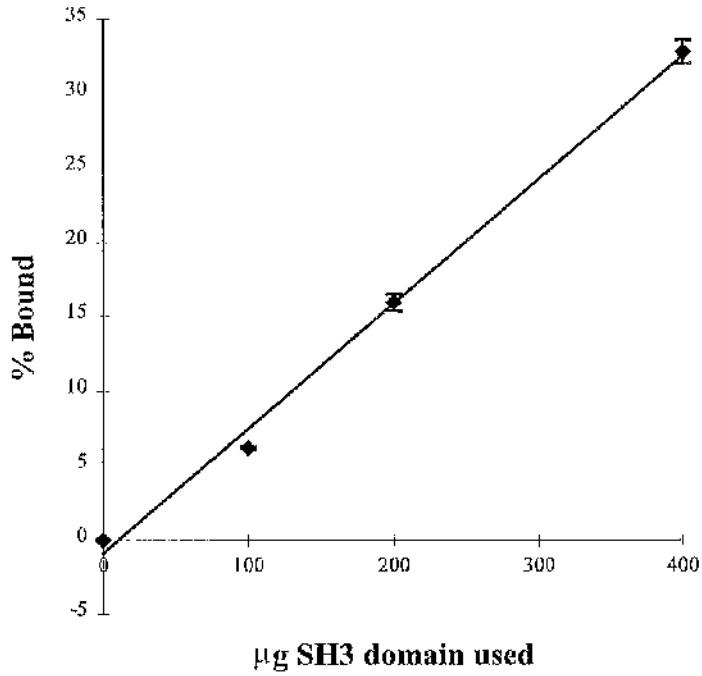

Figure 4.2.5. Relationship between binding and amount of SH3 domain.

Shows the percentage ± standard error for two separate experiments of the rpde6 added in 25µg of COS cytosol that bound to various amounts of the Src SH3 domain linked to glutathione beads. Bindings were performed for 10 minutes at 4°C and the SH3-PDE complex release from the beads for assay.

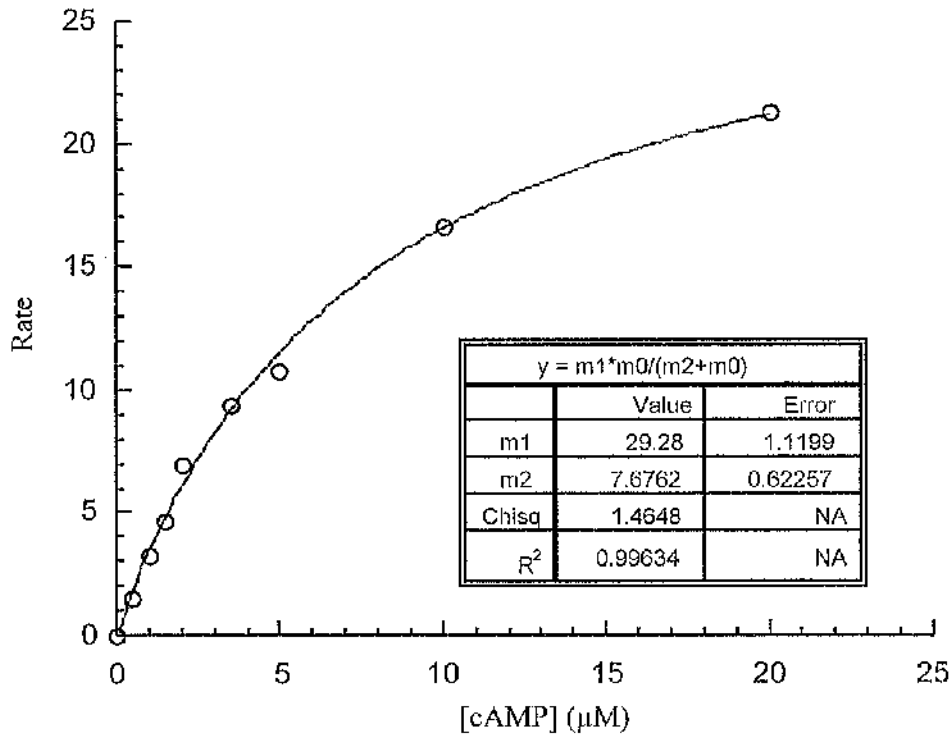

Figure 4.2.6. K_m determination for rpde6 bound to the Src SH3 domain

Shows a plot of concentration of cAMP against the rate of catalysis expressed as pmols cAMP hydrolysed per minute. The inset box shows the kinetic and statistical analysis 'm2' represents K_m and 'm1' the V_{max}. Shows an experiment identical to one done three times.

4.2.5.1. Determination of K_m and V_{max} for rpde6 bound to Src SH3

To determine the K_m of rpde6 bound to the Src SH3 domain, catalytic activity was measured at a number of cAMP concentrations, with assays done at 30°C. The bound PDE-SH3 complex was released from the glutathione beads prior to assay. Figure 4.2.6. shows a typical experiment which gives K_m and apparent V_{max} values that are almost identical to those published for both cytosolic and membrane associated rpde6 [McPhee, I., *et. al.* 1995]. Clearly the kinetic properties with respect to cAMP hydrolysis were unaffected by binding to the SH3 domain of Src.

4.2.5.2 Determination of rolipram IC_{50} values for rpde6 when bound to Src SH3

To investigate if the IC_{50} values for rolipram corresponded to the values for membrane (1.2μM) or cytosolic (0.16μM) rpde6, the inhibition of rpde6 bound to Src SH3 was measured at 0.15μM and 1.5μM rolipram, similar to the IC_{50} values for cytosolic and membrane bound, respectively. Table 4.5. demonstrates that 0.15μM rolipram gave approximately 50% inhibition of the activity of rpde6 bound to Src SH3. This suggests that rpde6 when bound to the Src SH3 domain alone, resembles its cytosolic form.

4.2.7. Other PDE4A splice variants do not bind.

To address the question of which region of rpde6 is responsible for binding to the SH3 domain of Src, the binding of rpde39 and met^{26}RD1 were investigated. met^{26}RD1 lacks any N-terminal splice regions (figure 4.1.1.) and it can be seen

Table 4.5. Inhibition of rpde6 bound to Src SH3 by rolipram

Shows the inhibition of rpde6 by rolipram at two concentrations. Assays were done on rpde6 that had been bound to 400μg of Src SH3 on glutathione beads at 4°C for 10 minutes and the complex then released with 10mM glutathione or 5μg of either cytosolic of membrane associated rpde6. Figures are given ± standard error for three experiments.

	Activity (pmol/min/25μg rpde6)	% Inhibition
rpde6 - Src SH3	2441 ± 32	
rpde6 - Src SH3 + 0.15μM rolipram	1220 ± 17	50 ± 1
rpde6 - Src SH3 + 1.5μM rolipram	445 ± 43	82 ± 2
rpde6 -cytosolic (5μg)	6259 ± 188	
rpde6 - cytosolic (5μg) + 0.15μM rolipram	3352 ± 60	46
rpde6 - cytosolic (5μg) + 1.5μM rolipram	911 ± 19	85
rpde6 - membrane (5μg)	1822 ± 76	
rpde6 - membrane (5μg) + 0.15μM rolipram	1526 ± 61	16
rpde6 - membrane (5μg) + 1.5μM rolipram	779 ± 23	57

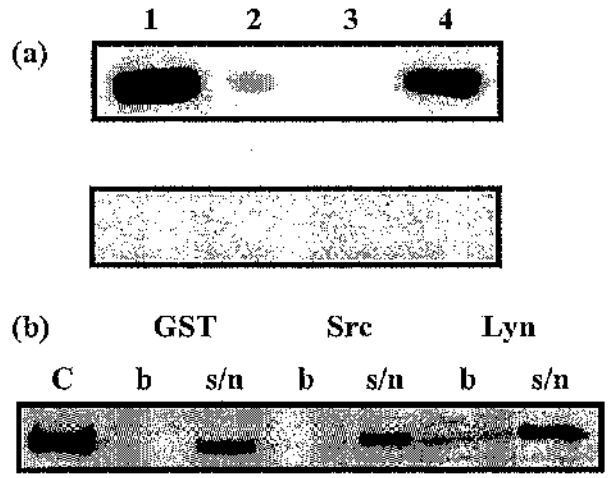

Figure 4.2.7. met^{26}RD1 and rpde39 do not interact with SH3 domains.

Panel (a) shows experiments done using met^{26}RD1 (met26) and mock (vector only) extracts of COS7 cells (mock) as the enzyme source. The data show immunoblots using the rat PDE4A specific antiserum. In track 1 is shown the soluble extract of COS7 cells used in the experiments. The pelleted beads harvested after incubation with either GST-agarose (track 2) or with GST-v-Src-SH3 agarose (track 3) were immunoblotted as was the supernatant fraction from the GST-v-Src-SH3 agarose (track 4) experiment. This experiment is typical of one done three times. The upper segment shows an identical set of experiments to those described above for the lower segment except that cytosol from mock (vector only) transfected COS-7 cells was used. This shows that the immunoreactive species detected by the PDE4A specific antisera are dependent upon transfection and expression of RPDE6. This data represents a typical experiment of one done at least three times

Panel (b) shows experiments done using rpde39 with GST alone and with GST fusion proteins formed with the SH3 domains of Src and Lyn as indicated in the figure panel. 'b' represents lanes containing bound PDE and 's/n' represents lanes showing unbound PDE. Lane 'C' shows COS cell expressed rpde39. rpde39 was detected using a PDE4A specific polyclonal antibody. This data represents a typical experiment of one done at least three times.

from figure 4.2.7a. that it did not interact at all with the SH3 domain of Src. Therefore, the N-terminal region of rpde6 is required for binding to SH3 domains.

The N-terminal splice region of rpde6 is 256 amino acids, 154 of which are shared with rpde39 (figure 4.1.1.). When, however, the binding of rpde39 to Src SH3 domain was investigated, again, as with met^{26}RD1 no binding was seen, figure 4.2.7b. This demonstrated that the extreme N-terminus of rpde6, which is unique, was required for binding to the v-Src SH3 domain and that the longer common region between rpde6 and rpde39 is not responsible. It maybe that this is the reason for their different subcellular distributions, The SH3 domain interaction may determine association with the low speed pellet and the common region between rpde6 and rpde39 might be involved with membrane association.

4.2.8. The use of dot blots to screen a number of SH3 domains for interaction.

It has been shown above, that rpde6 interacts with the SH3 domain of v-Src. In order to try and speed up the assay to facilitate the investigation of binding to a number of other SH3 domains from a variety of sources, a 'dot blot' procedure was developed. The hypothesis was that if SH3 domains were immobilised onto nitrocellulose then rpde6 could be overlaid and interaction detected using antibody directed to the PDE.

4.2.8.1. rpde6 used for overlay.

Experiments were designed such that 10μg, 20μg and 40μg of SH3 domains from Src, p85, lck, crk, csk and grb2 were loaded onto nitrocellulose. A vacuum system was used to load the protein onto a small area of 3mm in diameter, thus enabling 96 samples to be loaded onto a single piece of nitrocellulose. The

SH3 domains to be loaded were purified on glutathione beads and then released from the beads into 10mM glutathione in 50mM Tris, pH 8.0, as described in section 2.5.2. (figure 4.2.1.). The nitrocellulose was then blocked with 5% marvel in TBS and overlaid with 100μg of cytosol from rpde6 transfected COS cells for 2hrs at room temperature. It was then probed with a PDE4A specific polyclonal antisera, followed by a anti-rabbit HRP conjugated second antibody, essentially treated identically to an immunoblot (Section 2.2.3.).

Figure 4.2.8. shows an example of such a 'dot blot'. Unfortunately this method did not prove effective for screening for interactions. The use of the vacuum system for loading proteins onto the nitrocellulose caused small indentations, into which the ECL reagent used for detection settled. This made it impossible to get comparative data and ECL from positive dots often ran into negative ones, giving false positives, for example the 10μg Grb2 SH3 domain in figure 4.2.8.

4.2.8.2. Biotinylated N-terminal rpde6 used for overlay.

In parallel with the method used in 4.2.4.1., the nitrocellulose was overlaid with 100μg of a biotinylated peptide encoding the unique N-terminal region of rpde6 [O'Connell, JC., *et. al.* 1996] instead of COS cell expressed rpde6. This allowed for one step detection using HRP-conjugated streptavadin (SAPU) which bound to the biotin on the peptide. Unfortunately this method failed to be effective for screening SH3 domains for exactly the same reasons as section 4.2.4.1.

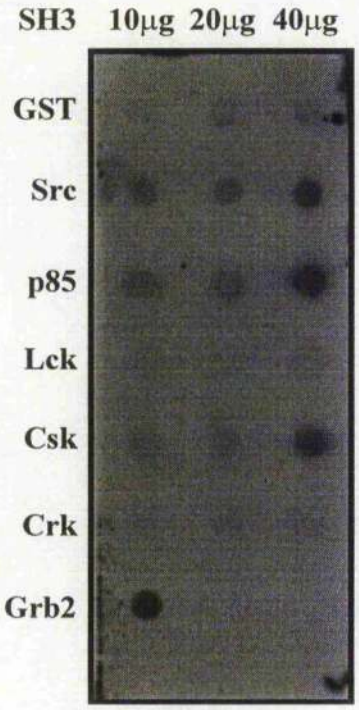

Figure 4.2.8. A 'dot blot', used for screening of rpde6-SH3 interactions.

10μg, 20μg and 40μg of the various SH3 domains were loaded onto the nitrocellulose which was then blocked with 5% marvel in TBS. The nitrocellulose was overlaid with 100μg of cytosol from rpde6 transfected COS cells for 2hrs at room temperature. Detection of rpde6 was via PDE4A specific polyclonal antisera.

4.2.9. Screening a number of SH3 domains for interaction with rpde6.

Since a rapid method for studying the interaction of rpde6 with SH3 domains could not be easily developed, binding was performed as described in section 4.2.2. SH3 domains have previously been shown to display selectivity for interaction with target species [Tersawa, H., *et. al.* 1994, Ramos-Morales, F., 1994]. This same selectivity can be seen for their interaction with rpde6, as measured by immunoblotting, in figure 4.2.9. The binding of rpde6 to SH3 domains was measured both by densitometry scanning of immunoblots and by assaying PDE activity associated with the SH3-GST beads and is tabulated in table 4.2.6.

If the relative affinities of rpde6 for various SH3 domains were compared by immunoblotting, table 4.2.6., it was evident that the SH3 domains with the highest affinity were those of Lyn and Fyn, which are tyrosyl kinases related to Src [Bolen, JB. 1993, Courtneidge, SA., *et. al.* 1993]. In contrast, another Src-family tyrosyl kinase, lck [Bolen, JB. 1993, Courtneidge, SA., *et. al.* 1993] showed only a very low binding. Additionally, it should be noted that while Lyn-SH3 showed an 8.8 fold increase in binding to rpde6 over Src-SH3, it still did not interact with the other PDE4A splice variant, rpde39 (figure 4.2.7b.). This supports the theory that the association of rpde6 with SH3 domains was conferred by its unique N-terminal region that contained the proline rich sequences.

Using an immunoblotting procedure [McPhee, I., *et. al.* 1995] to determine the relative activities of soluble and particulate forms of rpde6, it was shown that the PDE activity of rpde6, when bound to the SH3 domain of Src, was changed by

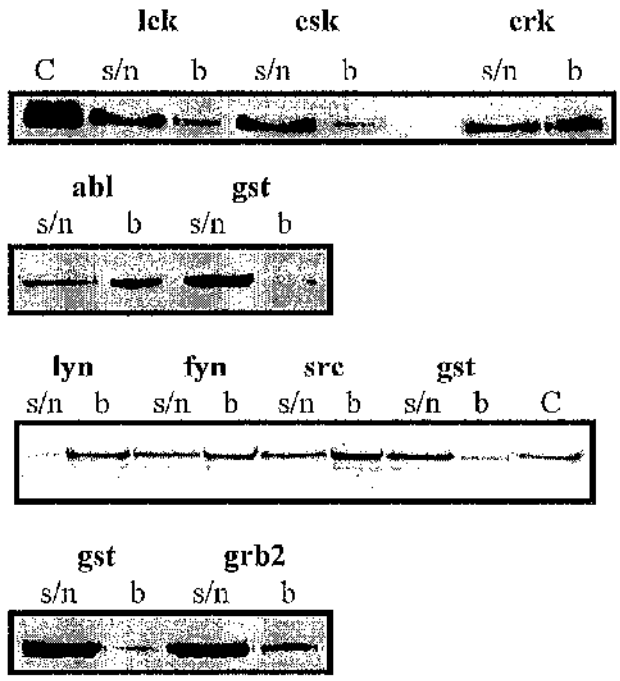

Figure 4.2.9. Selectivity for the binding of rpde6 to various SH3 domains expressed as GST fusion proteins.

Experiments were performed using 400µg of SH3 domain linked to glutathione sepharose beads and 15µg of cytosolic rpde6 from COS cells. Any rpde6 that became immobilised on the SH3 beads can be seen in lanes 'b'. That PDE that did not interact can be seen in lanes 's/n'. Lane 'C' represents COS cell cytosolic rpde6. Detection was via a polyclonal antibody to PDE4A. These immunoblots are typical of ones done at least three times.

Table 4.2.6. Assessment of the binding of rpde6 to SH3 domains

Detection of the amount of associated PDE was done by following immunoreactive protein and also by following PDE activity. For comparison, these data are shown relative to those found for v-src SH3 (set equal to 1). Errors are SD on the indicated number of experiments (n).

PDE4A species	GST fusion protein species	relative binding	relative activity	(n)
rpde6	src-SH3	(1)	(1)	(25)
rpde6	GST alone	0.05 ± 0.03	0.04 ± 0.03	(25)
rpde6	Src-SH3 + (1-256 NT-RPDE6/biotin)	0.08 ± 0.6	0.1 ± 0.5	(3)
rpde39	GST alone	0.04 ± 0.04	0.07 ± 0.05	(4)
rpde39	Src-SH3	0.05 ± 0.04	0.05 ± 0.03	(4)
rpde39	Lyn-SH3	0.09 ± 0.05	0.08 ± 0.05	(4)
rpde6	Lck-SH3	0.39 ± 0.09	0.07 ± 0.04	(6)
rpde6	Crk-SH3	0.40 ± 0.12	0.05 ± 0.04	(6)
rpde6	Csk-SH3	0.25 ± 0.06	0.06 ± 0.05	(6)
rpde6	Abl-SH3	0.58 ± 0.14	0.48 ± 0.09	(6)
rpde6	Fyn-SH3	2.1 ± 1.1	3.1 ± 1.2	(4)
rpde6	Lyn-SH3	8.8 ± 1.5	9.1 ± 1.7	(4)
rpde6	Grb2-(SH3-SH2-SH3)	0.08 ± 0.05	0.07 ± 0.04	(3)
rpde6	Src kinase	7.8 ± 1.2	7.0 ± 0.9	(4)
rpde6	Src-SH2	0.04 ± 0.04	0.05 ± 0.03	(4)
rpde6	Src-(SH2+SH3)	8.1 ± 0.8	7.9 ± 0.5	(4)

less than 7% (n=6). If, however, the relative affinities of rpde6 for various SH3 domains were compared by measuring the PDE activity versus immunoblotting, then a slightly different pattern was evident. Binding to the SH3 domains of Lyn, Fyn and Abl were similar by both immunoblotting and PDE activity. However, the SH3 domains that displayed weaker affinity Crk, Csk and Lck, had virtually no PDE activity associated with them, which would not have been expected by if the levels of protein on an immunoblot are considered. It would appear that although binding to these domains was weak, the PDE that associated with them displayed a marked diminution of activity.

From the analyses done, the strongest interactions with rpde6 were those of the SH3 domains of Src, Fyn and Lyn. However, SH3 domains from these proteins need not necessarily be the actual proteins that rpde6 interacts with *in vivo*, since in intact cells, interaction will depend on availability of suitable SH3 domain containing proteins and competition with other species for the interaction. A potential for modulation of PDE catalytic activity was demonstrated on association with the SH3 domains of Crk, Lck and Csk. It may be that other SH3 domains can interact with a higher affinity and modulate activity.

4.2.10. Binding of rpde6 to full length Src

It has been well documented that SH3 domains, when generated as distinct species, fold into active conformations [Tersawa, H., *et. al.* 1994, Goudreau, N., *et. al.* 1994, Booker, GW., *et. al.* 1993, Borchert, TV., *et. al.* 1994, Yu, H., *et. al.* 1993, Guruprasad, L., *et. al.* 1995]. It was decided to confirm the interaction of rpde6 with an intact protein containing an SH3 domain. It was shown that rpde6

could interact with a full length Src tyrosyl kinase expressed as a GST fusion construct, figure 4.2.10. Indeed, when the cytosol from v-Src transfected COS cells was mixed with cytosol from rpde6 transfected COS cells, rpde6 could be co-immunoprecipitated with Src using anti Src antisera, figure 4.2.12. This data demonstrated that intact Src and intact rpde6 would interact when mixed together.

4.2.11. rpde6 does not interact with the SH2 domain of Src.

Src also has an SH2 domain, it was shown which binds to phosphorylated tyrosine residues in proteins. However, using the SH2 domain of Src, expressed as a GST fusion construct, it was shown (figure 4.2.10. and table 4.2.6.) that rpde6 did not interact with this species. Indeed, for rpde6 to interact with an SH2 domain, it would have needed to be tyrosine phosphorylated and not only was it not possible to demonstrate any tyrosine phosphorylation of rpde6, figure 4.2.11. but rpde6 does not contain a consensus tyrosine phosphorylation site within its coding sequence.

4.2.11.1. Increased affinity of the Src SH2-SH3 construct over SH3 alone.

Despite the inability of rpde6 to interact with the SH2 domain of Src, table 4.2.6. and figure 4.2.9 show that a GST construct with the SH2 and SH3 domains of Src together was much more effective in binding rpde6 than the SH3 domain alone. A similar potentiation of SH3 binding has been noted for the binding of PI-3 kinase to the Src SH3 domain in a construct made from the Src SH2 and SH3 domains [Haefner, R., *et. al.* 1995]. This was also shown not to be due to any interaction with the SH2 domain of Src but was presumed to be due to a more

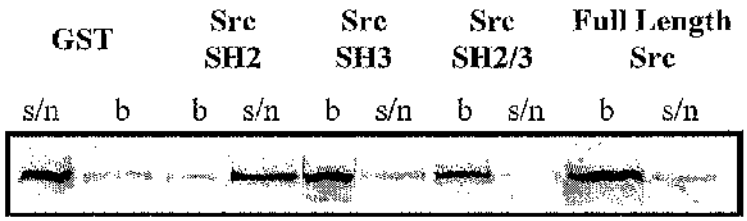

Figure 4.2.10. rpde6 binds to full length Src but not to the Src SH2 domain

Experiments were performed as described in the legend of fig. 4.2.9. but using GST fusion proteins of Src-SH2 domain, Src-SH3 domain, Src-(SH2+SH3) domain and full length Src. The immobilised (b) and remaining soluble (s/n) fractions are shown. The presence of associated rpde6 was detected using immunoblotting with the PDE4A antiserum. Experiments are typical of those done at least three times.

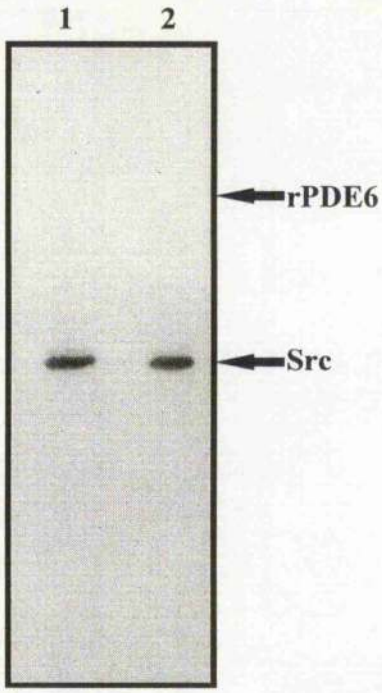

Figure 4.2.11. rpde6 is not tyrosine phosphorylated

Shows immunoblots using anti-phosphotyrosine antiserum probing an immunoprecipitate of v-Src incubated in a buffer system which allows for the functional tyrosyl kinase activity of Src to be expressed. In track (1) data is shown for incubation of the Src immunoprecipitate alone, with the single auto-phosphotyrosyl phosphorylated Src protein being identified. In track (2) incubations were done with the addition of immunoprecipitated rpde6. phosphotyrosyl immunoblotting of Src and rpde6. No evidence of any phosphotyrosine associated with rpde6 was obtained. The position where rpde6 migrated on these gels, as detected by stripping the blots and re-probing with antibody for rpde6, is shown. The immunoprecipitated Src protein kinase was able to phosphorylate exogenously enolase on tyrosine residues (data not shown). Experiments are typical of those done at least three times.

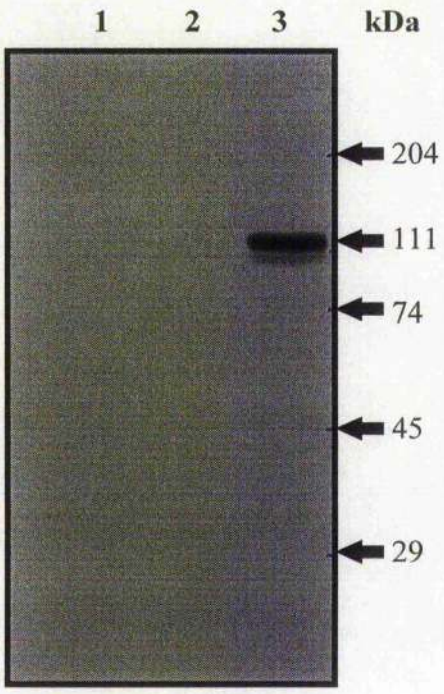

Figure 4.2.12. rpde6 and Src can be co-immunoprecipitated

The cytosol fractions from v-Src transfected cells were mixed with those from COS7 cells transiently expressing rpde6. In track (3) anti-Src antibody was added and the immunoprecipitate probed by Western blotting with antibody for rpde6. In track (2) a non-specific antibody was used and in track (1) no antibody was added to the immunoprecipitation system. Experiments are typical of those done at three times.

effective folding of the SH3 domain as a result of the presence of the SH2 domain which is normally adjacent to it in the native protein [Haefner, R., *et. al.* 1995]. It appears, therefore, that a similar phenomenon exists for Src SH3 interaction with rpde6.

A Grb2 construct, however, which contained two SH3 and an SH2 domain failed to interact with rpde6 at all, table 4.2.6. Thus rpde6 does not interact with this adapter protein, again reflecting the specificity of the interaction with SH3 domain containing proteins.

4.3. CONCLUSIONS

I have demonstrated that COS cell expressed rpde6 appears to bind to SH3 domains via its N-terminal splice region. This interaction is both specific and rapid and cannot be disrupted by high concentrations of either salt or detergent. The rat PDE4A splice variants, rpde39 and the 'core' species met^{26}RD1 do not interact with SH3 domains, which, given the differences that are seen in subcellular localisation, indicates that the SH3 interaction of rpde6 may be involved in regulating this. rpde6 is the only rat PDE4A splice variant that associates with the low speed pellet, whereas both rpde6 and rpde39 associate with the membrane and are found in the cytosol [McPhee, I., *et. al.* 1995]. The only difference between rpde6 and rpde39 is their extreme N-terminal regions, which in the case of rpde6 contains the proline rich regions, so perhaps the SH3 binding of rpde6 confers its association with the low speed pellet. If the IC_{50} values for rolipram are considered, they are identical for rpde6 bound to an SH3 domain to those seen for the cytosol form but 10-fold lower than the membrane

bound form. Therefore, either SH3 domain interactions do not confer membrane association or rpde6 or another factor, such as another interacting protein, might alter the properties of the membrane bound form.

The following chapter goes on to investigate the binding of rpde6 to other SH3 domains, looks at the binding to SH3 domains of PDEs that are expressed in rat tissues and investigates the potential binding of other PDE isoforms.

Chapter 5

SH3 Domain Interaction of PDE4D

5.1. INTRODUCTION

In chapter 4, it was shown that a PDE4A splice variant, rpde6, could associate with the SH3 domains of Src family tyrosyl kinases. This association was characterised and shown to be conferred by its' N-terminal splice region which contained proline rich sequences [Chapter 4, O'Connell, JC., *et. al.* 1996]. Such sequences are know to interact with SH3 domains [Alexandropoulos, K., *et. al.* 1995]. All the investigations performed in chapter 4 used COS cell expressed PDEs which raised the questions 'Can endogenously expressed rpde6 interact with SH3 domains?' and 'Do any other PDEs interact?'. The species rpde6 is predominately expressed in brain [Bolger, G., *et. al.* 1996], together with RD1 (figure 4.1.1.) and rPDE39 is expressed in testis [Bolger, G., 1994a], which are also PDE4A splice variants. These consequently made two good target tissues for investigating binding of PDE4A to SH3 domains.

PDE4s are encoded by four genes, PDE4A, PDE4B, PDE4C and PDE4D. The structure of the PDE4A gene is discussed in chapters 1 and 4. The PDE4D gene, in contrast to the PDE4A gene, has been better characterised in human tissue than in rat. As with the PDE4A gene, there are a number of splice variants, each with unique N-terminal domains [Nemoz, G., *et. al.* 1995, Bolger, G., *et. al.* 1996a]. Figure 5.1.1. illustrates the PDE4D splice variants. These PDE4D species showed distinct expression patterns in a number of cell lines, indicative of distinct functions conferred by their N-terminal domains [Nemoz, G., *et. al.* 1995, Bolger, G., *et. al.* 1996a]. They also showed remarkable similarity to the PDE4A species in their subcellular distribution, PDE4D1 and PDE4D2 show very little, <3%,

association with the membrane, PDE4D3, PDE4D4 and PDE4D5 each display 20-35% membrane association, with a further 10% being associated with the low speed pellet [Bolger, G., *et. al.* 1996a]. Given that the shorter species, PDE4D1 and PDE4D2 showed little membrane association then it is likely that subcellular targeting was conferred by the N-terminal splice regions of the other species.

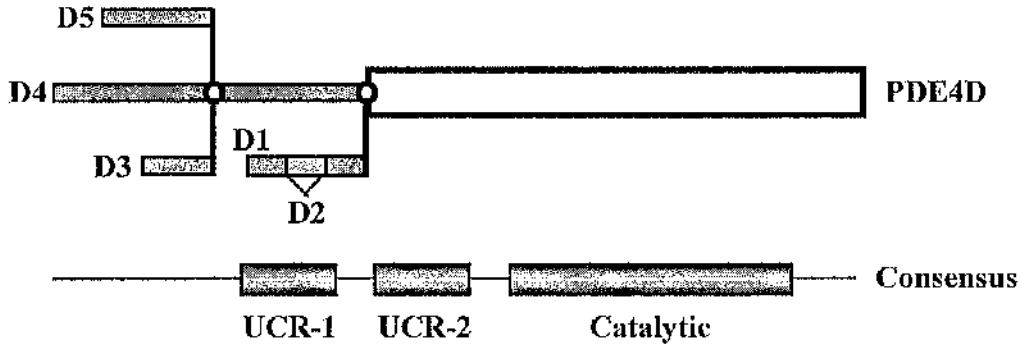

Figure 5.1.1. PDE4D splice variants.

Shows splice variants of the human PDE4D gene. The empty rectangle represents the core, catalytic region common to all species. The shaded areas are unique, alternatively spliced, regions and the circles splice junctions. The positions of the homologous regions, UCR1 and UCR2 are indicated.

In this chapter, the binding of endogenously expressed rpde6 (RNPDE4A5) to SH3 domains is investigated. It also demonstrates that another PDE, the PDE4D4 isoform, interacts with SH3 domains.

5.2. RESULTS AND DISCUSSION

5.2.1. Generation of a fodrin SH3-GST fusion protein.

It has been shown in chapter 4 that rpde6 preferentially binds to SH3 domains of Src family tyrosyl kinases, having very little or no affinity for the SH3 domains of adapter proteins Grb2 and Crk. Another class of proteins that SH3 domains are commonly found in are cytoskeletal proteins. Association of rpde6 with SH3 domains of such proteins might help to explain the distribution pattern of rpde6 between the cytosol, membrane and low speed pellet [McPhee, I., *et. al.* 1995, Section 1.3.5.2.]. A cytoskeletal protein that contains an SH3 domain is fodrin [Moon, RT., and McMahon, AP. 1990]. In order to investigate binding of PDEs to this protein, a GST fusion protein was made with the SH3 domain so that it could be expressed and purified from *E.coli*.

5.2.1.1. Design of primers to amplify the fodrin SH3 domain

The complete coding sequence of fodrin (nonerythroid alpha-spectrin) was obtained from GenBank (accession number J05243). Sequence homology with the SH3 domain of Src and information from the SwissProt database indicated that amino acids 974-1021, from the initiating methionine, form the SH3 domain. The expression vector that the SH3 domain was to be cloned into was pGEX-5X-1 from Promega. This vector allowed for induction of the GST-SH3 fusion protein with IPTG, as described in methods. The multiple cloning site of this vector is immediately downstream of the GST protein, to allow an N-terminal in-frame fusion protein to be generated (figure 5.2.1.).

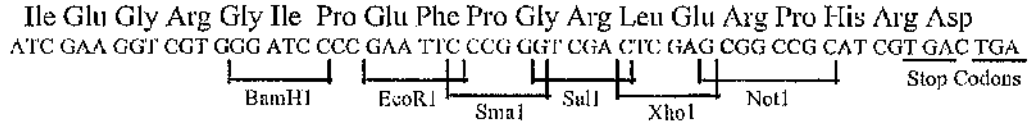

Figure 5.2.1.(a) Multiple cloning site of pGEX-5X-1

Shows the amino acid and nucleotide sequence of the multiple cloning site of pGEX-5X-1. The unique restriction sites are indicated.

```
 975 Leu Tyr Asp Asp Gln Glu Lys Ser Pro Arg Glu Val Thr Met Lys Lys
3025 CTC TAC GAC TAT CAG GAG AAG AGT CCC CGA GAC GTC ACC ATG AAG AAG

     Gly Asp Ile Leu Thr Leu Leu Asn Ser Thr Asn Lys Asp Trp Trp Lys
     GGA GAT ATC CTT ACC TTA CTC AAC AGC ACC AAC AAG GAT TGG TGG AAA

     Val Glu Val Asn Asp Arg Gln Gly Phe Val Pro Ala Ala Tyr Val Lys     1022
     GTG GAA GTG AAC GAT CGT CAG GGT TTT GTG CCG GCT GCG TAC GTG AAG AA 3170
```

Figure 5.2.1.(b) DNA and Protein sequence of the fodrin SH3 domain

Show the protein and DNA sequence of the fodrin SH3 domain that was cloned into pGEX-5X-1. The residue numbers from the initiating methionine or ATG are indicated.

PCR primers were designed to amplify the SH3 domain of fodrin given in figure 5.2.1.(b) and add restriction sites to the fragment for EcoR1 and BamH1 to allow insertion into the vector. The sequences of the primers used are given below.

N-terminal: 5'--CTGGTCGGATCCCTCTACGACTATCAGGAGAAG--3'

C-terminal: 5'--GGGTCCGAATTCTTCACGTACGCAGCCGGCAC--3'

First strand cDNA was made using RNA from Jurkats cells (human T-cell line) with a kit from Pharmacia. PCR was performed with 30 cycles, using 26pmols of each of the primers.

5.2.1.2. Cloning of the fodrin SH3 domain

Both the PCR fragment and the vector were digested with EcoR1 and BamH1 and purified using Promega's Wizard kit. They were then ligated overnight with T4 DNA ligase and competent *E.coli* transformed. Transformed bacteria showed resistance to ampicillin and six colonies were picked, grown and mini-preps of their plasmid DNA made. When each of the colonies 1-6 were grown and induced with 100μM IPTG for 5hrs, a protein species was produced that could be visualised on Coomassie-stained 12% SDS-PAGE (Figure 5.2.2.). However clone FOD5 produce a band that was smaller than the others, approximately 25kDa, the same size as GST alone. The other clones produced proteins of about 30kDa, the predicted size of an SH3-GST fusion. Restriction

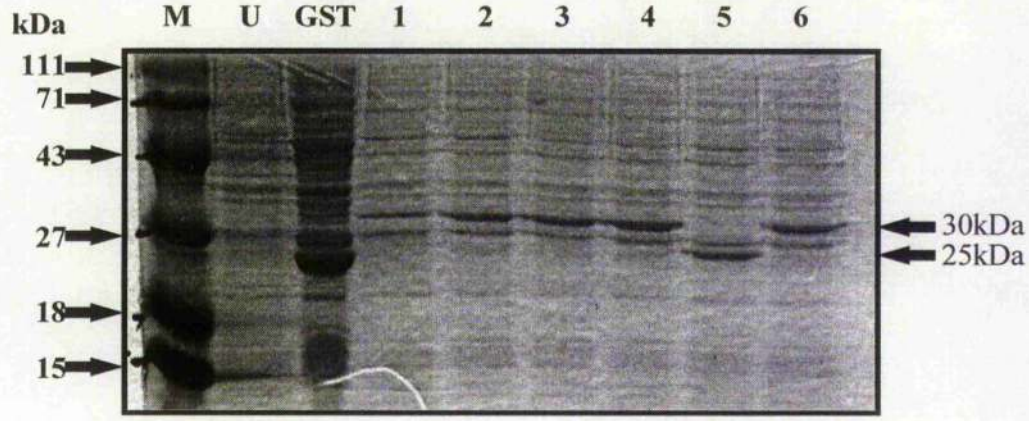

Figure 5.2.2. Coomassie stained SDS-PAGE of fodrin SH3 domain indications

Shows 12% SDS-PAGE of six bacterial clones transformed with the fodrin SH3-GST fusion protein, induced with 100μM IPTG and stained with Coomassie blue (lanes 1-6). Lane 'M' contains molecular weight markers, lane 'U' uninduced bacteria and lane 'GST' induced vector alone transformed bacteria.

digests using EcoRV, which cut the vector once and the insertonce, confirmed that clone FOD4 contained the fodrin SH3 domain and FOD5 contained vector alone.

5.2.2. rpde6 but not rPDE39 from rat tissue binds the Src SH3 domain

In order to investigate if any endogenous rpde6 (RNPDE4A5) could interact with SH3 domains, a cytosolic fraction from rat brain was used since rpde6 is known to be expressed in brain [McPhee, I., *et. al.* 1995]. Similarly rPDE39 is expressed in the testis [Bolger, G., *et. al.* 1996] so rat testis was used to investigate the binding of rPDE39, a PDE4A which lacks the proline-rich regions found in rpde6 (figure 4.1.1.). As with the COS cell expressed rpde6, experiments were performed using immobilised GST-Src SH3 fusion protein, the difference being only that brain or testis cytosol was used instead of COS cell cytosol. The PDEs were detected using polyclonal antisera which recognised all rat PDE4A species and a typical immunoblot is given in figure 5.2.3. It is clear that native rpde6 did associate with the SH3 domain of Src and that native rPDE39 did not. Thus endogenous PDE4A species showed a similar selectivity in binding SH3 domains as did the COS cell expressed species. The lower band seen in testis, as detected with an anti-PDE4A antibody, was of unknown origin. It is not known to date if this represents a novel PDE4A species, however, it did not associate with the SH3 domain of Src.

5.2.3. PDE activity can be bound from rat brain

Given that rpde6 from rat brain was shown, by immunodetection, to bind to SH3 domains, the next step was to see if catalytically active PDE could be extracted from rat brain cytosol using various SH3 domains. Figure 5.2.4.

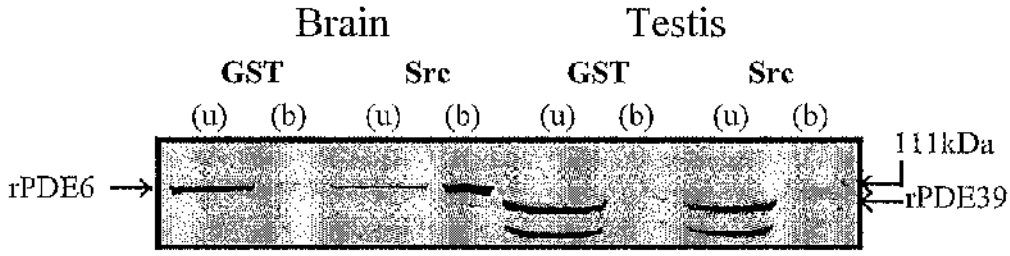

Figure 5.2.3. rpde6 from brain but not rPDE39 from testis binds to Src SH3

Figure shows binding of 100µg of brain or testis cytosol to 400µg of Src-GST fusion protein. GST alone is included as a control. Lanes (u) represent immunoreactive PDE that did not bind and lanes (b) represent PDE that did bind. Detection was via a polyclonal antisera that will recognise all rat PDE4A species.

demonstrates that PDE activity from brain cytosol bound to the SH3 domains of Src and Fyn, but not the SH3 domains of either the cytoskeletal protein, fodrin, or the N- or C-terminal SH3 domains of the adapter protein, Grb2. This specificity for the SH3 domains of the Src family tyrosine kinases reflects the same specificity that was seen with the COS cell expressed rpde6 in chapter 4. It is worth noting that while the SH2 domain of Grb2 showed no affinity for any PDEs, the SH2 domain of src displayed some affinity for PDE activity. This however was very variable between experiments, as reflected by the error bars. If, indeed, any PDE binds then it is unlikely to be rpde6 as it was shown not to interact with the SH2 domain of Src when expressed in COS cells [Chapter 4]. Furthermore, the primary sequence of rpde6 does not contain any consensus sites for tyrosine phosphorylation which would be required since SH2 domains bind to phosphorylated tyrosine residues (Chapter 1). It does not however rule out the possibility that another PDE was interacting with the Src SH2 domain, although by immunodetection, no PDE4A species was found to bind to the Src SH2 domain. The variation seen may have been effected by the phosphorylation state of the enzyme in the preparation, which was perhaps related to the lack of protein phosphatase inhibitors when preparing brain cytosol.

4.2.4. Estimation of the proportion of PDE4 from brain cytosol that could bind to SH3 domains

By measuring the total PDE activity in rat brain cytosol that was inhibited by rolipram, a PDE4 specific inhibitor, an estimation was made as to the total amount of PDE4 activity that was present. Consequently the amount of PDE4

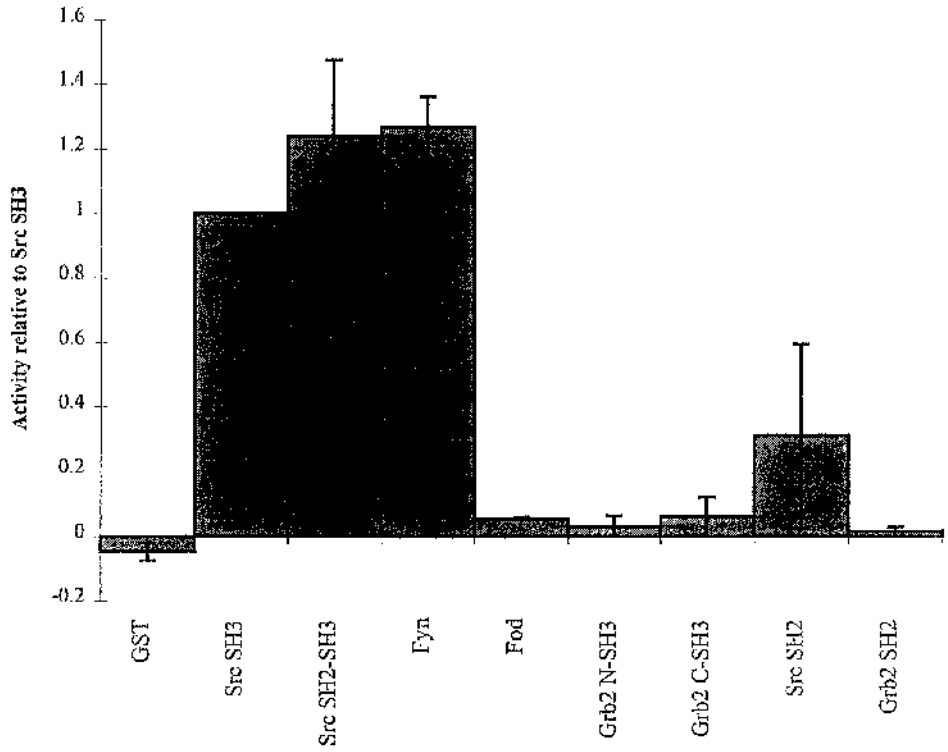

Figure 5.2.4. PDE Activity Bound to SH3 Domains from Rat Brain

Shows the total PDE activity that bound to 400μg of various SH3 domains from 100μg of rat brain cytosol. 'Fod' represents fodrin, 'Grb2-N SH3' represents the N-terminal Grb2 SH3 domain and 'Grb2-C SH3' represents the C-terminal Grb2 SH3 domain Values are expressed relative to those for the Src SH3 domain ± standard error for three experiments.

activity that bound to SH3 domains could be calculated as a percentage of the total PDE4 activity (figure 5.2.5.). It should be noted that not all of the PDE4 activity is contributed by rpde6 (RNPDE4A5), in fact rpde6 is reported to represent only 8-14% of the PDE4 activity in the cytosol [McPhee, I., *et. al.* 1995]. Consequently, one would not have expected to achieve 100% binding, nor at this stage was it known if rpde6 was the only PDE4 that was capable of interacting with SH3 domains. The data in figure 5.2.5. showed a high level of variation between experiments, with the proportion of PDE4 bound ranging between 20 and 50%. While the reasons for the variation remain unknown, it is possible that any endogenous associations of PDE4s may have changed with the age of the brain preparation, thus effecting the pool of PDE4 that is free for binding exogenous SH3 domain. Regardless of variation, figures anywhere within the range, represent a significant proportion of cytosolic brain PDE4s and in fact are much higher than the proportion constituted by rpde6 [McPhee, I., *et. al.* 1995]. It is likely therefore than other PDE4 species from brain might be capable of interacting with SH3 domains.

5.2.5. Assessment of the interaction of other PDE families from various tissues with SH3 domains.

Having already shown that PDE4 activity can be bound to SH3 domains from rat brain using SH3 domains as GST-fusion proteins, linked to glutathione sepharose beads, the next step was to determine if PDE activity could be bound from any other tissues. Additionally it is not a forgone conclusion that because all the activity found to bind to SH3 domains in section 5.2.4. could be inhibited by

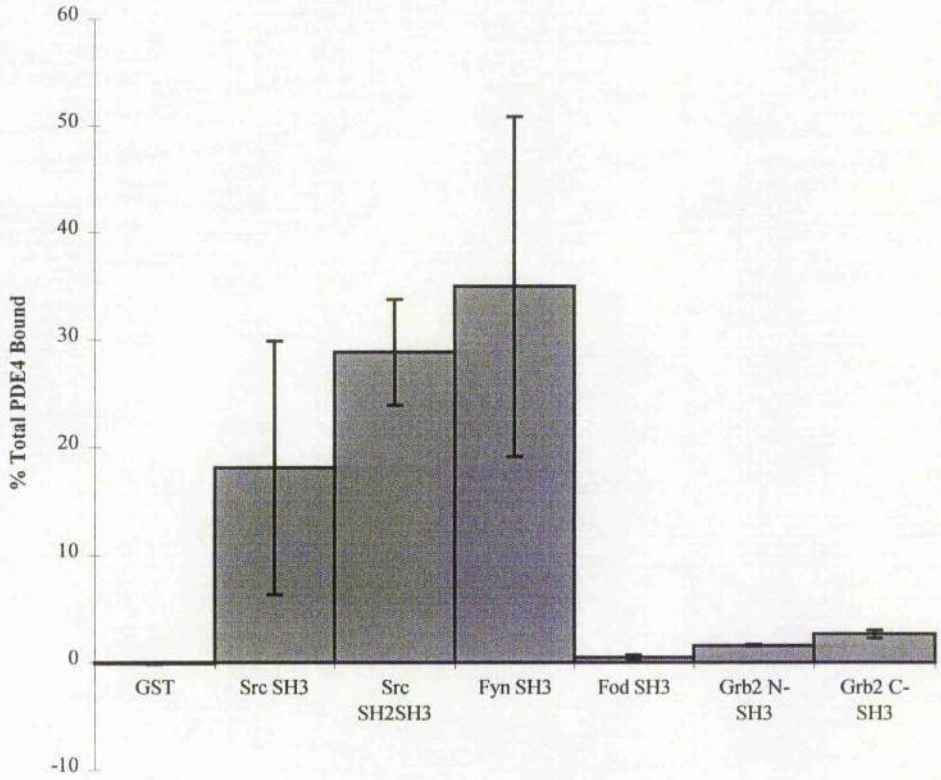

Figure 5.2.5. Percent of total brain PDE4 activity that binds to various SH3 domains.

Shows the proportion of brain cytosolic PDE4s that can interact with SH3 domains. Expressed as a percentage of the total brain cytosolic PDE4 activity in 100μg that bound to 400μg SH3 domain ± standard error for three experiments. PDE4 activity was measured using 10μM rolipram as an inhibitor.

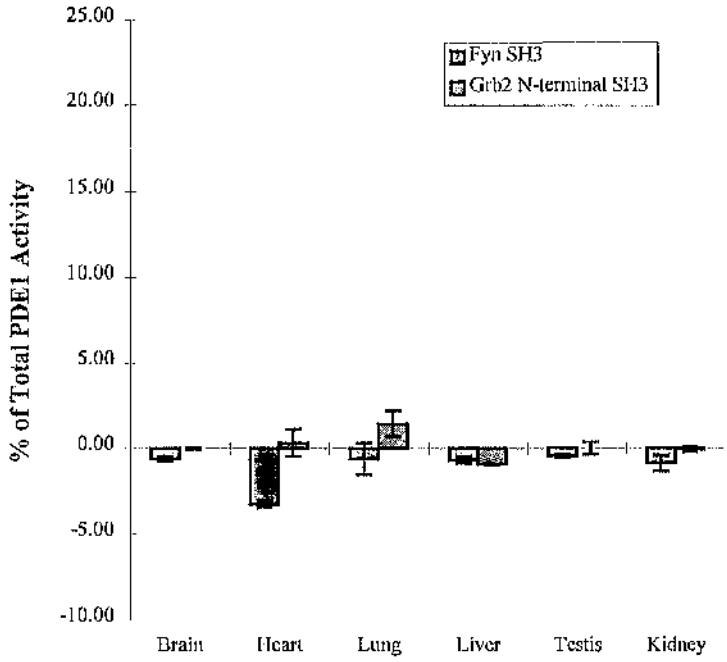

Figure 5.2.6.(a) Assessment of cytosolic PDE1 activity associating with the SH3 domains of Fyn and Grb2.

Shows PDE1 activity from 100µg of tissue cytosols that was pulled down by 400µg of either the Fyn SH3 domain or the N-terminal Grb2 SH3 domain with the GST controls subtracted. The PDE1 activity was measured as that which was activated by Ca^{2+} (5mM) and calmodulin (10U/100µl). Values are given as percent of total PDE1 activity (Table5.1) ± standard error for three measurements per tissue.

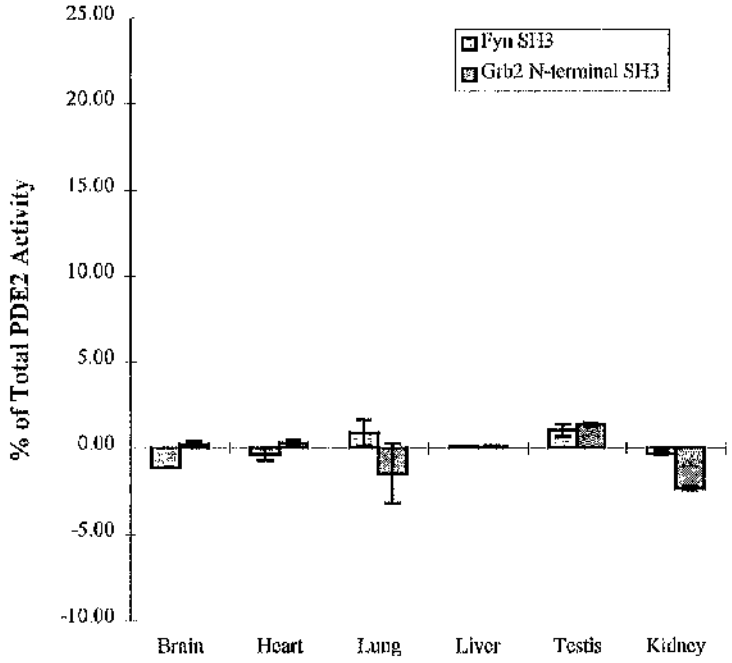

Figure 5.2.6.(b) Assessment of cytosolic PDE2 activity that associated with the SH3 domains of Fyn and Grb2.

Shows PDE2 activity from 100µg of tissue cytosols that was 'pulled down' by 400µg of either the Fyn SH3 domain or the N-terminal Grb2 SH3 domain with the GST controls subtracted. The PDE2 activity was measured as that which was inhibited by EHNA following stimulation by cGMP. Values are given as percent of total PDE2 activity (Table 5.1.) ± standard error for three measurements per tissue.

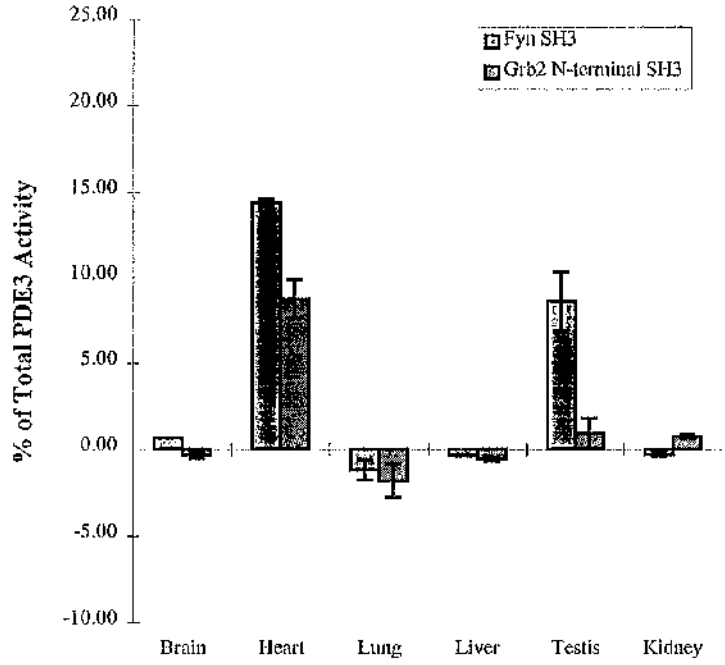

Figure 5.2.6.(c) Assessment of cytosolic PDE3 activity that associated with the SH3 domain of Fyn and Grb2.

Shows PDE3 activity from 100μg of tissue cytosols that was 'pulled down' by 400μg of either the Fyn SH3 domain or the N-terminal Grb2 SH3 domain with the GST controls subtracted. The PDE3 activity was measured as that which was inhibited by cilostamide. Values are given as percent of total PDE3 activity (Table 5.1.) ± standard error for three measurements per tissue.

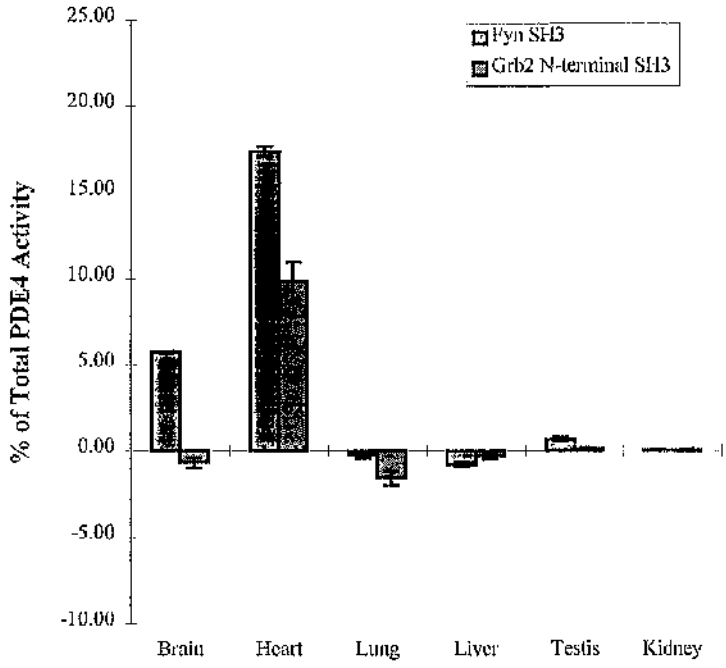

Figure 5.2.6.(d) Assessment of cytosolic PDE4 activity that associated with the SH3 domain of Fyn and Grb2.

Shows PDE4 activity from 100μg of tissue cytosols that was 'pulled down' by 400μg of either the Fyn SH3 domain or the N-terminal Grb2 SH3 domain with the GST controls subtracted. The PDE4 activity was measured as that which was inhibited by rolipram. Values are given as percent of total PDE4 activity (Table 5.1.) ± standard error for three measurements per tissue.

Table 5.1. Total PDE activities in tissues used for binding profiles

Shows the total cytosolic PDE activity for the tissues used in figures 5.2.6.(a-d). PDE activity is expressed as pmols cAMP hydrolysed per minute per unit of sample used at 1μM cAMP for the SH3-binding studies ± the standard error for three measurements per tissue.

	Brain	Heart	Lung	Liver	Testes	Kidney
PDE1	18640	713	855	3900	2990	3390
	± 4320	± 50	± 65	± 760	± 230	± 530
PDE2	4940	2337	330	11110	1150	1900
	± 1470	± 65	± 165	± 1095	± 180	± 630
PDE3	5530	535	580	3320	520	4430
	± 1690	± 8	± 35	± 920	± 280	± 68
PDE4	3820	525	2035	2320	6700	6760
	± 300	± 38	±260	± 720	± 60	± 1190

rolipram, the only PDEs that bind SH3 domains are PDE4s. For instance PDE1 activity would not be detected without adding Ca^{2+}/Calmodulin to activate it and PDE2 activity may not be detected without the presence of cGMP. In order to evaluate this, cytosolic fractions were taken from a number of tissues, namely brain, heart, lung, liver, kidney and testis and over a number of experiments probed with the SH3 domains of Fyn and Grb2, with GST alone as a control, and assayed for the presence of the various PDE families (figures 5.2.6.(a), (b), (c) and (d)). Figure 5.2.6.(d) shows that significant proportions of PDE4 activity bound from both brain and heart to the SH3 domain of Fyn, with no binding seen from the other tissues. The PDE4A species, rpde6 is expressed at high levels in the brain [Bolger, G., 1994a], which might explain this level of binding. The identity of PDE4 species in heart has not been reported, so it is not known if rpde6 was present. However, the levels of total PDE4 activity in heart were very low (table 5.1.), so such a low level of expression might account for the 15% of total activity that associated with the SH3 domain. However, in a manner that was very different to that in brain, binding of heart PDE4 activity to the Grb2 SH3 domains occurred. This might indicate that a different PDE4 form is expressed in heart which can bind to Grb2, unlike in brain where rpde6 has a negligible affinity for the Grb2 SH3 domains (chapter 4). A potential candidate might be PDE4B3, which has been shown to be expressed in heart by PCR and a low level expression detected by immunoblotting [Huston, E. and Houslay, MD., unpublished data]. In the sequence of PDE4B3 [Owens, R. and Houslay, MD. personal communication] can be seen two PxxP motifs within its unique N-terminal region (figure 5.2.7.). Although one PxxP motif is also found in both PDE4B1 and PDE4B2, the

```
4B1 MKKSRSVMTVMADDNVKDYFECSLSKSYSSSSNTLGIDLWRGRRCCSGNL
4B2 MKEHGG--------------------TFSSTGISGG----------SGDS
4B3 MTAKDSSKELTASEPEV----CI--KTFKEQ-----MHL---------EL

4B1 QLPPLSQRQSERARTPEGDGISRPTTLPLTTLPSIAIT-----TVSQECF
4B2 AMDSLQ-------------------------------------------
4B3 ELPRLPGNRPTSPKISPRSSPRNSPCFFRKLLVNKSIRQRRRFTVAHTCF

4B1 DVENGPSPGRSPLDPQASSSAGLVLHATFPGHSQRRESFLYRSDSDYDLS
4B2 ----------PLQP-----------------------------NY---
4B3 DVENGPSPGRSPLDPQASSSAGLVLHATFPGHSQRRESFLYRSDSDYDLS

4B1 PKAMSRNSSLPSEQHGDDLIVTPFAQVLASLRSVRNNFTILTNLHGTSNK
4B2 ----------------MPVCLFA------------------------
4B3 PKAMSRNSSLPSEQHGDDLIVTPFAQVLASLRSVRNNFTILTNLHGTSNK

4B1 RSPAASQPPVSRVNPQEESYQKLAMETLEELDWCLDQLETIQTYRSVSEM
4B2 ----------------EESYQKLAMETLEELDWCLDQLETIQTYRSVSEM
4B3 RSPAASQPPVSRVNPQEESYQKLAMETLEELDWCLDQLETIQTYRSVSEM
```

Figure 5.2.7. Alignment of the N-terminal regions of the PDE4B species.

Shows sequences of the N-terminal regions of the PDE4B splice variants* to their region of homology. Proline residues are indicated in bold. Consensus SH3 binding sequences on the basis of a PxxP motif [Ren, R., *et. al.* 1993, Yu, H., *et. al.* 1994, Feng, S.,*et. al.* 1994] are underlined.

*Owens, R. and Houslay, MD., unpublished data

sequence surrounding the other PxxP motif in PDE4B3 is rich in prolines. Such a proline-rich sequence can function to stabilise the formation of a poly-proline helix, a structure which is reported to be required for SH3 domain binding [Yu, H., *et. al.* 1994].

Figure 5.2.6.(c) shows binding of a PDE3 species from heart and testes to Fyn and a PDE3 species binding from heart but not brain to Grb2 SH3. It is not known what PDE species may have contributed to this. However, examination of the sequence of PDE3A revealed that it too contains a proline-rich sequence in its N-terminal splice region (figure 5.2.8.). PDE3A is expressed in heart [Taira, M., *et. al.* 1993] but no evidence has been published concerning its expression in

MRKDERERDT**P**AMRS**PPPPPPP**ATATAAS

PPESLRNGYVKSCVS**P**LRQD**PP**RSFFFHLCR

FCNVE**PP**AASLRAGARLSLAALAAFVLAALL

GAG**P**ERWAAAATGLRTLLSACSLSLS**P**LFSIA

CAFFFLT

Figure 5.2.8. The amino acid sequence of the extreme N-terminus of human PDE3B.

Shows the first 130 amino acids of human PDE3A. Prolines are indicated in large bold type. This sequence has no homology to any other PDE3 species.

testis. A proline-rich sequence was not found within the coding sequence of any known PDE3B splice variants, so the difference in affinity of the PDE3 species between the two tissues for the SH3 domains of Grb2 and Fyn might indicate the presence of further splice variants that have yet to be discovered or that a modification occurs in some tissues that prevents association with SH3 domains. It should be noted that, although a large proportion of total PDE3 activity bound from these tissues, the total PDE3 activity was low. For example in testes, PDE3 activity was 13-fold lower than PDE4 activity (table 5.1). This meant that, although ~10% of the PDE3 activity in testis associated with the SH3 domain of Fyn, the actual activity associated with the beads was only one fifth of the PDE4 activity that associated from brain. Low levels of activity would have made further characterisation difficult.

Figures 5.2.6 (a) and (b) demonstrate that no detectable PDE1 or PDE2 activity associated with the SH3 domains of Fyn or Grb2. Negative values in the case of PDE1 are likely to have been because, although Ca^{2+} is used to stimulate PDE1, it also inhibits PDE4 [Wilkinson, IR. and Houslay, MD., unpublished data], so a drop in activity upon the addition of Ca^{2+} is consistent with the presence of bound PDE4 activity.

5.2.6. Two PDE4 splice variants from rat brain become associated with the Src SH3 domain

Since the PDE4 activity that associated with SH3 domains was the highest in terms of total activity, irrespective of percentage of total PDE4, when rat brain was used, the next stage was to determine which PDE4 species were responsible

for this activity. It has already been shown in section 5.2.2. that rpde6 binds, but this need not have been the only species. To determine if any other PDE4 species contributed to the activity associated with the SH3 domains, rat brain cytosol was probed with immobilised SH3 domains and which were then loaded onto SDS gels and analysed with antisera specific to PDE4A, PDE4B, PDE4C and PDE4D.

No PDEs were detected on immunoblots with either the PDE4B or the PDE4C antisera, indicating that no PDE4B or PDE4C species from rat brain were capable of interacting with SH3 domains.

Figure 5.2.9. shows such a PDE4D immunoblot. It is clearly evident that a PDE4D species also possessed the ability to associate with SH3 domains. The PDE4D species that interacted was likely to be PDE4D4, as it comigrated with the PDE4D4 transfected COS cell cytosol. Rat brain could be seen to express species that comigrated with PDE4D3, PDE4D4 and PDE4D5, PDE4D3 apparently being expressed higher levels than the other two. The interaction of PDE4D4 with the SH3 domains was therefore specific since neither of the other two species expressed displayed any binding capabilities at all. Furthermore, the specificity for particular SH3 domains was also high since PDE4D4 interacted with the SH3 domains of Src and Fyn but not with that of fodrin.

Given that PDE4D4 interacted with Src family tyrosine kinases and that neither PDE4D5 or PDE4D3 interacted, then the interaction must have been conferred by its N-terminal splice region, since the C-terminal regions are identical (figure 5.1.1.). When the sequence of the extreme N-terminal region of PDE4D4 was studied, a large proline-rich region was seen (figure 5.2.10.). It is

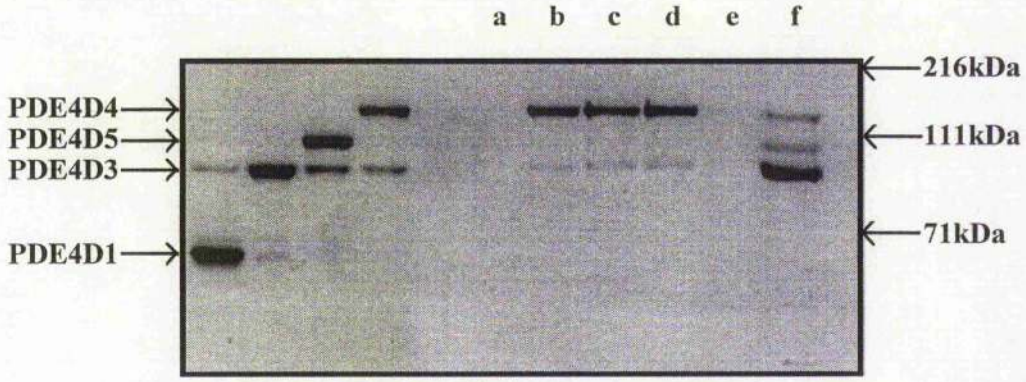

Figure 5.2.9. PDE4D4 binds to SH3 domains

A typical immunoblot with a PDE4D specific monoclonal antibody. It shows that only PDE4D4 of the PDE4D species expressed in rat brain bound to SH3 domains. COS cell expressed PDE4D splice variants are indicated in the figure. PDEs that bound to 400μg of SH3 domain from 100μg of rat brain cytosol are indicated in lanes (a)-(f): (a) GST control. (400μg) (b) Src SH3-GST. (400μg) (c) Src SH2SH3-GST. (400μg) (d) Fyn SH3-GST. (400μg) (e) Fodrin SH3-GST. (400μg) (f) 25μg of rat brain cytosol.

proline-rich sequences that confer interaction with SH3 domains (chapters 1 and 4).

As can be seen from figure 5.2.10., the N-terminal region of PDE4D4 is extremely rich in prolines, 74% proline, within a stretch of 31 amino acids. Thus, PDE4D4 is remarkably similar to rpde6 (RNPDE4A5) in that it possesses an N-terminal region that enables it to interact with SH3 domains and that both species are able to interact with SH3 domains from Src family tyrosyl kinases.

MEAEGSSA**P**ARAGSGEGSDSAGGATLKA**P**KHLWR

HEQHHQY**P**LRQ**P**QFRLLH**P**HHHL**PPPPPP**S**P**QP

QPQC**P**LQ**PPPPPP**L**PPPPPPP**GAARGRYASSG

ATGRVRHRGYSDTERYLYCRAMDRTSYAVETGHR**P**

GLKKSRMSW**P**SSFQGLRR

Figure 5.2.10. The N-terminal sequence of PDE4D4.

Shows the amino acid sequence of the first 150 amino acids of the unique N-terminal region of PDE4D4. Each proline is indicated as a large bold 'P'.

5.2.7. PDE4D4 interacts with SH3 domains

In section 5.2.6. it was demonstrated that a protein from rat brain cytosol could be detected on an immunoblot, with a PDE4D specific antibody, that bound to the SH3 domains of Src and Fyn and comigrated with PDE4D4 transfected COS cell cytosol. Consequently, it was assumed that this was in fact PDE4D4. To confirm this, a range of PDE4D species were expressed in COS cells and the cytosolic extracts pooled together before being probed with SH3 domains (figure 5.2.12.). It can be seen that only PDE4D4 bound to the SH3 domains and in the cases of Src and Fyn, virtually all the PDE4D4 that was available for binding was found associated with the SH3 domain. The specificity was exactly the same as with the PDE4D4 from rat brain, with binding to the SH3 domains of Src and Fyn but not to the SH3 domain of fodrin.

5.2.8. PDE4D4 binds in an active form

As PDE4D4 could be detected as associating with SH3 domains by immunoblotting, it was necessary to determine if PDE activity could be detected associated with SH3 domains. To check this, bindings to the SH3 domains of Fyn, Src and fodrin were performed with both PDE4D4 and also with PDE4D1, a PDE4D species that lacks the proline-rich region seen in PDE4D4 (figure 5.2.11.). As would have been expected, PDE4D4 activity could be detected associated with the SH3 domains of Src and Fyn but not to fodrin and no PDE4D1 activity associated at all, thus confirming the immunoblotting data.

5.2.9. PDE4D4 shows a different specificity for SH3 interaction to rpde6 (RNPDE4A5) and rpde6 is inactivated upon binding to fodrin and cortactin.

It has already been shown that PDE4D4 does not interact with the SH3 domain of fodrin, as detected on an immunoblot (figures 5.2.9. and 5.2.12) and if the activity data for rpde6 (RNPDE4A5) (figures 5.2.4. and 5.2.5.) is studied, then it appears that rpde6 did not bind to fodrin either. When, however, samples of rpde6 were incubated with the SH3 domains of fodrin and cortactin and binding assayed by immunoblotting, then binding was evident (figure 5.2.13.). The PDE4A species, rpde6 must therefore have been catalytically inactivated upon binding to the SH3 domains of fodrin and cortactin. Significantly, also, the interaction of PDE4D4 with these SH3 domains displayed differences in specificity. While PDE4D4 showed similar affinity for the SH3 domains of Src family tyrosyl kinases, little or no affinity was seen for the cytoskeletal SH3 domains, either by measuring PDE activity or by immunodetection. Evidently, although both PDEs belong to the same family and interact with SH3 domains, they differ in selectivity for SH3 domains and properties once bound. This demonstrated that PDE4D4 and rpde6 are likely to have unique and finely defined functional roles within the cell.

5.3. CONCLUSIONS

It has now been conclusively shown that two PDE4 species interacted with SH3 domains. These PDEs were are encoded by different PDE4 genes, PDE4A and PDE4D, with only one splice variant of each gene possessing the ability to interact with SH3 domains. PDE4D4 showed a different specificity to rpde6,

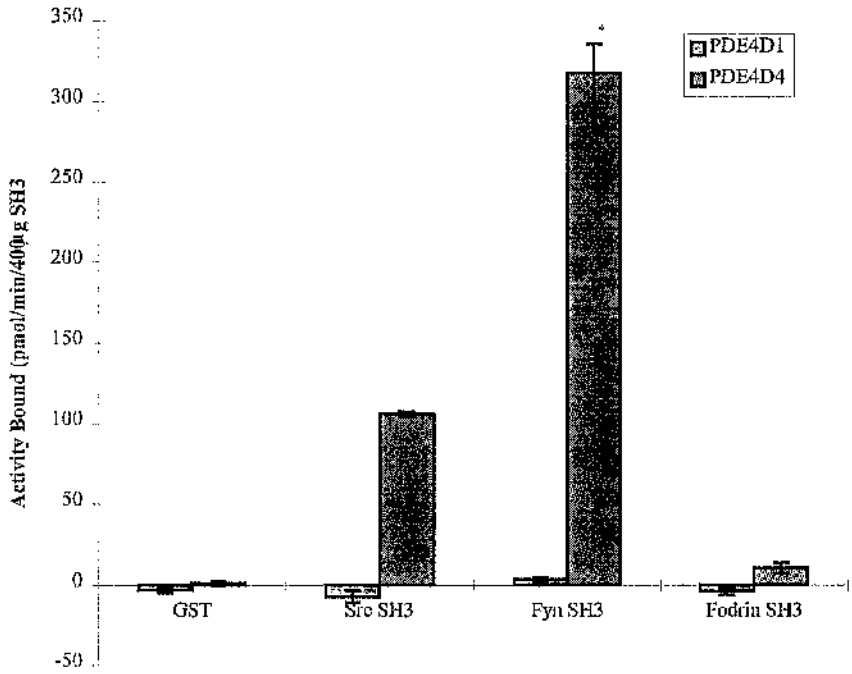

Figure 5.2.11. Association of PDE4D4 activity with SH3 domains

Shows PDE4D4 and PDE4D1 activity that associated with 400µg of SH3 domains from 15µg of COS cell cytosols. PDE activity was measured after releasing the GST-SH3-(PDE) complex from glutathione sepharose beads with 10mM glutathione. Values are expressed as PDE activity per 400µg of SH3 domain ± standard error for two separate experiments.

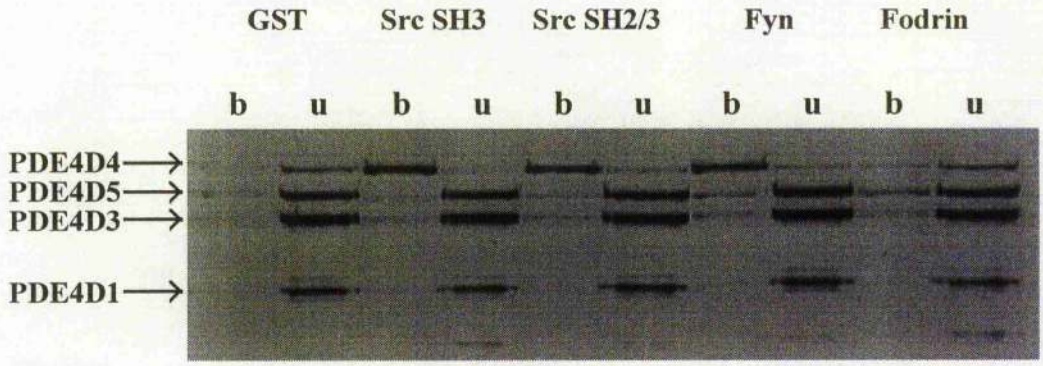

Figure 5.2.12 PDE4D4 binds to SH3 domains

Shows a typical immunoblot with a PDE4D specific monoclonal antibody. It demonstrates that when 15μg each of cytosolic PDE4D1, PDE4D3, PDE4D4 and PDE4D5 from COS cells were mixed together, and incubated with 400μg of various SH3 domains, only the PDE4D4 species bound to the SH3 domains. Each of the splice variants used are clearly marked on the figure. Lanes marked 'b' show PDEs that bound to the SH3 domain, lanes marked 'u' show PDEs that did not bind to the SH3 domain. Only 50% of the unbound fraction was loaded onto the gel.

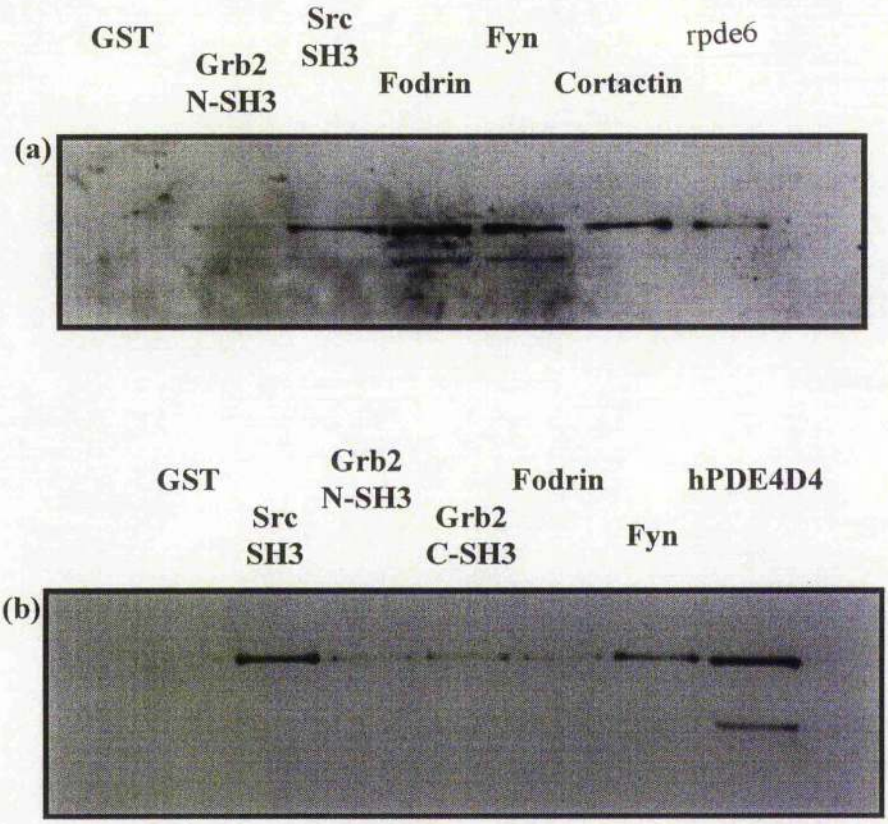

Figure 5.2.13. Different specificity of SH3 binding between rpde6 and PDE4D4

Panel (a) shows a typical immunoblot with a PDE4A specific antibody. COS cell transfected rpde6 was incubated with glutathione beads linked to GST fusion proteins of the SH3 domains from the indicated proteins. The beads were loaded onto the gel to measure binding. Binding to the SH3 domains of Src, Fyn, Fodrin and Cortactin was seen. Panel (b) shows a typical immunoblot with a PDE4D specific antibody. COS cell transfected PDE4D4 was incubated with glutathione beads linked to GST fusion proteins of the SH3 domains from the indicated proteins. The beads were loaded onto the gel to measure binding. Binding to the SH3 domains of Src and Fyn was seen.

PDE4D4 only binding to SH3 domains of the Src family tyrosyl kinases, Fyn and Lyn, and rpde6 binding to SH3 domains of both Src family tyrosyl kinases and the cytoskeletal proteins, fodrin and cortactin. The interaction of rpde6 with the SH3 domains of fodrin and cortactin but not Src family tyrosyl kinase SH3 domains profoundly attenuated the catalytic activity.

In addition to the binding of PDE4D4 and rpde6, evidence was suggested for the potential binding of another PDE4 species, a PDE4B, although this remains to be confirmed. Also, a PDE3 species was detected, associating with SH3 domains from heart and testes. It is likely that this is PDE3B1, since it contains a proline-rich region that fits with the SH3 binding peptide consensus [Yu, H., *et. al.* 1993], although again, this has yet to be confirmed.

Such interactions must clearly possess some functional role. Clearly they may serve to localise PDEs to particular subcellular compartments, the implications of which will be discussed in the next chapter.

Chapter 6

General Discussion and Conclusions

6.1. GENERAL DISCUSSION AND CONCLUSIONS

The introduction to this thesis summarised current knowledge about the PDE4 family of enzymes which is encoded by four genes, each of which is alternatively spliced. The tissue and subcellular distributions of very few of these splice variants has been documented in detail. There is also little insight into how the intracellular targeting of particulate associated species is determined and its functional significance. However, work performed recently in this laboratory has been fundamental in demonstrating that the N-terminal splice domains of various PDE4 isoforms can determine their intracellular localisation. The appreciation of a functional role for the N-terminal regions of certain PDE isoforms came originally from studies done on the membrane association of RD1 [Shakur, Y., *et. al.*, 1994, Scotland, G., *et. al.* 1995]. I have extended this to the study of the PDE4A splice variant, rpde6 and the PDE4D splice variant PDE4D4, where I have demonstrated their ability to interact with SH3 domains. rpde6 was shown to bind to the SH3 domains of a number of proteins, particularly those of Src family tyrosyl kinases. This SH3 binding was shown to be conferred by the N-terminal region since met^{26}RD1, which lacks the splice region, did not interact. Furthermore, other rat PDE4A splice variants, which have different N-terminal domains, were shown not to possess the ability to bind SH3 domains. Additionally, it was demonstrated that another PDE4 species, namely PDE4D4, was also able to bind to the SH3 domains of Src family tyrosyl kinases. As with rpde6, the interaction involving PDE4D4 appeared to be determined by the uniquely spliced N-terminal domain of this isoform. In both these instances, the N-terminal domain contains proline-rich

sequences which are known to define interaction with SH3 domains [Ren, R., *et. al.* 1993].

Specificity for SH3 domain interaction has been shown to be conferred by residues surrounding a simple PxxP motif in the primary sequence [Ren, R., *et. al.* 1993, Yu, H., *et. al.* 1994, Feng, S., *et. al.* 1994]. PxxP motifs are split into two categories, those that contain the sequence RxL immediately N-terminal to PxxP, (Class I) and those that don't (Class II) [Yu, H., *et. al.* 1994] as shown below.

Class I motif consensus	**R**	X	**L**	**P**	X	X	**P**	X	X
Class II motif consensus	X	X	X	**P**	X	X	**P**	$X_{n=1-3}$	**R**

Where X represents any amino acid

A number of groups have studied the interaction of proline containing peptides with SH3 domains so as to produce consensus SH3-binding sequences. Initial work, performed by Yu, H., *et. al.* 1994 and Rickles, RJ., *et. al.* 1994, used peptides generated by studying SH3 binding sequences in a number of natural ligands. In all these studies, done for Class I motifs, the constitutive PxxP motif was of the form PPxP, where only x was variable. Work performed more recently [Sparks, AB., *et. al.* 1996] has shown that the second proline is not a constitutive requirement for SH3 binding and, in most cases, can be replaced by any amino acid (Figure 6.1). Based upon this, I have performed an alignment of consensus sequences information from Sparks, AB., *et. al.* 1996 (Figure 6.1), the implications

SH3 Domain	Ligand Consensus													
Src[1]	L	X	X	R	P	L	**P**	X	Ψ	**P**				
Yes[1]	Ψ	X	X	R	P	L	**P**	X	L	**P**				
Cortactin[1]			+	P	P	Ψ	**P**	X	K	**P**	X	W	L	
Crk[1]						Ψ	**P**	Ψ	L	**P**	Ψ	K		
Grb2 N-term[1]		Φ	D	X	P	L	**P**	X	L	**P**				
PLCγ[1]				P	P	V	**P**	P	R	**P**	X	X	T	L
Abl[2]	P	P	P	X	P	P	**P**	P	I	**P**	X	X		
Fodrin[3,*]	P	P	L	A	L	T	A	P	P	**P**	A			
rpde6 1-11				M	E	P	**P**	A	A	**P**	S	E	R	S
rpde6 30-42	Q	H	L	W	R	G	**P**	R	T	**P**	I	R	I	Q
rpde6 54-66	S	E	T	E	R	S	**P**	H	R	**P**	I	E	R	A
rpde6 24-29					T	L	K	P	P	**P**	Q	H	L	W
4D4 72-85	L	Q	P	P	P	P	**P**	P	L	**P**	P	P	P	P
4B3 27-36	H	L	E	L	E	L	**P**	R	L	**P**	G	N	R	P
4B3 85-95	P	S	P	G	R	S	**P**	L	D	**P**	Q	A	S	S

Figure 6.1. Proline-rich peptide ligand consensus for various SH3 domains aligned with proline-rich sequences from PDE4 isoforms.

Shows consensus SH3 binding regions. Prolines of the PxxP motif are in bold. Homology to the Src SH3 binding consensus is shaded, homology to the Grb2 consensus is underlined. Lower part of the table shows proline-rich regions in PDE4 isoforms. 'X' represents any amino acid, '+' basic, 'Ψ' aliphatic and 'Φ' aromatic. '1' from Sparks, AB., *et. al.* 1996, '2' from Rickles, RJ., *et. al.* 1994, '3' from Rotin, D., *et. al.* 1994. '*' Not consensus, simply region known to bind from a single protein.

of which are discussed in the following paragraphs. While the consensus sequences for class I sequences are well documented [Yu, H., *et. al.* 1994 and Rickles, RJ., *et. al.* 1994, Sparks, AB., 1996] the class II sequences are less so. Alexandropoulos [Alexandropoulos, K., *et. al.* 1995] reports that sequences fitting the general consensus **P**xx**P**x(x)(x)R or **PP**xx**P**x(x)R is sufficient for interaction with the SH3 domains of Abl, Src, Fyn, Crk, Grb2 and Nck, where P represents proline, x any amino acid and (x) any amino acid but may be deleted. The PDE4A species, rpde6, contains three such sites that appear to fit with this consensus. These correspond to residues 4-10, 36-41 and 60-66 (Figure 6.2.). This might explain why rpde6 was found to interact with the SH3 domains of Src, Fyn, Abl and Crk

Class II consensus	X/P	**P**	X	X	**P**	X	**R**		
	X/P	**P**	X	X	**P**	X	X	**R**	
	X	**P**	X	X	**P**	X	X	X	**R**
rpde6 (residues 3-11)	P	**P**	A	A	**P**	S	E	**R**	S
rpde6 (residues 35-43)	G	**P**	R	T	**P**	I	**R**	I	Q
rpde6 (residues 59-67)	S	**P**	H	R	**P**	I	E	**R**	A

Figure 6.2. Alignment of rpde6 sequence with consensus class II SH3 domain binding motifs

Shows the consensus class II binding motifs for interaction with the SH3 domains of Src, Fyn, Abl, Crk, Grb2 and Nck [Alexandropoulos, K., *et. al.* 1995, Tersawa, H., *et. al.* 1994]. Proline and arginine residues, fitting with the class II consensus given in the table are in bold text.

It is not clear why rpde6 preferentially bound to the SH3 domains of Src, Fyn and Lyn than to those of Crk and Abl. However, specificity is known to be determined by residues surrounding the PxxP motif [Ren, R., *et. al.* 1994, Yu, H., *et. al.* 1994, Feng, S., *et. al.* 1994]. It is likely, therefore, that specificity for interaction with Src and Fyn maybe determined by such residues, although the specific preferences of the SH3 domains of Src and Fyn are not known. Furthermore, it has been shown [Grzesiek, S., *et. al.* 1996]* that the binding sequence of the HIV protein Nef to the SH3 domain of Hck tyrosine protein kinase occurs through a non-contiguous interaction. Therefore, it may be that additional amino acid residues in the sequence of rpde6 contribute to the interaction with the Fyn and Src SH3 domains when the three dimensional folding of the N-terminal region of rpde6 is considered. The requirement for such residues may differ between SH3 domains. Thus, it is possible that rpde6 may be prevented from associating with Crk and Abl, by a process of steric hindrance caused by other regions of this protein.

PDE4D4 appears to contain no absolute consensus for either class I or class II SH3 domain binding motifs within its N-terminal splice region. However, the sequence between amino acid residues 72 and 81 is similar to the class I consensus sequence, LXXRPLPXΨP, required for interaction with the SH3 domain of Src (figure 6.1.) [Alexandropoulos, K., *et. al.* 1995]. The absence of RxL, which is reported to define class I motifs [Yu, H., *et. al.* 1994], suggests that the interaction of PDE4D4 with SH3 domains differs to those published to date.

The consensus site for Abl reported by Rickles is highly distinctive, with a requirement for a string of proline residues, **PPP**x**PPPP**(I/V)Pxx, [Rickles, RJ.,

* [Lee, C.H., *et. al.* 1996]

et.al. 1994]. This is not evident in rpde6, although interaction with Abl was observed, albeit at a far lower level than with either Src or Fyn. The proline rich region in PDE4D4 does, however, resemble the preferred sequence for interaction with Abl more closely (figure 6.1 and 6.3.) and I would predict that it may preferentially bind to the Abl SH3 domain than to that of Src.

Abl consensus[1]	**P**	**P**	**P**	**X**	**P**	**P**	**P**	**P**	**I**	**P**	**X**	**X**
PDE4D4 (75-83)	L	Q	**P**	**P**	**P**	**P**	**P**	**P**	**L**	**P**	**P**	**P**

Figure 6.3. Alignment of PDE4D4 with the consensus SH3-binding sequence for Abl

1- Alexandropoulos, K., *et. al.* 1995

Binding of a PDE4 species from rat heart was seen to the SH3 domain of Grb2 but not to Fyn. It was hypothesised in chapter 5 that this may have been a novel (unpublished) form of PDE4B, namely PDE4B3, since it is has been detected to be expressed in heart [Huston, E. and Houslay, MD., unpublished data]. The sequence of PDE4B3, residues 29-36 is very similar to the consensus binding sequence for the N-terminal SH3 domain of Grb2 (underlined in Figure 6.1. and 6.4.). This suggests that PDE4B3 may make a good candidate for such an interaction.

A further level of complexity for the SH3 interaction came from the discovery that binding of rpde6 to the SH3 domain of fodrin significantly

inhibited the catalytic activity of rpde6. Interaction with this domain represented a stark difference in the ability of rpde6 and PDE4D4 to bind to SH3 domains, since

Grb2 consensus[1]						**P**	X	X	**P**	X	X	R
Grb2 consensus[1]					P	**P**	X	X	**P**	X	R	
Grb2 consensus[2]	Φ	D	X	P	L	**P**	X	L	**P**			
PDE4B3 (28-39)	L	E	L	E	L	**P**	R	L	**P**	G	N	R

Figure 6.4. Alignment of PDE4B3 with consensus binding domains for the N-terminal SH3 domain of Grb2

Shows the alignment of PDE4B3 residues 28-39 with two published consensus binding sequences for the N-terminal Grb2 SH3 domain. Homology is underlined in the sequence of PDE4B3. 1-Tersawa, H., *et. al.* 1994. 2-Sparks, AB., *et. al.* 1996.

PDE4D4 failed to interact with the fodrin SH3 domain at all. The consensus binding sequence for the SH3 domain of fodrin is not known. However, work done by Rotin localised the region of the epithelial sodium channel that bound to the fodrin SH3 domain to a sequence that contained the following proline rich sequence, **PPLALTAPPPA** [Rotin, D., *et. al.* 1994]. This sequence is unique in that it does not contain the consensus PxxP motif, perhaps indicating that the SH3 domain of fodrin is less selective in the distance between the two prolines. It is very noticeable that four of the five amino acid residues N-terminal to the three

prolines, PPP, are aliphatic and hydrophobic. This may relate to the specificity for interaction with the SH3 domain of fodrin.

PDE46 is the human homologue of rpde6 [Bolger, G., *et. al.* 1993, Bolger, G., *et. al.* 1996]. If the consensus SH3 domain-binding motifs of rpde6 and PDE46 are compared (figure 6.5.), they are seen to be highly homologous. However, if the first consensus sequence is considered, the amino acids between the two prolines of the PxxP motif (residues 4-7) are different. While one of these is a conserved substitution of Ala^6 to Val^6, the other is a change of an aliphatic residue to an aromatic residue, Ala^5 to Tyr^5. If this sequence confers association with SH3 domains in both species, then it may represent a divergence in specificity of SH3 domain interaction between rat and human. Furthermore, Gly^{36} in rpde6, which is immediately N-terminal to the second PxxP motif (figure 6.5) is changed to Gln^{36} in PDE46. A similar change of Ser^{59} to Gln^{59} occurs in the third PxxP motif, which might imply that this mutation also reflects an evolutionary divergence.

The functional significance of PDEs binding to SH3 domains remains to be determined. One possible role is to form part of a system allowing the compartmentalisation of cAMP signals. It has been known for a number of years that, although a number of hormones work by elevating cAMP levels, they each have discrete effects within the same cell, as discussed in the introduction to this

rpde6 (1-11)			M	E	P	**P**	A	A	**P**	S	E	R	S
pde46 (1-11)			M	E	P	**P**	T	V	**P**	S	E	R	S
rpde6 (31-42)	Q	H	L	W	R	G	**P**	R	T	**P**	I	R	I	Q
pde46 (31-42)	Q	H	L	W	R	Q	**P**	R	T	**P**	I	R	I	Q
rpde6 (54-66)	S	E	T	E	R	S	**P**	H	R	**P**	I	E	R	A
pde46 (54-66)	A	E	R	E	R	Q	**P**	H	R	**P**	I	E	R	A

Figure 6.5. Alignment of the SH3-binding consensus sequences in rpde6 with its human homologue pde46

Shows alignment of the rat PDE4A species, rpde6 and the human PDE4A species, PDE46. Prolines of the SH3-binding consensus motif, PxxP are in bold text. Absolute homology between the rat and human species is shaded.

---

thesis. Clearly for this to occur, cAMP produced from certain receptor systems must only activate specific populations of PKA and be prevented from activating other populations. A means of achieving this may be via the localisation of PDE enzymes to specific subcellular compartments where they could prevent cAMP from diffusing into other regions of the cell. As discussed in the introduction, PKA-II, itself can be localised to specific areas of the cell via interaction with a number of AKAP isoforms. Colocalisation of PDEs would serve to ensure activation of a specific PKA population. A means by which PDEs could be localised themselves is via protein-protein interactions, or more specifically SH3 domain binding, such as that that has been demonstrated in this thesis.

Binding of PDE4 isoforms to a number of SH3 domains has been demonstrated in this thesis. Further work, investigating the binding of more SH3 domains will be necessary, since evidence for binding by the methods used does not conclusively prove that they represent the domains that the PDEs bind to *in vivo*. Mutagenesis studies would be interesting to discover which proline-rich regions in rpde6 and PDE4D4 are responsible for interaction with SH3 domains. It is also possible that figures may be put to affinities for SH3 domains with the use of a Biacore machine. The work does, however, demonstrate the first link of PDEs to SH3 domain containing proteins and provides the first suggestion as to a mechanism by which PDEs may be localised to specific locales within the cell. It also assigns a function to the alternatively spliced N-terminal domains of the PDE4A species rpde6 and the PDE4D species PDE4D4, giving insight into the necessity of the multiple splice variants.

References

7.1. REFERENCES

Alexandropoulos, K., Cheng, G. and Baltimore, D. (1995) Proceedings of the National Academy of Science USA **92**, 3110-3114.

Alvarez, R., Sette., C., Yang, D., Eglen, RM., Wilhelm, R., Shelton, ER. and Conti, M. (1995) Molecular Pharmacology **48**, 616-622.

Appleman, MM., Rall. TW. and Dedman, JR. (1985) Cyclic Nucleotide Protein Phosphorylation Res., **10**, 417-421.

Arshavsky, VY., Dumke, CL, and Bownds, MD. (1992) Journal of Biological Chemistry **267**, 24501-24507.

Baecker, PG., Obernolte, R., Bach, C., Yee., C. and Shelton, ER. (1994) Gene **138**, 253-256.

Bachr, W., Devlin, MJ. and Applebury, ML. (1979) Journal of Biological Chemistry **254**, 11669-11677.

Bakalyar, HA. and Reed, RR. (1990) Science **250**, 1403-1406.

Barnette, MS., Manning, CD., Cieslinski, LB., Burman, M., Christensen, SB. and Torphy, TJ. (1995) J. Pharmacol. Exp. Ther. **273**, 647-649.

Barnette, MS., Christensen, SB., Essayen, DM., Essre, KM., Grous, M., Huang, S-K., Manning, CD., Prabhaker, U., Rush, J. and Torphy, TJ. (1994) Am. J. Resp. Crit. Care Med. **149**, A209.

Bar-Sagi, D., Rotin, D., Batzer, A., Mandiyan, V. and Schlessinger, J. (1993) Cell **74**, 83-91.

Barsony, J. and Marx, SJ. (1990) Proceedings of the National Academy of Science USA **87**, 1188-1192.

Beavo, JA., Hardman, JG. and Sutherland, EW. (1970) Journal of Biological Chemistry **245**, 5649-5655.

Beavo, JA., Hardman, JG. and Sutherland, EW. (1971) Journal of Biological Chemistry **246**, 3841-3846.

Beavo, JA. and Reifsnyder, DH. (1990) Trends in Pharmacology **11**, 150-155.

Beavo, JA., Conti, M. and Heaslip, RJ. (1994) Molecular Pharmacology **46**, 399-405.

Beebe, S., Oyen, O., Sandberg, M., Froyas, A., Namsson, V. and Jahnsen, T. (1990) Molecular Endocrinology **4**, 465-475.

Beltman, J., Sonnenberg, WK. and Beavo, JA. (1993) Molecular and Cellular Biochemistry **127** 239-253.

Bentley, JK., Dadlecek, A., Sherbert, C., Seger, D., Sonnenberg, WK., Charbonneau, H., Novack, Jp. and Beavo, JA. (1992) Journal of Biological Chemistry **267**,18676-18682.

Bolen, JB. (1993) Oncogene **8**, 2025-2031.

Bolger, G., Michaeli, T., Martins, T., St. John, T., Steiner, B., Rodgers, L., Riggs, M., Wigler, M. and Ferguson, K. (1993) Molecular and Cellular Biology **13**, 6558-6571.

Bolger, G. (1994) Cellular Signalling **6**, 851-859.

Bolger, G., Rodgers, L. and Riggs, M. (1994a) Gene **149**, 237-244.

Bolger, G., McPhee, I. and Houslay, MD. (1996) Journal of Biological Chemistry **271**, 1065-1071.

Bolger, G., Erdogan, S., Wilkinson, IR., Jones, R., Loughney, K. and Houslay, MD. (1996a) Biochemical Journal **in press**

Bönigk, W., Altenhofen, W., Müller, F., Dose, A., Illing, M., Molday, RS. and Kaupp, UB. (1993) Neuron **10**, 865-877.

Booker, GW., Gout, I., Downing, AK., Driscoll, PC., Boyd, J., Waterfield, MD. and Campbell, ID. (1993) Cell **73**, 813-817.

Borchert, TV., Mathieu, M., Zeelen, JPH., Courtneige, SA. and Wierega, RK. (1994) FEBS letters **341**, 76-86.

Bork, P. and Sudol, M. (1994) Trends in Biochemical Sciences **19**, 531-533.

Borrelli, E., Montmayeur, JP., Foulkes, NS. and Sassone-Corsi, P. (1992) Critical Reviews of Oncology **3**, 321-338.

Bray, P., Carter, A., Guo, V., Puckett, C., Kamholz, J., Speigel, A. and Nirenberg, M (1986) Proceedings of the National Academy of Science USA **83**, 8893-8897.

Brechler, V.,Pavoine, C., Hanf, R., Garbarz, E., Fischmeister, R. and Pecker, F. (1992) Journal of Biological Chemistry **267**, 15496-15501.

Bregman, DB., Bhattacharyya, N. and Rubin, CS. (1989) Journal of Biological Chemistry **264**, 4648-4656.

Brunton, LL., Hayes, JS. and Mayer, SE. (1981) Advances in Cyclic nucleotide Research **14**, 391-397.

Butt, E., Geiger, J., Jarchau, T., Lohmann, SM. and Walter, U. (1993) Neurochem. Res. **18**, 27-42.

Cali, JJ., Zwaagstra, JC., Mons, N., Cooper, DMF. and Krupinski, J. (1994) Journal of Biological Chemistry **269**, 12190-12195.

Cantly, LC., Auger, KR., Carpenter,C., Duckworth, B., Graziani, A., Kapeller, R. and Soltoff, S. (1991) Cell **64**, 281-302.

Carr, DW., Hausken, ZE., Fraser, IDC., Stofko-Hahn, RE. and Scott, JD, (1992) Journal of Biological Chemistry **267**, 13376-13382.

Charbonneau, H. (1990) In Cyclic Nucleotide Phosphodiesterases: Stucture, Regulation and Drug Action (Beavo, JA. and Houslay, MD., Eds) pp. 267-296, John Wiley and Sons, Chichester UK

Charbonneau, H., Kumar, S., Novack, JP., Blumenthal, DK., Griffin, PR., Shabanowitz, J., Hunt, DF., Beavo, JA. and Walsh, KA. (1991) Biochemistry, **30**, 7931-7940.

Chaudhry, PS. and Cassilas, ER. (1988) Arch. Biochem. Biophys. **262**, 439-444.

Chen, HI. and Sudol, M. (1995) Proceedings of the National Academy of Science USA **92**, 7819-7823.

Cheung, WY. (1967) Biochem. Biophys. Res. Commun., **29**, 478-482.

Cheung, WY. (1970) Biochem. Biophys. Res. Commun., **38**, 533-538.

Cheung, WY. (1971) Journal of Biological Chemistry **246**, 2859-2869.

Chinkers, M. and Grabers, DL. (1991) Annu. Rev. Biochem. **60**, 553-575.

Chinkers, M., Singh, S. and Grabers, DL. (1991) Journal of Biological Chemistry **266**, 4088-4093.

Cicchetti, P., Mayer, BJ., Thiel, G. and Baltimore, D. (1992) Science **257**, 803-806.

Coghlan, VM., Langeberg, LK., Fenandez, A., Lamb, NJC. and Scott, JD. (1994) Journal of Biological Chemistry **269**, 7658-7665.

Cohen, P., Holmes, CFB. and Tsukitani, Y. (1990) Trends in Biochemical Sciences **15**, 98-102.

Cohen, GB., Ren, R. and Baltimore, D (1995) Cell, **80**, 237-248.

Colicelli, J., Birchmeister, C., Michaeli, T., O'Neill, K., Riggs, M. and Wigler, M. (1989) Proceedings of the National Academy of Science USA **86**, 3599-3603.

Colicelli, J., Nicolette, C., Birchmeister, C., Rodgers, L., Riggs, M. and Wigler, M. (1991) Proceedings of the National Academy of Science USA **88**, 2913-2917.

Conti, M. and Swinnen, JV. (1990) In Cyclic Nucleotide Phosphodiesterases: Stucture, Regulation and Drug Action (Beavo, JA. and Houslay, MD., Eds) pp. 61-85, John Wiley and Sons, Chichester UK

Conti, M., Jin., S-C., Monaco, L., Repaske, DR. and Swinnen, JV. (1991) Endocrine Reviews **12**, 218-234.

Conti, M., Nemoz, G., Sette, C. and Vicini, E. (1995) Endocrine Reviews **16**, 370-389.

Coquil, J-F. (1983) Biochim. Biophys. Acta **743**, 359-369.

Corbin, JD., Keeley, SL. and Park, CR. (1975) Journal of Biological Chemistry **250**, 218-255.

Courtneidge, SA., Fumagalli, S., Koegl, M., Superlifurga, G. and Twamley-Stein, GM. 1993 Development **119**, 57-64.

David, M., Daveran, M-L., Batut, J., Dedieu, A., Domergue, O., Ghai, J., Hertig, C., Boistard, P. and Kahn, D. (1988) Cell **54**, 671-683.

Davis, RL., Takayasu, H., Eberwine, M., Myres, J. (1989) Proc. Natl. Acad. Sci. USA **86**, 3604-3608.

Davis, RL. (1990) in Molecular Pharmacology of Cell Regulation (Beavo, JA. and Houslay, MD., Eds) vol 2, pp. 243-266, John Wiley and Sons, Chichester UK.

de Groot, RP., den Hertog, J., Vandenheede, JR., Goris, J. and Sassone-Corsi, P. (1993) EMBO J. **12**, 3903-3911.

de Jonge, HR., (1981) Advances in cyclic nucleotide research **14**, 315-323.

Degerman, E., Smith, CJ., Tornqvist, H., Vasta, V., Belfrage, P. and Manganiello, VC. (1990) Proceedings of the National Academy of Science USA **87**, 533-537.

Degerman, E., Moos, Jr., M., Rascon, A., Vasta, V., Meacci, E., Smith, CJ., Anderson, KE., Belfrage, P. and Manganiello, VC. (1995) Biochem. Biophys. Acta. **1205**, 189-198.

Denton, RM. and Tavare, JM. (1995) European Journal of Biochemistry **227**, 597-611.

Doskeland, SO., Maronde, E. and Gjertsen, BT. (1993) Biochim. Biophys. Acta Mol. Cell. Res. **1178**, 249-258.

Downing, AK., Driscoll, PC., Gout, I., Salim, K., Zvelebil, MJ. and Waterfield, MD. (1994) Current Biology, **4**, 884-891.

Eck, MJ., Atwell, SK., Shoelson, SE. and Harrison, SC. (1994) Nature, **368**, 764-769.

Eck, MJ., Pluskey, S., Trüb, T. and Harrison, SC. (1996) Nature, **379**, 277-280.

Engles, P., Abdel'Al, S., Hulley, P. and Lübbuert, H. (1995) Journal of Neuroscience Research **41**, 169-178.

Epstein, P., Yang, Q., Paskind, M., Salfeld, J., Kamen, R., Bolger, G., Thompson, WJ. and Cutler, L. (1994) FASEB J. **8**, A82.

Feinstein, PG., Schrader, KA., Bakalyar, HA., Tang, W-J., Krupinski, J., Gilman, AG. and Reed, RR. (1991) Proceedings of the National Academy of Science USA **88**, 10173-10177.

Feng, S., Chen, JK., Yu, H., Simon, JA. and Schreiber, SL. (1994) Science **266**, 1241-1247.

Ferguson, KM., Lemmon, MA., Schlessinger, J. and Sigler, PB. (1995) Cell **83**, 1037-1046.

Feuerstein, GZ., Liu, T. and Barone, FC. (1994) Cerebrovascular Brain Metabolism Reviews **6**, 341-360.

Finan, P., Shimizu, Y., Gout, I., Hsuan, J., Truong, O., Butcher, P., Bennett, P., Waterfield, MD. and Kellie, S. (1994) Journal of Biological Chemistry **269**, 13752-13755.

Flockhart, DA. and Corbin, JA (1982) CRC Crit. Rev. Biochem. **12**, 133-186.

Flynn, DC., Leu, TH., Reynolds, AB. and Parsons, JT. (1993) Molecular Cell Biology **13**, 7892-7900.

Foulkes, NS., Borrelli, E., and Sassone-Corsi, P. (1991) Cell **64**, 739-749.

Francis, SH., Colbran, JL., McAllister-Lucas, LM. and Corbin, JD. (1994) Journal of Biological Chemistry **269**, 22477-22480.

Fransis, SH., Lincoln. TM. and Corbin, JD. (1980) Journal of Biological Chemistry **255**, 620-626.

Fransis, SH. and Corbin, JD. (1988) Methods in Enzymology **159**, 722-729.

Fransis, SH., Thomas, MK. and Corbin, JD. (1990) In Cyclic Nucleotide Phosphodiesterases: Stucture, Regulation and Drug Action (Beavo, JA. and Houslay, MD., Eds) pp. 117-140, John Wiley and Sons, Chichester UK.

Fresenko, EE., Kolesnikov, SS. and Lyubarsky, AL. (1985) Nature **313**, 310-313.

Fumagelli, S., Totty, NF., Hsuan, JJ. and Courtneidge, SA. (1994) Nature **368**, 871-874.

Gao, B. and Gilman, AG. (1991) Proceedings of the National Academy of Science USA **88**, 10178-10182.

Garbers, DL. (1992) Cell **71**, 1-4.

Garbers, DL., Koesling, D. and Schultz, G. (1994) Molecular Biology of the Cell **5**, 1-5.

Gerzer, R., Bohme, E., Hoffmann, F. and Schultz, G. (1981) FEBS letters **132**, 71-74.

Gilles-Gonzalez, MA., Gonzalez, G., Perutz, MF., Kiger, L., Marden, MC. and Poyart, C. (1994) Biochemistry **33**, 8067-8073.

Gillman, AG. (1984) Cell **36**, 577-579.

Glantz, SB., Li, Y. and Rubin, CS. (1993) Journal of Biological Chemistry **268**, 12796-12804.

Gonzalez, GA. and Montminy, MR. (1989) Cell **59**, 675-680.

Goudreau, N., Cornille, F., Duchesne, M., Parker, F., Tocque, B., Garbay, C. and Roques, BP., (1994) Nature Structural Biology **1**, 898-907.

Grzesiek, S., Bax, A., Clore, GM., Gronenborn, AM., Hu, J-S., Kaufman, J., Palmer, I., Stahl, SJ. and Wingfield, PT. (1996) Nature Structural Biology, **3**, 340-345.

Guruprasad, L., Dhanaraj, V., Timm, D., Blundell, TL., Gout, I. and Waterfield, MD. (1995) Journal of Molecular Biology **248**, 856-866.

Haefner, R., Baxter, R., Fincham, VJ., Downes, CP. and Frame, MC. (1995) Journal of Biological Chemistry **270**, 7937-7943.

Hamet, P. and Coquil, J-F. (1978) Journal of Cyclic Nucleotide Research **4**, 281-290.

Hamet, P., Coquil, J-F., Bousseau-Lafortune, S., Franks, DJ. and Tremblay, J. (1984) Advances in Cyclic Nucleotide Phosphorylation Research **16**, 119-136.

Hanks, EG., Quinn, AM. and Hunter, T. (1988) Science **241**, 42-52.

Lee, C.H., Saksela, K., Mirza, U. A., Chait, B.T. and Kuriyan, J. (1996) Cell, **85**, 931-942.

Harper, JF., Haddox, MK., Johanson, R., Hanley, RM. and Steiner, AL., (1985) Vitamins and Hormones **42**, 197-252.

Harris, AL., Connell, MJ., Ferguson, EW., Wallace, AM., Gordon, RJ., Pagani, ED. and Silver, PJ. (1989) J. Pharmacol. Exp. Ther. **251**, 199-206.

Hashimoto, Y., Sharma, RK. and Soderling, TR. (1989) Journal of Biological Chemistry **264**, 10884-10887.

Haslam, R., Kolde, HB. and Hemmings, BA. (1993) Nature **363**, 309-310.

Hausken, ZE., Coghlan, VM., Schafer-Hastings, CA., Reimann, EM. and Scott, JD. (1994) Journal of Biological Chemistry **269**, 24245-24251.

Henkel-Tiggs, J. and Davis, RL. (1990) Molecular Pharmacology **37**, 7-10.

Heyworth, CM., Wallace, AV. and Houslay, MD. (1983) Biochemical Journal **214**, 99-110.

Ho, HC., Teo, TS., Desai, R. and Wang, JH. (1976) Biochem. Biophys. Acta, **429**, 461-473.

Hoeffler, JP., Meyer, TE., Yun, Y., Jameson, JL. and Habener, JF. (1988) Science **242**, 1430-1433.

Hofmann, F., Beavo, JA., Bechtel, PJ. and Krebs, EG. (1975) Journal of Biological Chemistry **250**, 7795-7801.

Hofmann, F., Grensheimer, H-P. and Göbel, C. (1985) Eur. Biochem. **147**, 361-365.

Horton, Y., Sullivan, M. and Houslay, MD. (1995) Biochem J. **308**, 683-691.

Houslay, MD. and Kilgour, E. (1990) In Cyclic Nucleotide Phosphodiesterases: Stucture, Regulation and Drug Action (Beavo, JA. and Houslay, MD., Eds) pp. 185-227, John Wiley and Sons, Chichester UK.

Hurley, JB. and Stryer, L. (1982) Journal of Biological Chemistry **257**, 11094-11099.

Hyvönen, M., Macias, MJ., Nilges, M., Oschkinat, H., Saraste, M. and Wilmanns, M. (1995) EMBO J. **14**, 4676-4685.

Jackson, SP., Schoenwalder, S.M., Yuan, Y., Rabinowitz, I., Salem, HH. and Mitchell, CA. (1994) Journal of Biological Chemistry **269**, 27093-27099.

Jin, SLC., Swinnen, JV. and Conti, M. (1992) Journal of Biological Chemistry **267**, 18929-18939.

Joachim, S. and Schwock, G. (1990) European Journal of Cell Biology **51**, 76-84.

Kakiuchi, S. and Yamazaki, R., (1970) BBRC, **42**, 1104-1110.

Kakiuchi, S., Yamazaki, R. and Nakajima, H., (1970) Proc. Jap. Acad. **46**, 587-592.

Kakiuchi, S., Yamazaki, R., Teshima, Y. and Uenishi, K. (1973) Proceedings of the National Acadadmey of Science USA **70**, 3526-3530

Kakiuchi, S., Yamazaki, R., Teshima, Y. and Uenishi, K., and Miyamoto, E (1975) Biochemical Journal, **146**, 109-120.

Kaupp, UB. (1991) Trends in Neuroscience **14**, 150-157.

Kaupp, UB., Niidome, T., Tanabe. T., Terade, S., Bönigk, W., Stühmer, W., Cook, NJ., Kangawa, K., Matsuo, H., Hirose, T., Miyata, T. and Numa, S. (1989) Nature **342**, 762-766.

Kavanaugh, WM. and Williams, LT., (1994) Science, **266**, 1862-1865.

Kazlauskas, A., Kashishian, A., Cooper, JA. and Valius, M. (1992) Molecular and Cellular Biology **12**, 2534-2544.

Keely, SL. (1979) Molecular Pharmacology **15**, 235-245.

Kilgour, E., Anderson, NG. and Houslay, MD. (1989) Biochemical Journal **260**, 27-36.

Kincaid, RL., Balaban, CD. and Billingsley, ML. (1987) Proceedings of the National Academy of Science USA **84**, 1118-1122.

Koch, CA., Anderson, D., Moran, MF., Ellis, C. and Pawson, T. (1991) Science **252**, 668-674.

Kozac, M., (1991) Journal of Cell Biology **115**, 887-903.

Krebs, EG., (1986) Biochemical Society Transactions **13**, 813-820.

Krupinski, J., Coussen, F., Bakalyar, HA., Tang, W-J., Feinstein, PG., Orth, K., Slaughter, C., Reed, RR. and Gilman, AG., (1989) Science **244**, 1558-1564.

La Porte, DC., Toscano, WA. and storm, DR. (1979) Biochemistry **18**, 2820-2825.

Landschultz, WH., Johnson, PF. and McKnight, SL. (1988) Science **240**, 1759-1764.

Laoide, BM., Foulkes, NS., Schlotter, F. nad Sassone-Corsi, P. (1993) EMBO J. **12**, 1179-1191.

Lee, DC., Carmicheal, DF., Krebs, EG. and McKnight, GS. (1983) Proceedings of the National Academy of Science USA **80**, 3608-3612.

Lee, C., Kominos, D., Jacques, S., Margolis, B., Schlessinger, J., Shoelson, SE. and Kuriyan, J. (1994) Structure **2**, 423-428.

Lee, C., Murakami, T. and Simonds, WF. (1995) Journal of Biological Chemistry **270**, 8779-8784.

Leiser, M., Rubin, CS. and Erlichman, J. (1986) Journal of Biological Chemistry **261**, 1904-1908.

Li, N., Batzer, A., Daly, R., Yajnik, V., Skolnik, E., Chardin, P., Bar-Sagi, D., Margolis, B. and Schlessinger, J. (1993) Nature **363**, 85-88.

Li, T., Volpp, K. and Applebury, ML. (1990) Proceedings of the National Academy of Science USA **87**, 293-297.

Lincoln, TM., Thompson, M. and Cornwell, TL. (1988) Journal of Biological Chemistry **263**, 17632-17637.

Livi, GP., Kmetz, P., McHale, M., Cielinski, LB., Sathe, GM., Taylor, DJ., Davis, RL., Torphy, TJ. and Balcarek, JM. (1990) Molecular and Cellular Biology **10**, 2678-2686.

Lobban, M., Shakur, Y., Beattie, J. and Houslay, MD. (1994) Biochemical Journal **304**, 399-406.

Lohmann, SM., DeCamilli, P., Einig, I. and Walter, U. (1984) Proceedings of the National Academy of Science USA **81**, 6723-6727.

Loten, EG. and Sneyd, JGT., (1970) Biochemical Journal **120**, 187-193.

Lowe, DG., (1992) Biochemistry **31**, 10421-10425.

Manganiello, VC., Smith, CJ., Degerman, E. and Belfrage, P. (1990) In Cyclic Nucleotide Phosphodiesterases: Stucture, Regulation and Drug Action (Beavo, JA. and Houslay, MD., Eds) pp. 87-140, John Wiley and Sons, Chichester UK.

Manganiello, VC., Taira, M., Degerman, E. and Belfrage, P. (1995) Cellular Signalling **7**, 445-455.

Manganiello, VC., Degerman, E. Taira M., Kono, T., and Belfrage, P. (1995a) Current Topics in Cellular Regulation

Martins, TJ., Mumby, MC. and Beavo, JA. (1982) Journal of Biological Chemistry **257**, 1973-1979.

Mayer, BJ. and Baltimore, D. (1993) Trends in Cell Biology **3**, 8-13.

Mayer, BJ., Ren, R., Clark, KL. and Baltimore, D. (1993) Cell **73**, 629-630.

McCartney, S., Little, BM., Langeberg, LK. and Scott, JD. (1995) Journal of Biological Chemistry **270**, 1-7.

McKnight, GS. (1991) Current Opinion in Cell Biology **3**, 213-217.

McLaughlin, MM., Cieslinski, LB., Burman, M., Torphy, TJ. and Livi, G. (1993) Journal of Biological Chemistry **268**, 6470-6476.

McPhee, I., Pooley, L., Lobban, M., Bolger, G. and Houslay, MD (1995) Biochemical Journal **310**, 965-974.

Meacci, E., Taira, M., Moos, M., Smith, CJ., Movsesian, MA., Degerman, E., Belfrage, P. and Manganiello, VC. (1992) Proceedings of the National Academy of Science USA **89**, 3721-3725.

Mery, P-F., Pavoine, C., Pecker, F. and Fischmeister, R. (1995) Molecular Pharmacology **48**, 121-130.

Meyer, TE. and Habener, JF. (1993) Endocrinology Reviews **14**, 269-290.

McLaughlin, MM., Cielinski, LB., Burman, M., Torphy, TJ. and Livi, GP. (1993) Journal of Biological Chemistry **268**, 6470-6476.

Michaeli, T., Bloom, J., Martins, T., Loughney, K., Ferguson, K., Riggs, M., Rodgers, L., Beavo, J. and Wigler, M. (1993) Journal of Biological Chemistry **268**, 12925-12932.

Miki, N., Baraban, JM., Keirns, JJ., Boyce, JJ. and Bitenski, MW. (1975) Journal of Biological Chemistry **250**, 6320-6327.

Milatovich, A., Bolger. G., Michaeli, T. and Francke, U. (1994) Somat. Cell Molec. Genet. **20**, 75-86.

Miot, F., Van Haastert, P. and Erneux, C. (1985) European Journal of Biochemistry **149**, 59-65.

Mollner, S. and Pfeuffer, T. (1988) European Journal of Biochemistry **171**, 265-271.

Monaco, L., Vicini, E. and Conti, M. (1994) Journal of Biological Chemistry **269**, 347-357.

Moon, RT., and McMahon, AP. (1990) Journal of Biological Chemistry **265**, 4427-4433.

Moss, J., Manganiello, VC. and Vaughan, M. (1977) Journal of Biological Chemistry **252**, 5211-5215.

Mukai, J., Asai, T., Naka, M. and Tanaka, T. (1994) British Journal of Pharmacology **111**, 389-390.

Murashima, S., Tanaka, T., Hockman, S. and Manganiello, VC. (1990) Biochemistry **29**, 5285-5292.

Musacchio, A., Gibson, T., Rice, P., Thompson, J. and Saraste, M. (1993) Trends in Biochemical Sciences **18**, 343-348.

Musacchio, A., Wilmanns, M. and Saraste, M. (1994) Prog. Biophys. Mol. Biol. **61**, 283-297.

Nakane, M., Arai, K., Saheki, S., Kuno, T., Buechler, W. and Murad, F. (1990) Journal of Biological Chemistry **265**, 16841-16845.

Neer, EJ. (1994) Protein Science **3**, 3-14.

Nemoz, G., Zhang, R., Sette, C. and Conti, M. (1996) Febs letters **354**, 97-102.

Neubig, RR., Connelly, MP. and Remmers, AE. (1994) FEBS letters **355**, 251-253.

Nichols, M., Weih, F., Schmid, W., DeVack, C., Kowenz-Leutz, E., Luckow, B., Boshart, M. and Schutz, G. (1992) EMBO J. **11**, 3337-3346.

Nigg, EA., Hilz, H., Eppenberger, H. and Dutly, F. (1985) EMBO J. **4**, 2801-2806.

Nigg, EA., Schafer, G., Hilz, H. and Eppenberger, H. (1985a) Cell **41**, 1039-1051.

Novac, JP., Charbonneau, H., Bentley, JK., Walsh, KA. and Beavo, JA. (1991) Biochemistry **30**, 7940-7947.

O'Connell, JC., McCallum, JF., McPhee, I., Wakefield, J., Houslay, ES., Wishart, W., Bolger, G., Frame, M. and Houslay, MD. (1996) Biochemical Journal **318**, 255-262.

O'Neil, KT., Hoess, RH. and Delgado, WF. (1990) Science **249**, 774-778.

Palfreyman, MN. and Souness, JE. (1996) Progressive Medicinal Chemistry **33**, 1-52.

Pawson, T. and Gish, GD. (1992) Cell **71**, 359-362.

Pawson, T. and Schlessinger, J. (1993) Current Biology **3**, 434-442.

Pfeuffer, T. and Metzger, H. (1882) FEBS Letters **146**, 369-375.

Pfeuffer, E., Mollner, S. and Pfeuffer, T. (1985) EMBO Journal **4**, 3675-3679.

Pfister, C., Bennett, N., Bruckert, F., Catty, P., Clerc, A., Pages, F. and Deterre, P. (1993) Cellular Signalling **5**, 235-251.

Pronon, AN. and Gautam, N. (1992) Proceedings of the National Academy of Science USA **89**, 6220-6224.

Purvis, K., Olsen, A. and Hannson, V. (1981)) Journal of Biological Chemistry **256**, 11434-11441.

Pyne, N., Cooper, M. and Houslay, MD. (1986) Biochemical Journal **234**, 325-334.

Pyne, N., Cooper, M. and Houslay, MD. (1987) Biochemical Journal **242**, 33-42.

Qiu, Y., Chen, CN., Malone, T., Richter, L., Beckendorf, SK. and Davis, R. (1991) Journal of Molecular Biology **222**, 553-565.

Qiu, Y. and Davis, R. (1993) Genes Dev. **7**, 1447-1458.

Rahn, T., Riderstrale, M., Tornquivst, H., Fredrikksin, G., Manganiello, VC., Belfrage, P. and Degerman, E. (1994) FEBS Letters **350**, 314-318

Ramos-Morales, F., Druker, BJ. and Fischer, S. (1994) Oncogene **9**, 1917-1923.

Rascon, A., Lindgreen, S., Stavenow, L., Belfrage, P. and Manganiello, VC. (1992) Biochem. Biophys. Acta. **1134**, 149-152.

Ray, K., Kunsch, C., Bonner, LM. and Robishaw, JD. (1995) Journal of Biological Chemistry **270**, 21765-21771.

Reeves, ML., Leigh, BK. and England, PJ. (1987) Biochemical Journal **241**, 535-541.

Ren, R., Mayer, BJ., Cicchetti, P. and Baltimore, D. (1993) Science **259**, 1157-1161.

Repaske, DR., Swinnen, JV., Jin, SLC., Van Wyk, JJ. and Conti, M. (1992) Journal of Biological Chemistry **267**, 18683-18688.

Rossi, P., Giorgi, M., Geremia, R. and Kincaid, RL. (1988) Journal of Biological Chemistry **263**, 15521-15527.

Rotin, D., Bar-Sagi, D., O'Brodovich, H., Merilainen, J., Lehto, VP., Canesssa, CM., Rossier, BC. and Downey, GP. (1994) EMBO J., **13**, 4440-4450.

Schade, FU. and Schudt, C. (1993) European Journal of Pharmacology **230**, 9-14.

Schmiechen, R., Schneider, HH. and Wachel, H. (1990) Physiopharmacology **102**, 17-20.

Schneider, HH., Schmiechen, R., Brezinski, M. and Seidler, J. (1986) European Journal of Pharmacology **127**, 105-115.

Schultz, JE., Klumpp, S., Benz, R., Schüfhoff-Goeters, WSJC. and Schmid, JE. (1992) Science **255**, 600-603.

Schwabe, U., Miyake, M., Ohaga, Y. and Daly, JW. (1976) Molecular Pharmacology **12**, 900-910.

Scotland, G. and Houslay, M.D. (1995) Biochemical Journal **308**, 673-681.

Scott, JD. (1991) Pharmacol. Ther. **50**, 123-145.

Scott, JD. and Carr, DW. (1992) News in Physiological Science **7**, 143-148.

Scott, JD., Stofko, RE., McDonald, JR., Comer, JD., Vitalis, EA. and Mangili, J. (1990) Journal of Biological Chemistry **265**, 21561-21566.

Sekut, L., Yarnall, D., Stimpson, SA., Noel., LS., Batemanfite, R., Clarke, RL., Brackeen, MF., Menius, LA. and Connelly, KM (1995) Clin. Exp. Immunology, **100**, 126-132.

Sette, C., Vicini, E. and Conti, M. (1994) Journal of Biological Chemistry **269**, 18271-18274.

Sette, C. and Conti, M. (1995) FASEB J. **33**, A1262.

Sette, C. and Conti, M. (1996) Journal of Biological Chemistry **271**, 16526-16534.

Shakur, Y., Pryde, J.G. and Houslay, MD. (1993) Biochemical Journal **292**, 677-686.

Shakur, Y., Wilson, M., Pooley, L., Lobban, M., Griffiths, SL., Campbell, AM., Beattie, J., Daly, C. and Houslay, MD. (1995) Biochemical Journal **306**, 801-809.

Sharma, RK, and Wang, JH. (1985) Proceedings of the National Academy of Science USA **82**, 2603-2607.

Sharma, RK, and Wang, JH. (1986) Journal of Biological Chemistry **261**, 1322-1328.

Sharma, RK., Huang, CY., Chau, V. and Chock, PB. (1980) Ann. NY Acad. Sci. **356**, 190-204.

Sharma, RK., Wang, TH., Wirch, E. and Wang, JH. (1980) Journal of Biological Chemistry **255**, 5916-5923.

Shenolikar, S., Thompson, WJ. and Strada, SJ. (1985) Biochemistry **24**, 672-678.

Shibita, H., Robinson, FW., Soderling, TR. and Kono, T. (1991) Journal of Biological Chemistry **266**, 17948-17953.

Slusarewicz, P., Nilsson, T., Hui, N., Watson, R. and Warren, GB. (1994) Journal of Cell Biology **124**, 405-413.

Smigel, MD. (1986) Journal of Biological Chemistry **261**, 1976-1982.

Smith, CJ., Vasta, V., Degerman, E., Belfrage, P. and Manganiello, VC. (1991) Journal of Biological Chemistry **266**, 13385-13390.

Smith, KJ., Scotland, G., Beattie, J., Trayer, IP. and Houslay, MD. (1996) Journal of Biological Chemistry **in press.**

Songyang, Z., Shoelson, SE., Chaudhuri, M., Gish, G., Pawson, T., Haser, WG., King, F., Roberts, T., Ratnofsky, S. and Lechleider, RJ. (1993) Cell **72**, 767-778.

Songyang, Z., Shoelson, SE., McGlade, J., Olivier, P., Pawson, T., Bustelo, XR., Barbacid, M., Sabe, H., Hanafusa, H. and Yi, T. (1994) Molecular Cell Biology, **14**, 2777-2785.

Sonnenberg, WK., Mullaney, PJ. and Beavo, JA. (1991) Journal of Biological Chemistry **266**, 17655-17661.

Sonnenberg, WK., Seger, D. and Beavo, JA. (1993) Journal of Biological Chemistry **268**, 645-652.

Souness, JE. and Scott, LC. (1993) Biochemical Journal **291**, 389-395.

Souness, JE., Maslen, C., Webber, S., Foster, M., Raeburn, D., Palfreyman, MN., Ashton, MJ. and Karlsson, J-A. (1995) British Journal of Pharmacology **114**, 39-46.

Souness, JE. and Rao, S. (1996) Cellular Signalling, **in press**.

Souness, JE., Griffin, M., Maslen, C., Ebsworth, K., Scott, LC., Pollock, K., Palfreyman, MN. and Karlsson, J-A. (1996) British Journal of Pharmacology **118**, 649-658.

Stroop, SD, Charbonneau, H. and Beavo, JA. (1989) Journal of Biological Chemistry **254**, 13718-13725.

Stroop, S. and Beavo, JA. (1991) Journal of Biological Chemistry **266**, 23802-23809.

Stroop, S. and Beavo, JA. (1992) Adv. Second Messenger Phosphoprotein Res. **25**, 55-71.

Sudol, M., (1994) Oncogene, **9**, 2145-2152.

Sudol, M., Bork, P., Einbond, A., Kumar, K., Druck, T., Negrini, M., Huebner, K. and Lehman, D. (1995) Journal of Biological Chemistry **270**, 14733-14741.

Sugimoto, S., Wandless, TJ., Shoelson, SE., Neel, BG. and Walsh, CT. (1994) Journal of Biological Chemistry **269**, 13614-13622.

Superti-Furga, G., Furmagalli, S., Koegl, M., Courtneidge, SA. and Draetta, G. (1993) EMBO J. **12**, 2625-2634.

Swarup, G., Cohen, S. and Garbers, DL. (1982) Biochemical and Biophysical Research Communications **107**, 1104-1109.

Swinnen, JV., Joseph, DR. and Conti, M. (1989) Proc. Natl. Acad. Sci. USA **86**, 5325-5329.

Swinnen, JV., Tsikalas, KE. and Conti, M. (1991) Journal of Biological Chemistry **266**, 18370-18377.

Taira, M., Hockman, S., Calvo, JC., Belfrage, P. and Manganiello, VC. (1993) Journal of Biological Chemistry **268**, 18573-18579.

Takemoto, IJ., Hansen, J., Farber, DB., Souza, D., and Takemoto, DJ. (1984) Biochemical Journal, **217**, 129-133.

Takio, K., Wade, RD., Smith, SB., Krebs, EG., Walsh, KA. and Titani, K. (1984) Biochemistry **23**, 4207-4218.

Tanaka, T., Hockman, S., Moos, M., Taira, M., Meacci, E., Murashima, S. and Manganiello, VC. (1991) Second Messengers Phosphoproteins **13**, 87-98.

Tang, WJ. and Gilman, AG. (1991) Science **254**, 1500-1503.

Tang, WJ., Krupinski, J. and Gilman AG. (1991) Journal of Biological Chemistry **266**, 8595-8603.

Tang, WJ., Iñiguez-Lluhi, JA., Mumby, SM. and Gilman AG. (1992) Cold Spring Harbour Symp. Quant. Biol. **57**, 102-110.

Taussig, R. and Gilman, AG. (1995) Journal of Biological Chemistry **270**, 1-4.

Taylor, SJ. and Shalloway, D., (1994) Nature **368**, 867-871.

Teo, TS., Wang, TH. and Wang JH. (1973) Journal of Biological Chemistry **248**, 588-595.

Terasaki, WL. and Appleman, MM. (1975) Metabolism **24**, 311-319.

Tersawa, H., Kohda, D., Hatanaka, H., Tsuchiya, S., Ogura, K., Nagata, K., Ishii, S., Mandiyan, V., Ullrich, A., Schlessinger, J. and Inagaki, F. (1994) Nature Structural Biology **1**, 891-897.

Thomas, MK., Fransis, SH. and Corbin, JD. (1988) 14th International Congress of Biochemistry, MO256, p.122.

Thomas, MK., Fransis, SH., Todd, BW. and Corbin, JD. (1988a) FASEB J. **2**, A596

Thomas, MK., Fransis, SH. and Corbin, JD. (1990) Journal of Biological Chemistry **265**, 14964-14970.

Thomas, MK., Fransis, SH. and Corbin, JD. (1990a) Journal of Biological Chemistry **265**, 14971-14978.

Thompson, WJ, Ross, CP., Strada, SJ., Hersh, EM. and Lavis, VR. (1980) Cancer Research **40**, 1955-1960.

Thompson, WJ. (1991) Pharmacol. Ther. **57**, 13-33.

Torphy, TJ. and Cieslinski, LB (1990) Molecular Pharmacology **37**, 206-214.

Torphy, TJ., Stadel, JM., Burman, M., Cielinski, LB., McLaughlin, MM., White, JR. and Livi, GP. (1992) Journal of Biological Chemistry **267**, 1798-1804.

Tracey, KJ. and Cerami, A. (1993) Annual Review of Cell Biology **9**, 317-343.

Trong, HL., Beier, N., Sonnenberg, WK., Stroop, SD., Walsh, KA., Beavo, JA. and Charbonneau, H. (1990) Biochemistry **29**, 10280-10288.

Tuteja, N. and Farber, DB. (1988) Fedn Eur. Biochem. Socs. Lett. **232**, 182-186.

Vandermeers, A., Vandermeers-Piret, M-C., Rathe, J. and Christophe, J. (1983) Biochemical Journal, **211**, 341-347.

Vinson, CR., Sigler, PB. and McKnight, SL. (1989) Science **246**, 911-916.

Wachel, H. (1983) Neuropharmacology **22**, 267-272.

Walsh, DA. and Van Patten, SM (1994) FASEB Journal **8**, 1227-1236.

Walsh, DA., Perkins, JP. and Krebs, EG. (1968) Journal of Biological Chemistry **243**, 3763-3765.

Wang, LY., Salter MW. and MacDonald, JF. (1991) Science **253**, 1132-1134.

Wasco, WM. and Orr, GA., (1984) Biochem. Biophys. Res. Commun. **118**, 636-642.

Witthuhn, BA., Silvennoinen, O., Miura, O., Lai, KS., Cwik, C., Liu, ET. and Ihle, JN (1994) Nature **370**, 153-157.

White, MF. and Kahn, CR. (1994) Journal of Biological Chemistry **269**, 1-4.

Wolf, G., Trüb, T., Ottinger, E., Groninga, L., Lynch, A., White, M., Miyazaki, M., Lee, J. and Shoelson, SE. (1995) Journal of Biological Chemistry **270**, 27407-27410.

Wolfe, L., Corbin, JD. and Francis, SH. (1989) Journal of Biological Chemistry **264**, 7734-7741.

Wu, Z., Sharma, RK. and Wang. JH. (1992) Advances in Second Messenger and Phosphoprotein Research **25**, 29-43.

Yamamoto, T., Manganiello, VC. and Vaughan, M. (1983) Journal of Biological Chemistry **258**, 12526-12533.

Yamazaki, A. (1992) Advances in Second Messenger and Phosphoprotein Research **25**, 135-145.

Ye, Z-S. and Baltimore, D. (1995) Proceedings of the National Academy of Science USA. **92**,

Yoshimura, M. and Cooper, DMF. (1992) Proceedings of the National Academy of Science USA **89**, 6716-6720.

Yu, H., Rosen, MK. and Schreiber, SL. (1993) FEBS letters **324**, 87-93.

Yu, H., Chen, JK., Feng, S., Dalgarno, DC., Brauer, AW. and Schreiber, SL. (1994) Cell **76**, 933-945.

Yuen, PST., Doolittle, L. and Garbers, DL. (1994) Journal of Biological Chemistry **269**, 791-793.

Zhang, GY., Sharma, RK, and Wang, JH. (1990) Journal of Biological Chemistry **265**, 12454-12458.

Zhou, MM., Huang, B., Olejniczak, ET., Meadows, RP., Shuker, SB., Miyazaki, M., Trüb, T., Shoelson, SE. and Fesik, SW. (1996) Nature Structural Biology **3**, 388-393.